TECHNISCHE UNIVERSITÄT MÜNCHEN

Department Chemie

Lehrstuhl für Biotechnologie

Phospho-regulation of the Hsp90 chaperone machinery

Joanna Soroka

Vollständiger Abdruck der von der Fakultät für Chemie der Technischen Universität München zur Erlangung des akademischen Grades eines Doktors der Naturwissenschaften genehmigten Dissertation.

Vorsitzender:		Univ.-Prof. Dr. Stephan A. Sieber
Prüfer der Dissertation:	1.	Univ.-Prof. Dr. Johannes Buchner
	2.	Univ.-Prof. Dr. Thorsten Hugel
	3.	Priv.-Doz. Dr. Henrik Daub

Die Dissertation wurde am 19.10.2011 bei der Technischen Universität München eingereicht und durch die Fakultät für Chemie am 01.12.2011 angenommen.

For Muzio and my family

1 Index

2 Summary

Hsp90 is a molecular chaperone modulating the activity of hundreds of client proteins, many of which are important cellular effector proteins. This activation process is regulated on several levels: by ATP hydrolysis, various specific Hsp90 co-chaperones as well as posttranslational modifications. In this context, phosphorylation of Hsp90 is of particular importance as there is a conserved phosphatase Ppt1, which specifically associates with Hsp90 and dephosphorylates it (Wandinger et al., 2006). Little is known about how Ppt1-dependent phosphorylation sites affect Hsp90 activity.

The combination of SILAC and MS analysis allowed identifying ten *in vivo* phosphorylation sites of Hsp90 distributed in the M- and the C-domain of Hsp90 and determining a subset regulated by Ppt1. Further experiments revealed that the ten residues constitute the major phospho-acceptor sites in yeast Hsp90. Despite a highly conserved protein sequence, the phosphorylation pattern of yeast and human Hsp90 is not conserved. This is probably because many known human kinases evolved after the divergence of higher eukaryotes from yeast. Thus, Hsp90 phosphorylation may be an evolutionary mechanism to allow organism-specific functional variations and provide an adaptation to various environmental conditions.

By employing alanine and glutamate substitutions of the identified sites (mimicking non-phosphorylated and phosphorylated states, respectively), the functional consequences of phosphorylation were assessed. The analysis revealed that four phosphorylation sites were active, whereas six exhibited no effects on Hsp90 chaperone activity. This finding shows that there are ‘silent’ phosphorylation events without functional importance, except that they might enhance the solubility of the protein (Lienhard, 2008). In general, the active phosphorylation sites down regulate the Hsp90 machinery. In particular, one site (S485) disrupted the essential chaperone properties of Hsp90, whereas three other negatively affect Hsp90 activity *in vivo* including reduced client protein activation, hypersensitivity to Hsp90 inhibition and disruption of DNA repair processes.

Several biophysical techniques have been employed to determine the molecular mechanisms of the active phospho-sites such as intermolecular FRET and analytical ultracentrifugation combined with fluorescence detection. This analysis revealed that sites located in distant regions of Hsp90 protein affect the ATPase activity, co-chaperone binding and conformational transitions in Hsp90. Thus, phosphorylation of Hsp90 allows the manipulation of the conformational cycle at distinct steps by targeting switch points for the communication between remote regions within Hsp90.

3 Zusammenfassung

Das molekulare Chaperon Hsp90 ist an der Regulation der Aktivität von hunderten Substratproteinen beteiligt, welche zum Großteil eine wichtige Rolle als Effektorproteine in der Zelle spielen. Diese Aktivierung kann auf verschiedene Weise reguliert werden: durch ATP-Hydrolyse, durch Bindung Hsp90-spezifischer Co-Chaperone, sowie durch verschiedene Arten posttranslationaler Modifikationen. Bei letzteren spielt die Phosphorylierung von Hsp90 eine entscheidende Rolle, da die konservierte Phosphatase Ppt1 spezifisch am Hsp90 bindet und das Protein dephosphoryliert (Wandinger et al., 2006). Bisher ist jedoch wenig darüber bekannt, wie die Ppt1-spezifischen Phosphorylierungsstellen die Aktivität von Hsp90 beeinflussen.

Durch die Kombination von SILAC und MS Analysen konnten *in vivo* zehn Phosphorylierungsstellen innerhalb der M- und C-Domänen von Hsp90 identifiziert werden, wovon zwei durch Ppt1 reguliert werden. Weitere Untersuchungen zeigten, dass diese zehn Aminosäurereste die Hauptakzeptorstellen für die Phosphorylierung von Hsp90 in der Hefe darstellen. Trotz einer stark konservierten Aminosäuresequenz zeigte das Phosphorylierungsmuster des Hsp90 aus der Hefe und des humanen Hsp90 keine Übereinstimmung. Dies lässt sich dadurch erklären, dass die meisten bekannten humanen Proteinkinasen nach der evolutionären Trennung von Hefe und höheren Eukaryoten in ihrer Spezifität weiter evolvierten.

Um den Einfluss der Phosphorylierungsstellen auf die Funktion von Hefe Hsp90 zu untersuchen, wurden diese durch Alanin oder Glutamat substituiert, wodurch der nicht-phosphorylierte und phosphorylierte Status nachgahmt wurde. Vier der zehn untersuchten Phosphorylierungsstellen waren „aktiv“, wohingegen die weiteren sechs keinen Einfluss auf die Aktivität von Hsp90 hatten. Dies zeigt, dass es `stille` Phosphorylierungen gibt, die wahrscheinlich nur zur Löslichkeit des Proteins beitragen (Lienhard, 2008). Im Allgemeinen führt eine Phosphorylierung der aktiven Stellen zur einer Verlangsamung der Hsp90 Maschinerie. Nur die Phosphorylierung an S485 zerstört die essenziellen Chaperoneigenschaften von Hsp90. Drei weitere Phosphorylierungen beeinflussen *in vivo* die Aktivität von Hsp90 negativ. Dies äußert sich auch in einer verminderten Aktivierung der Substratproteine, in einer

Überempfindlichkeit von Hsp90 gegenüber Inhibierung, sowie in einer gestörten DNA-Reparatur.

Um die molekularen Mechanismen der aktiven Phosphorylierungsstellen zu bestimmen, wurden verschiedene biophysikalische Methoden angewandt, wie z.B. intermolekulare FRET-Experimente und analytische Ultrazentrifugation gekoppelt mit Fluoreszenzdetektion. Diese Analysen zeigen, dass auch weit von der ATPase Domäne entfernte Phosphorylierungsstellen des Hsp90 Proteins dessen ATPase Aktivität, sowie die Bindung von Co-Chaperonen und Konformationsänderungen von Hsp90 negativ beeinflussen. Zusammengefasst zeigen die vorgelegten Ergebnisse, dass die Phosphorylierung von Hsp90 die Manipulation des Konformationszyklus an bestimmten Schritten ermöglicht, indem sie an Schaltpunkten für die Kommunikation in Hsp90 angreift.

4 Introduction

4.1 The molecular chaperone Hsp90

Hsp90 is an abundant and highly conserved molecular chaperone found in all kingdoms except for archea (Figure 1) (Large et al., 2009). It is involved in the activation, stabilization or conformational maturation of hundreds of client proteins in eukaryotes (McClellan et al., 2007; Picard, 2002; Pratt and Toft, 1997; Zhao et al., 2005). These are important players in numerous cellular processes including gene expression, signal transduction and cell cycle regulation. These diverse cellular functions and the fact that several Hsp90 client proteins are essential components in signal transduction pathways require a strict regulation of this chaperone machinery. Consequently, attempts to discover specific Hsp90 inhibitors as novel anti-cancer therapeutics, which allow interfering with the proliferation of cancer cells, are actively pursued (Neckers, 2007; Whitesell and Lindquist, 2005). In cancer cells, Hsp90 plays a crucial role in buffering oncogenic mutations and protecting a large set of over-expressed oncoproteins from their degradation. Consequently, Hsp90 helps to stabilize tumorogenic cells. Therefore, cancer cells are often considered to be *'*addicted*'* to Hsp90 (Bagatell and Whitesell, 2004; Sangster et al., 2004). In normal cells, Hsp90 is also involved in evolutionary processes such as increasing the inherent genetic heterogeneity. This is achieved by buffering mutations that occur during normal morphological evolution (Jarosz and Lindquist, 2010; Queitsch et al., 2002; Rutherford and Lindquist, 1998).

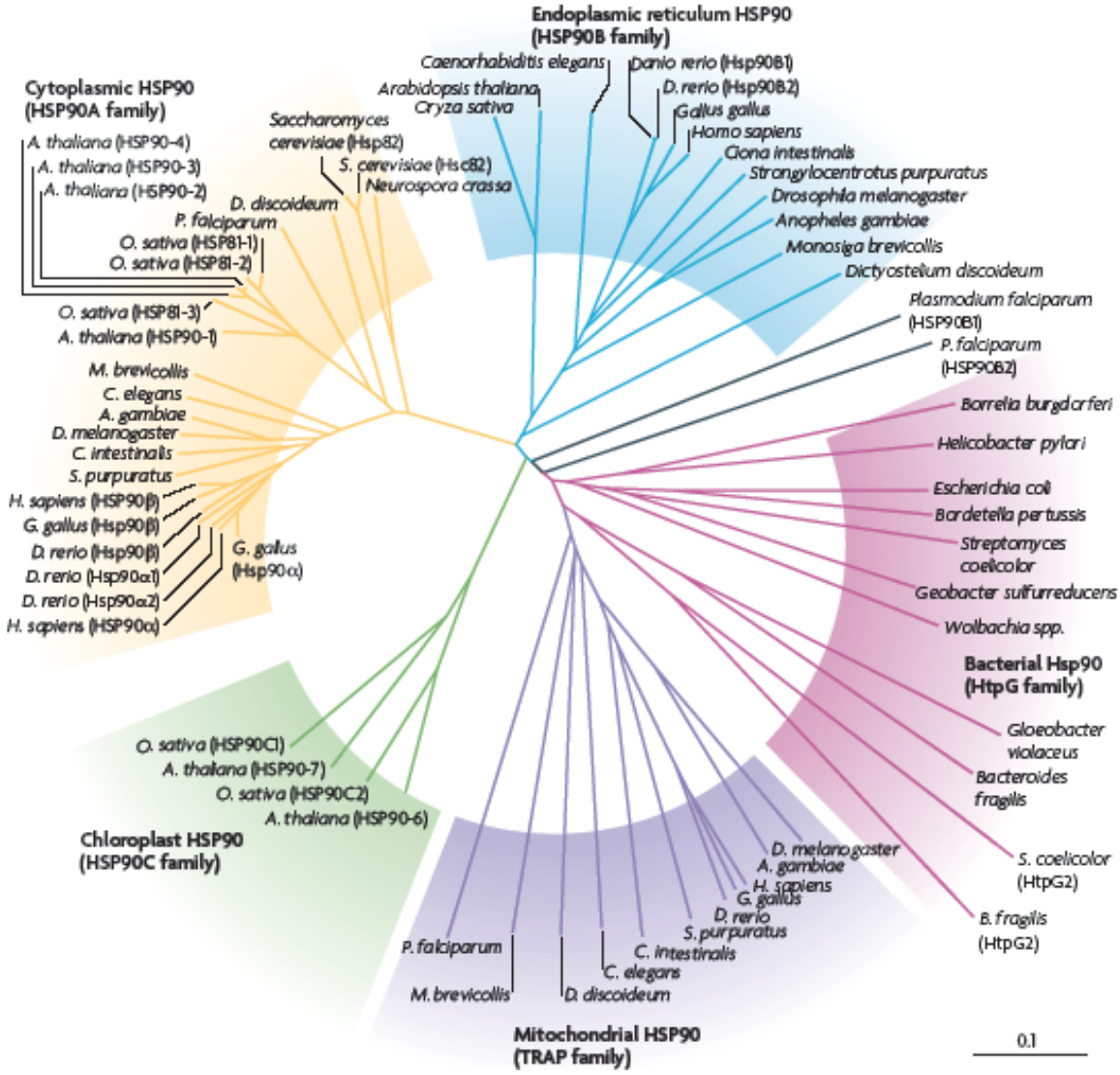

Figure 1. Evolution of Hsp90 protein family
Hsp90 family is highly conserved and present in all kingdoms of life except for archea. Several Hsp90 subfamilies can be distinguished: cytosolic Hsp90, endoplasmic reticulum Hsp90 (Grp94), chloroplast Hsp90 (Hsp90C), mitochondrial Hsp90 (TRAP), and bacterial Hsp90 (HtpG). The scale bar represents the genetic distance. Adopted from (Taipale et al., 2010).

4.2 The Hsp90 and Hsp70 chaperone machinery

Hsp90 is an important player in protein folding. Under physiological conditions it seems that Hsp90 does not assist general de novo folding processes, but its clients are already partly structured and may even adopt native-like conformations (Picard, 2002). To recruit and assemble with client proteins, eukaryotic Hsp90 collaborates with the Hsp70 system and a number of the accessory proteins termed 'co-chaperones' forming large dynamic multi-protein complexes (Pratt and Toft, 2003; Smith et al., 1993). Protein turnover is an essential cellular process needed for health

and survival. Thus, not only correct folding, but also degradation of misfolded proteins is critical for cellular homeostasis. To balance between folding and degradation, the Hsp70/Hsp90 machinery cooperates with the ubiquitin-proteosome system mediated by the Hsp90 co-chaperone CHIP directing misfolded proteins for degradation (Gamerdinger et al., 2009; Pratt et al., 2006; Pratt et al., 2010). Binding of CHIP to the chaperone complexes leads to the ubiquitination and ultimately degradation of the client proteins as well as the chaperones (Kundrat and Regan, 2010). Thus, CHIP functions as the quality control regulator of the folding pathway.

4.3 Hsp90 homologues and its localization in the cell

Hsp90 is present in nearly every compartment of the eukaryotic cell while it is most abundant in the cytosol. Two cytosolic Hsp90 isoforms exist: an inducible Hsp90α and a constitutive Hsp90β form (Hsp82 and Hsc82, respectively in yeast) (Csermely et al., 1998). A small pool of the cytosolic Hsp90 is also translocated to the nucleus. It is thought that Hsp90 is co-transported to the nucleus when associated with the client as the chaperone itself does not have a nuclear localization sequence (Pratt, 1993). Hsp90 can be also transported outside of the cell. Recently, a pool of Hsp90 has been identified at the cell surface of various cell types indicating diverse extracellular chaperoning activity (Sidera and Patsavoudi, 2008; Trepel et al., 2010). Particularly in cancer, extracellular Hsp90α was shown to be involved in cancer cell invasion (Eustace et al., 2004). Extracellular Hsp90α was also shown to be associated with wound healing (Li et al., 2007). Plants contain several copies of cytosolic Hsp90 which play a protective role against deleterious effects of environmental fluctuations and pathogens (Krishna and Gloor, 2001; Meiri and Breiman, 2009; Sangster and Queitsch, 2005). In addition, compartment-specific Hsp90 homologues are present in mitochondria (TRAP1), chloroplasts (Hsp90C) and the endoplasmic reticulum (Grp94) (Figure 2) (Felts et al., 2000; Shiu et al., 1977).

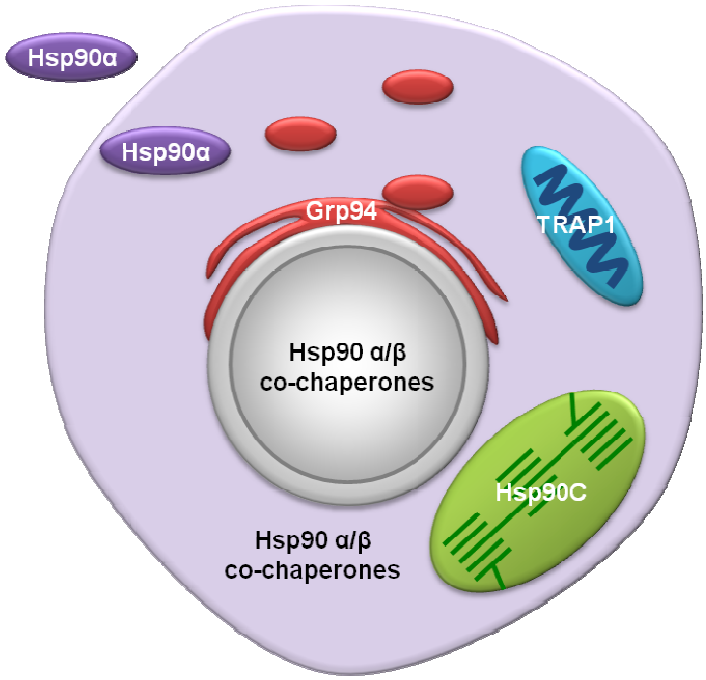

Figure 2. Hsp90 localization in the eukaryotic cell
Hsp90 is most prominent in the cytoplasm but it can also be found in different subcellular compartments including the nucleus (where it is transported from the cytoplasm), mitochondria (TRAP1), endoplasmic reticulum (Grp94) or chloroplasts (Hsp90C). Furthermore, Hsp90 can be exported from the cytoplasm outside the cell.

Found in nearly all organisms including bacteria and all branches of eukarya, Hsp90 appears to have evolved to exert diverse functions. Although dispensable in bacteria, it is an essential protein in eukaryotes (Bardwell and Craig, 1988; Borkovich et al., 1989). Further functional differences between eukaryotic and prokaryotic/organellar Hsp90 homologues exist. Cytosolic Hsp90 in eukaryotes is fine-tuned by a large set of co-chaperones which may serve to stabilize different conformational states of Hsp90 according to the requirements of the client protein. This complexity of eucaryotic Hsp90 makes it one of the most sophisticated chaperone machineries known to date. In contrast, its procaryotic (HtpG) or organellar homologues are stand-alone machines, which could reflect changes in the client specificity. In this context, numerous client proteins unrelated in sequence and structure are known for eukaryotic Hsp90, while the clientele of prokaryotic homologue awaits its identification (Buchner, 2010; Sato et al., 2010). Nevertheless, the structural organization and mechanistic basis of the ATPase cycle are conserved among its cytosolic and organellar species (Frey et al., 2007; Leskovar et al., 2008; Richter et al., 2008).

4.4 Hsp90 structure and conformational changes

Hsp90 is a flexible dimeric protein where each of the protomers contains an N-terminal domain (N-domain) responsible for binding and hydrolysis of ATP (Prodromou et al., 1997), connected in eukaryotes by a charged linked of variable length (Hainzl et al., 2009; Tsutsumi et al., 2009) to the middle domain (M-domain) - a binding site for many client proteins and co-chaperones (Fontana et al., 2002; Meyer et al., 2004; Retzlaff et al., 2010; Vaughan et al., 2006). Finally, the C-terminal dimerization domain (C-domain) possesses the MEEVD motif involved in interactions with co-chaperones via their TPR domains (Millson et al., 2008; Scheufler et al., 2000).

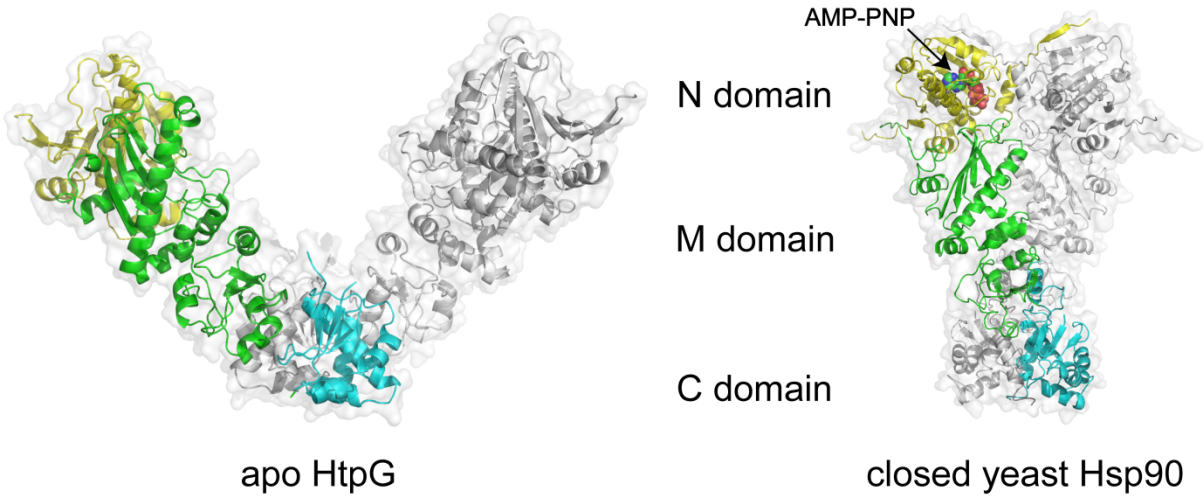

Figure 3. Hsp90 structures
Crystal structures of full length Hsp90 from *E. coli* (HtpG) in the open conformation (left, PDB 2IOQ) and nucleotide-bound yeast Hsp90 in the closed conformation (right, PDB 2CG9). The N-domain is depicted in yellow, the M-domain in green and the C-domain in blue.

Recently, crystal structures of both *Escherichia coli* (Huai et al., 2005; Shiau et al., 2006) and *Saccharomyces cerevisiae* (Ali et al., 2006) Hsp90s have been solved showing that different Hsp90 conformations exist and providing valuable snapshots of the conformational cycle (Figure 3). Not only the structural organization, but also the mechanism of the ATPase cycle, necessary for Hsp90 chaperone activity, is conserved (Richter et al., 2008). To define the molecular mechanism, a combination of various biophysical techiques has been applied. This allowed dissecting the ATPase cycle in detail and determining the rate-limiting steps (Figure 4) (Hessling et al., 2009; Mickler et al., 2009). In the apo state, Hsp90 is present predominantly in an open V-shaped conformation. Upon binding of ATP, a segment in the N-domain

called ATP-lid is repositioned and an N-terminal segment within the N-terminal domain is released. This accomplishes the formation of the first intermediate state (I1). Subsequent structural remodeling induces ATP-dependent dimerization of the N-domains and extensive intra-molecular contacts between the N- and the M-domains in a 'molecular clamp' mechanism. This conformational compaction defines the second intermediate state (I2). Subsequently, Hsp90 accommodates a closed catalytically active state. Here, R380 in the M-domain contacts the γ-phosphate of ATP and promotes catalysis. Concomitant hydrolysis of ATP triggers the dissociation of the N-domains and the products ADP, Pi are released. The return to its original open form completes the Hsp90 conformational cycle. Although this universal three-state conformational cycle is conserved among Hsp90 homologues, the intrinsic conformational equilibrium between various states can be highly species-dependent.

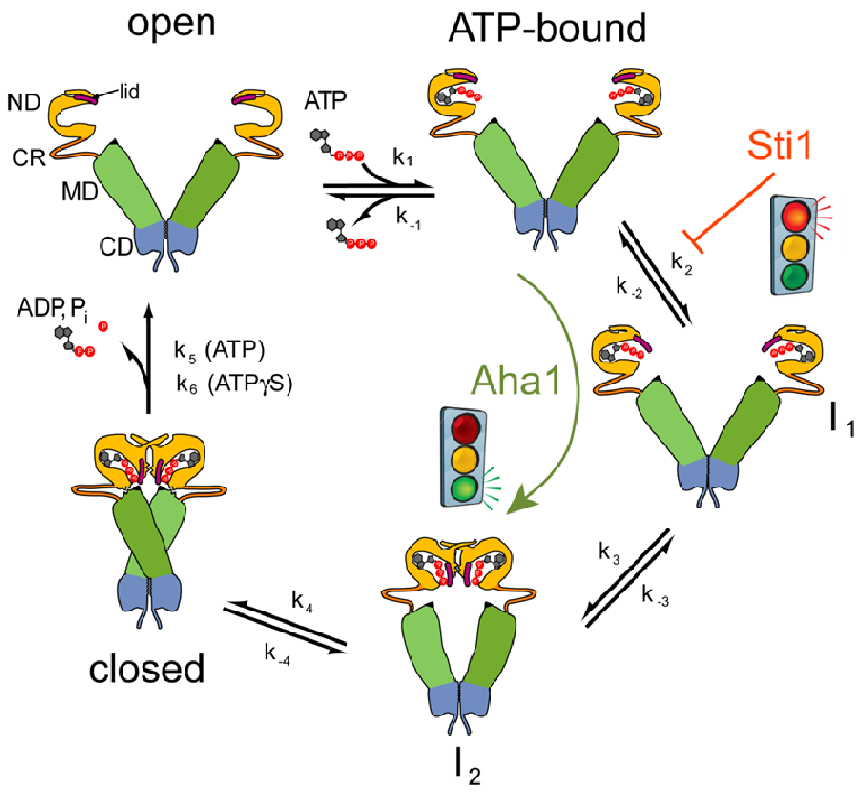

Figure 4. Conformational cycle of Hsp90
Binding of ATP induces conformational changes in Hsp90. First rearrangements in the N-domain take place. These involve repositioning of the N-domain segment and ATP-lid and lead to the formation of the first intermediate state (I1). Subsequent conformational transitions induce the N-terminal dimerization and association of the N-domains and the M-domains forming the second intermediate state (I2). Co-chaperones can modulate these structural changes. An inhibitor Hop/Sti1 locks Hsp90 in the open conformation. In contrast, the activator Aha1 promotes these rearrangements. It allows bypassing the I1 state and promotes formation of the I2 state thereby accelerating the conformational cycle.

Like other proteins belonging to so called the GHKL (gyrase–Hsp90–histidine kinase–MutL) ATPase family, Hsp90 is a 'split' ATPase that requires repositioning of motifs in both the M- and the N-domains to form the active ATPase site (Dutta and Inouye, 2000). Although Hsp90 chaperone function relies on the ATPase activity, the speed of the ATPase cycle, controlled by the conformational transitions, is slow. Importantly, all Hsp90 proteins can hydrolyze ATP but the hydrolysis rates significantly vary among different species. Hsp90 from yeast hydrolyzes one ATP molecule per 1-2 min (Panaretou et al., 1998; Scheibel et al., 1998). Grp94 has an ATP turnover rate comparable with or even higher than that of the cytosolic Hsp90 from yeast. The ATP hydrolysis by human Hsp90 is ten-fold slower than that of its yeast homologue, while HtpG and TRAP1 show an intermediate hydrolysis rates (Graf et al., 2009; McLaughlin et al., 2002; Richter et al., 2008; Frey et al., 2007; Leskovar et al., 2008). These differences arise from a higher conformational flexibility of yeast Hsp90 compared to its human or bacterial representatives.

The structural movements are not only restricted to nucleotide binding and can be detected also in the absence of nucleotide indicating that these rearrangements occur spontaneously. It has been proposed that Hsp90 fluctuates among different dynamic states and binding of ATP shifts this equilibrium towards more compact conformation (Mickler et al., 2009; Southworth and Agard, 2008). No structural data, however are available that would confirm whether these states are indeed structurally identical. Furthermore, analysis of the C-terminal dimerization revealed that the C- and the N-domains move in an anti-correlated way (Ratzke et al., 2010). Thus, communication between spatially distant regions within Hsp90 seems to play an important role in regulating the conformational cycle.

4.5 Hsp90 co-chaperones

Co-chaperones are important regulators of the Hsp90 conformational cycle and influence processing of client proteins. Up to date, over twenty co-chaperones have been identified to associate with eukaryotic Hsp90 in a conformation-specific manner and influence the chaperone cycle in various ways. Some can affect the ATPase cycle as activators or inhibitors, other specifically deliver clients to the Hsp90 folding machinery (Panaretou et al., 2002; Richter et al., 2003; Richter et al., 2004; Roe et

al., 2004). Co-chaperones themselves may additionally have chaperone activity. Overall, these accessory proteins provide directionality to the Hsp90 chaperone cycle. Based on their structural architecture, most of the co-chaperones fall into two distinct classes: those that possess TPR domains and those that do not. The tetratricopeptide (TPR) domain is a structural motif comprising a 34-amino acid degenerate sequence that forms two anti-parallel α helices separated by a turn (Figure 5) (Das et al., 1998). The TPR motifs pack in tandem arrays to form a structure with a superhelical groove, which associates with TPR acceptor modules (Scheufler et al., 2000). Hsp90 co-chaperones containing TPR domain are Hop/Sti1 (Johnson et al., 1998), protein phosphatase PP5/Ppt1 (Wandinger et al., 2006), members of peptidylprolylisomerase (PPIase) family including Fkbp52 (Riggs et al., 2003) and Fkbp51 (Nair et al., 1997), Cyp40 (Ratajczak and Carrello, 1996)/Cpr6 and Cpr7 (Mayr et al., 2000), myosin folding factor Unc45 (Barral et al., 2002) or CHIP (Pratt et al., 2010). Non-TPR-containing co-chaperones are Aha1, p23/Sba1 or Cdc37 (Ali et al., 2006; Retzlaff et al., 2010; Vaughan et al., 2006).

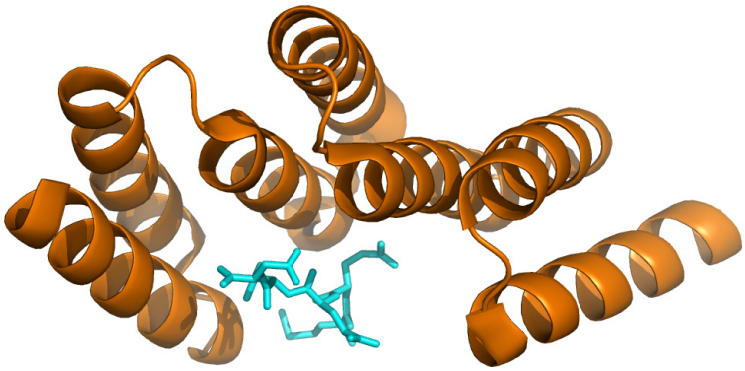

Figure 5. TPR domain architecture
TPR2A domain from Hop (orange) with the bound MEEVD peptide (blue) (PDB 1ELR).

4.5.1 Hop/Sti1

Hop/Sti1 serves as a non-competitive inhibitor of the Hsp90 ATPase activity (Figure 4) (Richter et al., 2003). It interacts with Hsp90 as a monomeric unit and stabilizes the open conformation of the dimeric Hsp90 (Li et al., 2011). Structurally, Hop/Sti1 is composed of three TPR domains. TPR1 binds to the EEVD motif in the C-terminus of Hsp70. The TPR2A domain associates with Hsp90, although recent studies revealed that multiple interaction sites between Hop/Sti1 and Hsp90 exist. The function of TPR2B is unknown (Brinker et al., 2002). Hop/Sti1 acts as a platform allowing simultaneous association of Hsp70 and Hsp90 and consequently transfer of client

proteins such as steroid hormone receptors (Wegele et al., 2006). In yeast, Hop/Sti1 is dispensable for viability, but causes synthetic lethality when knocked out with the Hsp40/Ydj1 or p23/Sba1 genes (Flom et al., 2006). The list of cellular functions of Hop/Sti1 is increasing. These include activation of progesterone receptor (Kosano et al., 1998) or phenotypic stability (mediated by a complex of Hop/Sti1, Hsp90 and the protein Piwi) (Gangaraju et al., 2011).

4.5.2 Cdc37

Another co-chaperone that is involved is client delivery and inhibits the ATPase activity of Hsp90 is Cdc37 (Vaughan et al., 2006; Gaiser et al., 2010). In the context of Hsp90 chaperone machinery, Cdc37 mediates recruitment of client kinases. Cdc37-kinase interaction is mediated via its N-terminal domain. Cdc37-Hsp90 interaction and the molecular mechanism of the Hsp90 ATPase arrest are now also known in structural details. The C-terminal region of Cdc37 binds between the N-domains of Hsp90 and interacts with the ATP-lid. This physically prevents the N-terminal dimerization of Hsp90 (Roe et al., 2004). Next, the insertion of the Cdc37 R167 side chain into the nucleotide binding pocket and the interaction with the catalytically important E33 of Hsp90 arrests ATP hydrolysis. It still remains unsolved how exactly the client kinase is transferred from Cdc37 to Hsp90 and whether this process requires any conformational transitions in the client protein. Since kinases control fundamental cellular processes, Cdc37 is absolutely essential for cell viability both in yeast (Gerber et al., 1995) and higher eukaryotic organisms, like Drosophila (Cutforth and Rubin, 1994) or Caenorhabditis elegans (Kamath et al., 2003). Moreover, Cdc37 displays Hsp90-independent activities and can function as a molecular chaperone on its own (Kimura et al., 1997). It has been also shown to directly interact with other components of Hsp90 chaperone machinery, including Hop/Sti1 (Abbas-Terki et al., 2002).

4.5.3 p23/Sba1

Unlike the two co-chaperones described above, p23/Sba1 is not associated with client protein transfer, but rather with its maturation process. Like Cdc37, p23/Sba1

possesses intrinsic chaperone activity mediated by its unstructured C-terminal tail (Weikl et al., 1999; Weaver et al., 2000). Binding of p23/Sba1 to Hsp90 is conformation-specific and occurs at the later stages of the conformational cycle when Hsp90 adopts the N-terminally dimerized closed form (Grenert et al., 1999). Structural studies revealed that the interaction involves predominantly the N-domain and, to minor extent, the M-domain of Hsp90 (Ali et al., 2006).

During the chaperone cycle p23/Sba1 appears to stabilize Hsp90-client complex (Morishima et al., 2003). A good example in this context is the maturation of steroid hormone receptors (Johnson and Toft, 1994; Smith et al., 1993). This process requires the stabilization of the N-terminal dimerization in Hsp90 by p23/Sba1, which locks Hsp90 in the closed conformation (Johnson and Toft, 1995). Structural studies showed that at the same time p23/Sba1 stabilizes the active conformation of the catalytic loop in the M-domain of Hsp90 (Ali et al., 2006). Thus, ATP is hydrolyzed, albeit slower. This explains why p23/Sba1 slows down ATP hydrolysis but not fully inhibits it. Return of Hsp90 to its open conformation induces p23/Sba1 dissociation and release of the client protein (McLaughlin et al., 2006; Obermann et al., 1998). Hence, p23/Sba1-mediated stabilization of Hsp90-client protein heterocomplex regulates the time a particular client is associated with Hsp90 (Morishima et al., 2003). Expression of p23/Sba1 is not required for cell survival and p23/Sba1 disruption in yeast has a modest effect on growth at both physiological and elevated temperature (Fang et al., 1998). In mice, p23/Sba1 is necessary for perinatal survival (Grad et al., 2006). p23/Sba1 has also additional function not related to Hsp90. p23/Sba1 was shown to modulate the activity of receptors in the nucleus and to participate in the disassembly of different transcription complexes allowing the cell to respond dynamically both to environmental stimuli and to intracellular needs on a transcriptional level (Freeman and Yamamoto, 2002; Echtenkamp et al., 2011).

4.5.4 Aha1

Co-chaperones can also accelerate Hsp90 ATP hydrolysis. This activation is mediated by Aha1. Structural studies revealed that both the M- and the N-domains of Hsp90 bind Aha1 (Lotz et al., 2003; Retzlaff et al., 2010). In the recently proposed asymmetric activation mechanism one Aha1 molecule fully stimulates the ATPase

activity of the dimeric Hsp90 (Retzlaff et al., 2010). Aha1 promotes conformational changes that result in the association of the N-domains and the formation of the closed state. Thus, Aha1 accelerates the progression of the ATPase cycle by bypassing the first intermediate I1 and helps to adopt I2 state (Figure 4) (Hessling et al., 2009). Although the Aha1 knockout is not deleterious, simultaneous deletion of the genes encoding Aha1 and its homolog Hch1 in yeast impaired activation of Hsp90-dependent clients (Lotz et al., 2003). Recent findings revealed a critical role of Aha1 in cystic fibrosis. Depletion of Aha1 can reverse defects in folding and trafficking of mutant cystic fibrosis transmembrane conductance regulator (CFTR) associated with cystic fibrosis (Wang et al., 2006). This suggests that Aha1 may be a potent therapeutic target for treatment of misfolding diseases.

4.5.5 Pp5/Ppt1

Interestingly, one of Hsp90's co-chaperones is the protein phosphatase Pp5/Ppt1. Ppt1 possesses a TPR domain which exhibits both regulatory and targeting functions (Andreeva and Kutuzov, 1999; Becker et al., 1994; Chen et al., 1996; Chinkers, 2001). Ppt1 is maintained inactive and the enzymatic activity is suppressed by the TPR domain stabilized by the C-terminal αJ domain, which together restrict access to the catalytic site (Figure 6) (Kang et al., 2001; Sinclair et al., 1999; Swingle et al., 2004). Binding to Hsp90 via the TPR domain activates the phosphatase. Ppt1 was shown to be associated with Hsp90 both *in vivo* and *in vitro* and to mediate dephosphorylation of Hsp90 and the co-chaperone Cdc37 (Vaughan et al., 2008; Wandinger et al., 2006). Ppt1 is present both in the cytoplasm and the nucleus, and thus may function in multiple subcellular compartments (Chen et al., 1994). Using genetic microarray studies in yeast it was shown that Ppt1 levels may be regulated depending on the environmental fluctuations (Gasch et al., 2000). Decreased phosphatase levels were detected under stress conditions such as metabolic, oxidative, osmotic and thermal stress, while Ppt1 expression was enhanced in cells approaching the stationary phase, cultivated in zinc-deficient medium or exposed to alpha factor.

Ppt1 is not essential for yeast viability and deletion of *ppt1* causes neither growth defects nor visible phenotype even under a variety of stress conditions (Chen et al.,

1994). However, in cells lacking Ppt1, decreased activation of Hsp90-specific clients was detected (Wandinger et al., 2006). This implies that the strict regulation of Hsp90 phosphorylation by Ppt1 is required for efficient processing of client proteins.

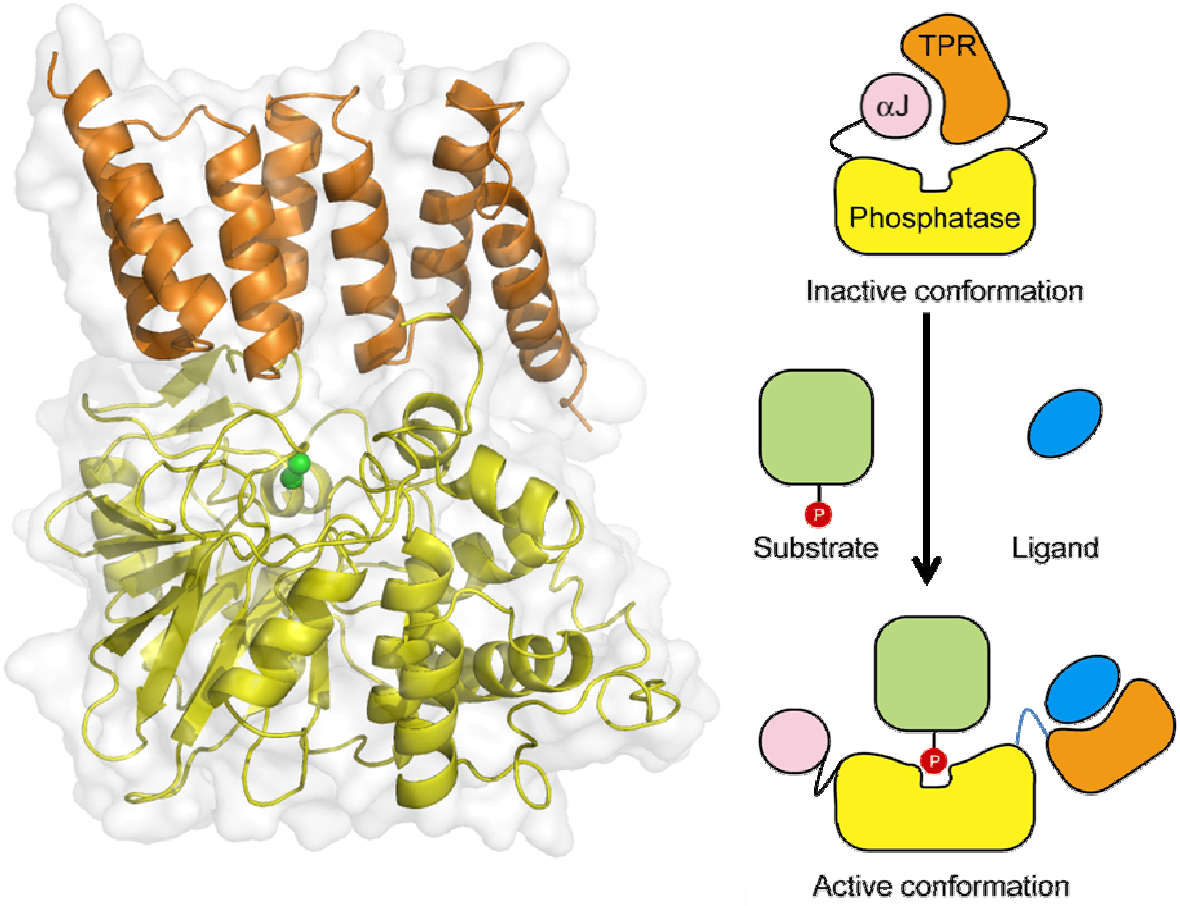

Figure 6. Structure of PP5 and the autoinhibition model
Crystal structure of PP5 in the inactive conformation (PDB 1WAO) (left panel). The TPR domain is depicted in orange and a phosphatase domain in yellow. Metal ions are highlighted in green. PP5 has low basal phosphatase activity due the autoinhibitory properties of its TPR and αJ domains (Sinclair et al., 1999). Binding of the TPR ligand exposes its catalytic center and substrate can be dephosphorylated (right panel).

4.5.6 Other co-chaperones

The list of Hsp90 co-chaperones is large and constantly growing, thus they will be further discussed only fragmentary. One group of co-chaperones are peptidylprolyl isomerases (PPIases) such as Fkbp51, Fkbp52, Cyp40 in mammals (Nair et al., 1997; Ratajczak and Carrello, 1996; Riggs et al., 2003) and Cpr6, Cpr7 in yeast (Mayr et al., 2000). PPIases catalyze the cis-trans interconversion of peptide bonds amino terminal to proline residues (Fanghanel and Fischer, 2004). In addition, they

possess a TPR domain, which anchors them to the C-terminus of Hsp90. Their role in the Hsp90 chaperone cycle is still to be determined. It is plausible that PPIases are recruited by specific clients. However, several studies indicate that their function goes beyond only loading of a client, as their incorporation into steroid hormone receptors takes place after the client is associated with Hsp90 (Smith et al., 1995; Smith and Toft, 2008). Another co-chaperone with the TPR domain is Sgt1. However, its binding to Hsp90 is somehow unusual. Although it contains a TPR domain, it associates to the N-terminal domain of Hsp90 via its CS domain (Kadota et al., 2008), which structurally resembles p23/Sba1. Unlike p23/Sba1, binding of Sgt1 does not affect the ATPase activity of Hsp90. Sgt1 and Hsp90 can form a ternary complex with the co-chaperone Rar1. This interaction is mediated via a CHORD domain of Rar1 (Zhang et al., 2010). Functionally, this heterocomplex modulates the innate immunity response in plants and mammals (Austin et al., 2002). Hsp90 also assembles in ternary complexes with the co-chaperones Tah1 and Pih1. Tah1 binds to Hsp90 with its TPR domain, while its C-terminus serves as the anchoring region for Pih1. The interaction with the Hsp90-Tah1 complex helps to stabilize the intrinsically unstable Pih1 (Zhao et al., 2008). While Tah1 alone is a weak activator of the Hsp90 ATPase activity, the Tah1-Pih1 complex inhibits the ATP hydrolysis of Hsp90 (Eckert et al., 2010; Millson et al., 2008). Thus, the effect of individual co-chaperones may depend on other components of the Hsp90 chaperone complex. Further specific Hsp90 functions are mediated by its association with certain co-chaperones, which include mitochondrial/chloroplast protein import (Tom70/Toc64) (Young et al., 2003; Qbadou et al., 2006), nuclear migration (NudC) (Zhu et al., 2010) or the aforementioned Hsp90/Hsp70-dependent protein degradation (CHIP).

The above examples show that co-chaperones provide a strict regulation of the Hsp90 chaperone cycle at different conformational stages and their large variety allows Hsp90 assisting various cellular processes.

4.6 The chaperone cycle of Hsp90

To promote maturation of client proteins, Hsp90 collaborates with a cohort of co-chaperones, which deliver clients and drive its conformational cycle (Riggs et al., 2003; Vaughan et al., 2006). The best studied example is the activation of steroid

hormone receptors (SHRs), which strongly depends on the Hsp90 chaperone machinery (Figure 7) (Picard et al., 1990; Smith et al., 1993). Activation of SHRs involves the formation of several distinct complexes comprising Hsp90 and different sets of co-chaperones in a multistep process. The progression of the cycle occurs in a sequential manner and ultimately leads to the release of a mature client. First, the unfolded substrate is recognized by Hsp70 and together with Hsp40 they form the 'early complex' (Cintron and Toft, 2006; Smith et al., 1992). The transfer of the client receptor from Hsp70 to Hsp90 occurs via the adaptor protein Hop/Sti1 in the 'intermediate complex' (Chen and Smith, 1998; Wegele et al., 2006). In the next stage, other co-chaperone components are recruited to the Hsp90 chaperone machinery, like PPIases and p23/Sba1 and the 'late complex' is formed (McLaughlin et al., 2006; Smith, 1993). Apparently a client protein is not required for these multi-protein complexes to be assembled.

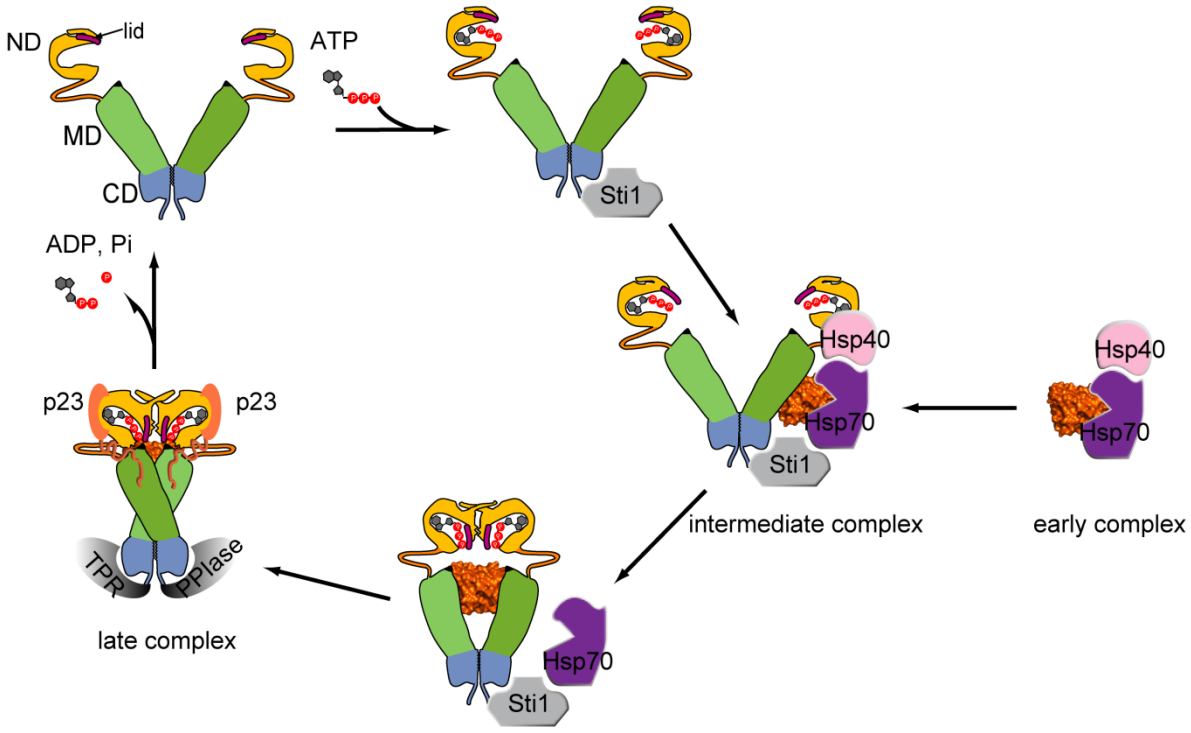

Figure 7. Hsp70-Hsp90 chaperone cycle
Hsp90 collaborates with the Hsp70 chaperone machinery in promoting maturation of client proteins. First, the client is bound in the early complex which involves Hsp70 and Hsp40. The client protein is transferred to the Hsp90 machinery via the adaptor protein Hop/Sti1 in the intermediate complex. Binding of ATP leads to conformational changes which induce Hop/Sti1 dissociation and promote recruitment of p23/Sba1. This leads to the formation of the late complex. Both in the intermediate and the late complex, Hsp90 can associate with PPIases or other TPR co-chaperones. Upon hydrolysis of ATP, p23/Sba1 and the folded client are released and Hsp90 returns to the open state which completes the chaperone cycle.

To uncover how the progression from one complex to another occurs, distinct biophysical methods have been applied (Li et al., 2011). This allowed dissecting a sequence of events during the chaperone cycle. Based on the results from previous studies, dimeric Hsp90 binds in its open conformation to one Hop/Sti1, which inhibits its ATPase activity. The second TPR-acceptor site is free and can anchor a PPIase forming an asymmetric Hsp90 intermediate complex. Binding of ATP induces conformational rearrangements that result in Hsp90 closure by dimerization of the N-domains followed by a recruitment of p23/Sba1. The structural transitions in Hsp90 weakens the association with Hop/Sti1 and results in its dissociation. This binding site can now be occupied by a PPIase or a TPR co-chaperone leading to the assembly of the final complex. Subsequent ATP hydrolysis triggers dissociation of p23/Sba1, PPIase and folding of the client protein is completed.

4.7 Posttranslational modifications of Hsp90

Hsp90 is subjected to a number of posttranslational modifications including phosphorylation, acetylation, nitrosylation, oxidation and ubiquitination that alter its chaperone activity in various ways. Transient posttranslational modifications can regulate Hsp90 functions by modifying its enzymatic activity, cellular location or dynamic interactions with other components of the chaperone cycle. This precise fine-tuning of Hsp90 permits adjusting its chaperone activity to cellular needs. Up to date, it was possible to map a number of modified sites and for some of them the mechanism of their action has been elucidated (Figure 8).

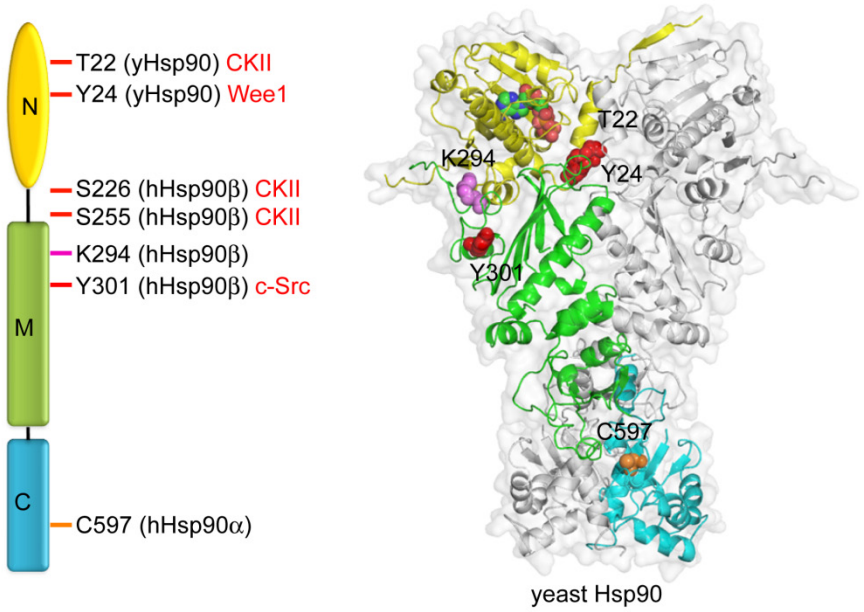

Figure 8. Posttranslational modifications of Hsp90
Hsp90 is modified by several posttranslational modifications including most prominent phosphorylation (red), acetylation (magenta) and nitrosylation (orange). Several functionally important modification sites throughout Hsp90 protein have been identified to influence its chaperone activity. The Hsp90 N-domain is depicted in yellow, the M-domain in green and the C-domain in blue. The numbering corresponds to yeast Hsp90, human Hsp90α or β, as indicated.

4.7.1 Phosphorylation

Hsp90 is most frequently modified by phosphorylation at multiple sites distributed throughout the dimeric protein. Serine residues are the major phospho-acceptor sites, though modifications of threonines and tyrosines were also reported (Scroggins and Neckers, 2007). Hsp90 phosphorylation levels are modulated by environmental conditions and the physiological state of the cell. Hsp90 phosphorylation appears to have also a species-specific pattern. Under heat stress, the turnover of Hsp90 phosphate groups is decreased in yeast and increased in HeLa cells (Legagneux et al., 1991; Mollapour et al., 2010b). Generally, hyper-phosphorylated Hsp90 interacts weaker with its client proteins and deletion of its specific phosphatase Ppt1 in *S. cerevisiae* leads to a reduced chaperone activity (Wandinger et al., 2006). Phosphorylation seems to be a general mechanism to down-regulate Hsp90 activity globally as maturation of different classes of clients such as kinases or SHRs was affected by this modification. Studies on the assembly of the C-terminal globular head of the reovirus attachment protein σ1 (Zhao et al., 2001) revealed that Hsp90 phosphorylation promotes a release of the chaperone from its client and therefore

dynamic phosphorylation/dephosphorylation is a mechanism that can modulate Hsp90-client interaction. Although most of the studies collectively demonstrated that phosphorylation negatively affects Hsp90 activity, recent reports suggest also stimulatory effects of Hsp90 phosphorylation. Phosphorylation of Hsp90β on Y301 by c-Src kinase enhances Hsp90 association with eNOS. This leads to an increased eNOS activity and promotes NO release from endothelial cells (Duval et al., 2007). Apoptotic processes also depend on Hsp90 phosphorylation (Kurokawa et al., 2008). In leukemic cells, constitutive phosphorylation of Hsp90β at S226 and S255 is suppressed. Dephosphorylated Hsp90 interacts stronger with apoptotic peptidase activating factor 1 (APAF1) and thus prevents cytochrome c-induced Apaf-1 oligomerization and apoptosome assembly.

In yeast, Hsp90 is phosphorylated at two important residues in the N-domain (Mollapour et al., 2010a; Mollapour et al., 2011b). Phosphorylation at Y24 was shown to be cell-cycle associated and to mediate Hsp90 translocation from the nucleus to the cytoplasm, where its polyubiquitination and subsequent degradation takes place. Hence, phosphorylation may be considered as a mechanism to regulate Hsp90 levels in a cell-cycle dependent fashion. The tyrosine kinase responsible for phosphorylating this tyrosine residue is Wee1/Swe1. Functionally, phosphorylation of Y24 affected the Hsp90 ATPase activity and its ability to chaperone a selected group of clients, comprised primarily of protein kinases. Another phosphorylation site identified in the N-domain is T22. Modification of this site diminished association with specific clients and co-chaperones, however over-expression of the co-chaperone Aha1 could correct these defects. Since both phospho-sites are important determinants of Hsp90 drug sensitivity, these observations might provide novel strategies to increase drug sensitivity (Mollapour et al., 2011a).

Cellular secretion of Hsp90 is controlled by phosphorylation. Here, modification of T90 in Hsp90α by protein kinase A (PKA) plays an important role. This finding has a particular importance as Hsp90 secretion is involved in wound healing and is correlated with cancer metastasis (Eustace et al., 2004; Li et al., 2007). Furthermore, isoform-specific Hsp90 phospho-species exist. DNA-dependent protein kinase (DNA-PK) mediates phosphorylation of Hsp90α at two unique threonine residues (T5 and T7), which are not present in the β isoform (Lees-Miller and Anderson, 1989a).

Similarly, non-ubiquitous calmodulin kinase Pnck phosphorylates Hsp90α in an isoform-specific way (Deb et al., 2011).

Distinct Hsp90 functions can be altered by phosphorylation. These include binding to co-chaperones and client proteins, translocation, degradation etc. The examples described here indicate that phosphorylation may act as a modulator of the conformational cycle. Interestingly, Hsp90 is responsible for activation of many kinases that in turn phosphorylate this chaperone, including CKII, Wee1/Swe1, Src, Raf1 or Cdk4 (Miyata, 2009; Mollapour et al., 2010a) which could serve as a feedback loop to regulate the phosphorylation status of Hsp90.

4.7.2 Acetylation

Hsp90 can be also modified by acetylation which is the second, most commonly occurring modification, after phosphorylation. First reports on Hsp90 acetylation came from studies performed by Yu and co-workers who found that specific inhibition of HDAC deacetylase activity caused Hsp90 hyper-acetylation and consequently affected ATP binding and destabilized interaction with several client proteins including key oncogenic proteins (Bali et al., 2005; de Zoeten et al., 2011; Kovacs et al., 2005). Although numerous studies focused on the effects of HADC6 inhibition, other HDACs can target Hsp90 in different cellular compartments. For instance, HDAC1 acts on Hsp90 in the nucleus (Zhou et al., 2008). Several Hsp90 lysine residues were identified to be modified by acetylation in human cells. Their substitutions with glutamine impaired association with co-chaperones, negatively affected ATPase activity and chaperoning action *in vivo*. Thus, hyper-acetylation leads to loss of Hsp90 protective function in the cell.

Neckers and colleagues identified one Hsp90 acetylation site and determined its relevance using a mutagenesis approach *in vivo* and *in vitro*. Their study demonstrated that the acetylation state of K294 (hHsp90α) is a key regulator of Hsp90 function both in yeast and man with consequence for co-chaperone binding and maturation of client proteins (Scroggins et al., 2007). Importantly, these studies revealed a connection between Hsp90 acetylation and various cellular processes like cell signaling or nuclear transport suggesting a general role of this modification.

4.7.3 Nitrosylation

NO-mediated S-nitrosylation of Hsp90 has also been observed. Hsp90 is modified at C597 in human Hsp90α causing an inhibition of the ATPase activity and a decrease in its chaperone function. Furthermore, Hsp90 nitrosylation was correlated with a reduced association with eNOS in endothelial cells (Garcia-Cardena et al., 1998; Martinez-Ruiz et al., 2005). In a current model, S-nitrosylation decreases Hsp90 chaperone capacity and provides a feedback mechanism to inhibit further activation of eNOS. Retzlaff and colleagues (Retzlaff et al., 2009) investigated the molecular mechanism of C597 modification and showed that this cysteine residue located in a conformational switch region propagates inter-domain communication between the N- and the C-domain in the Hsp90 dimer.

4.7.4 Oxidation

Hsp90 has been shown to be modified under oxidative stress conditions, which induce formation of reactive oxygen species and decrease the intracellular glutathione pool. Ultimately, this resulted in thiol oxidation of Hsp90 and enhanced degradation of Hsp90-dependent clients, such as Raf1, Cdk4 or Akt1 implying that under oxidative stress, the Hsp90 chaperone function is impaired (Chen et al., 2008). Oxidative stress also caused lipid peroxidation, promoting the formation of thiol-reactive aldehydes that modified Hsp90 at cysteine residues. Functionally, Hsp90 oxidation negatively affected refolding of client proteins (Carbone et al., 2004; Carbone et al., 2005).

4.7.5 Ubiquitination

Ubiquitination is another posttranslational modification that is linked to Hsp90 function. Increased Hsp90 ubiquitination has been observed after photodynamic signal transduction inhibitor hypericin treatment (Blank et al., 2003). This inhibited Hsp90 chaperone function and induced increased degradation of Hsp90-specific clients. A recent study from Neckers and colleagues demonstrated that Swe1-mediated phosphorylation of Hsp90 promotes its ubiquitination and targets Hsp90 for

degradation (Mollapour et al., 2010a). This is a good example, when different posttranslational modifications act in a cooperative manner.

5 Objectives

The primary objective of this work was to identify *in vivo* phosphorylation sites in yeast Hsp90 and assess a specific function of the phosphatase Ppt1. This should be achieved by applying a combination of SILAC and MS analysis. In the next step, phospho-mimicking mutants would be engineered to test their effects both *in vivo* and *in vitro* using various biophysical methods and determine their mechanisms of action.

Hsp90 has been known as a phospho-protein and numerous phosphorylation sites for human Hsp90 have been identified so far (Lees-Miller and Anderson, 1989a; Lees-Miller and Anderson, 1989b). However, little is known about yeast Hsp90 phosphorylation. It had been shown that Hsp90 has its own phosphatase, Ppt1, and its deletion leads to down-regulation of Hsp90-dependent client maturation (Wandinger et al., 2006). In this context, two important phosphorylation sites in the N-domain (T22 and Y24) of yeast Hsp90 have been identified recently (Mollapour et al., 2010a; Mollapour et al., 2011b). Though, how Hsp90 is globally regulated by phosphorylation in yeast was not clear. Understanding the molecular mechanisms of phospho-regulation would add new insight into this complex chaperone machinery. To identify Hsp90 phosphorylation sites and their regulation by Ppt1 *in vivo*, a combination of SILAC and MS approaches should be applied in collaboration with Dr. Henrik Daub from the MPI of Biochemistry in Martinsried. This strategy should allow confident phospho-peptide identification, phospho-site localization and enable quantitative comparisons. In the next step, the MS analysis should be applied to test the phosphorylation sites in human HeLa cell line in order to compare the Hsp90 phosphorylation pattern in different organisms. These experiments would help to understand whether, despite its highly conserved protein sequence, Hsp90 phospho-regulation has universal or species-specific nature.

To determine the role of the identified phosphorylation sites, the identified phospho-sites were replaced by alanines (the mimic of the dephosphorylated state) or glutamates (the mimic of a constitutively phosphorylated state). To test for *in vivo* effects, the phospho-variants should be expressed in yeast as the sole Hsp90 and their influence on the maturation of model Hsp90 clients, Hsp90 inhibition or DNA damage response was to be tested. Determination of the molecular mechanisms was

possible by applying a number of biophysical techniques such as FRET, aUC, or standard protein analysis methods such as CD, cross-linking or ATPase assays. Together, the experiments aimed at answering the question how phosphorylation affects the enzymatic and chaperone activity of Hsp90, its conformation and the interaction and regulation by co-chaperones. This should allow elucidating molecular mechanisms underlying phospho-regulation and assign a specific role for Ppt1.

6 Results

6.1 Analysis of yeast Hsp90 phosphorylation

6.1.1 Identification of Hsp90 phosphorylation sites

To analyze *in vivo* phosphorylation sites of yeast Hsp90, a proteomics approach based on stable isotope labeling with amino acids in cell culture (SILAC) was applied (Cox and Mann, 2008). Hsp90 was immunoprecipitated, trypsin-digested and enriched phospho-peptides were analyzed by LC-MS on a high-resolution linear ion trap-orbitrap (LTQ-Orbitrap) hybrid mass spectrometer (Figure 9).

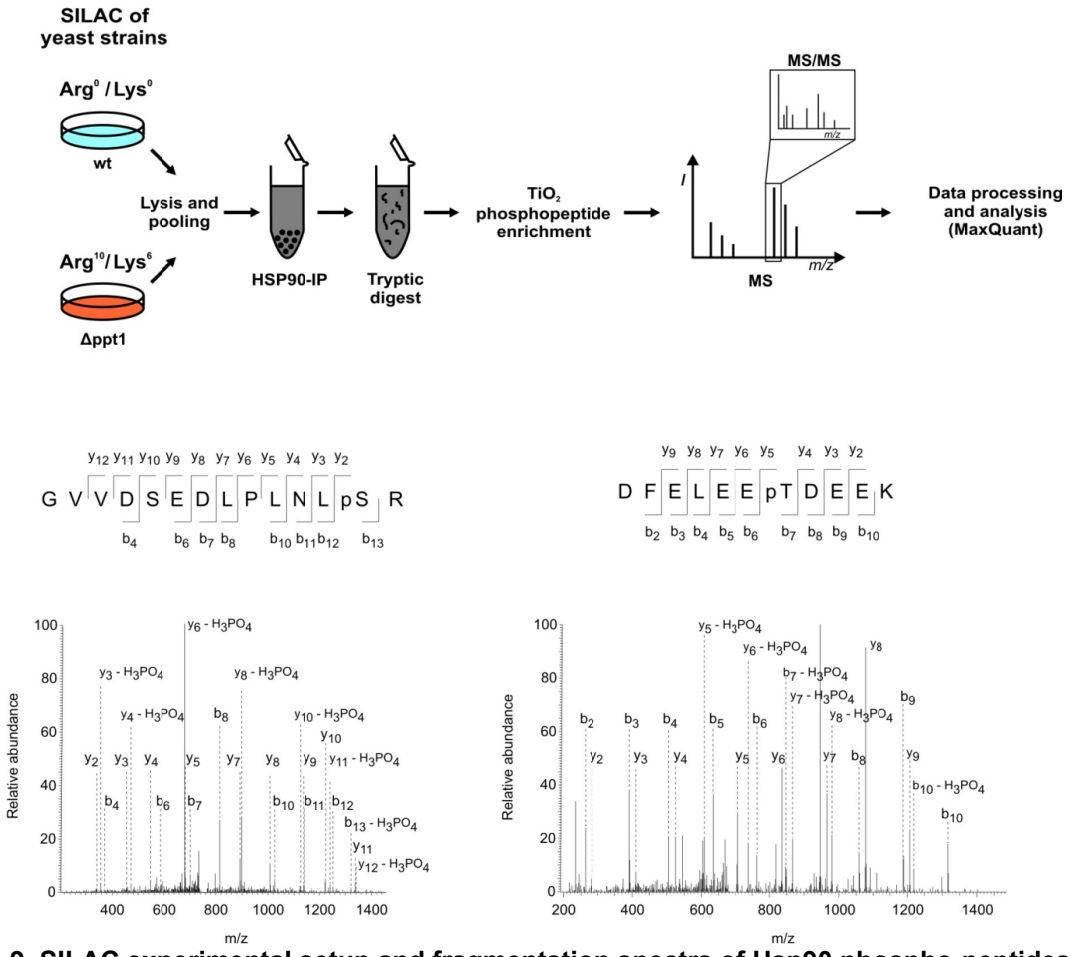

Figure 9. SILAC experimental setup and fragmentation spectra of Hsp90 phospho-peptides
Schematic presentation of a SILAC experiment including sample preparation and MS analysis (upper panel). Fragmentation spectra of the identified Hsp90 phospho-peptides GVVDSEDLPLNLpSR and DFELEEpTDEEK harboring the phosphorylation sites S379 and T533, respectively. The numbering of phosphorylated residues in Hsp82 is used (lower panel) (kindly provided by Dr. H. Daub).

All sites were found on singly phosphorylated peptides shared by the two yeast Hsp90 variants Hsp82 and Hsc82. As an example, fragmentation spectra of peptides harboring the phosphorylation sites S379 and T533 are shown in Figure 9. In several SILAC screens in total ten different phosphorylation sites (S282, S297, S334, S379, S450, S456, S485, T533, S602, S604) were identified which were distributed in the M- and the C-domain (Figure 10), consistent with recent phospho-proteomic studies (Albuquerque et al., 2008; Holt et al., 2009).

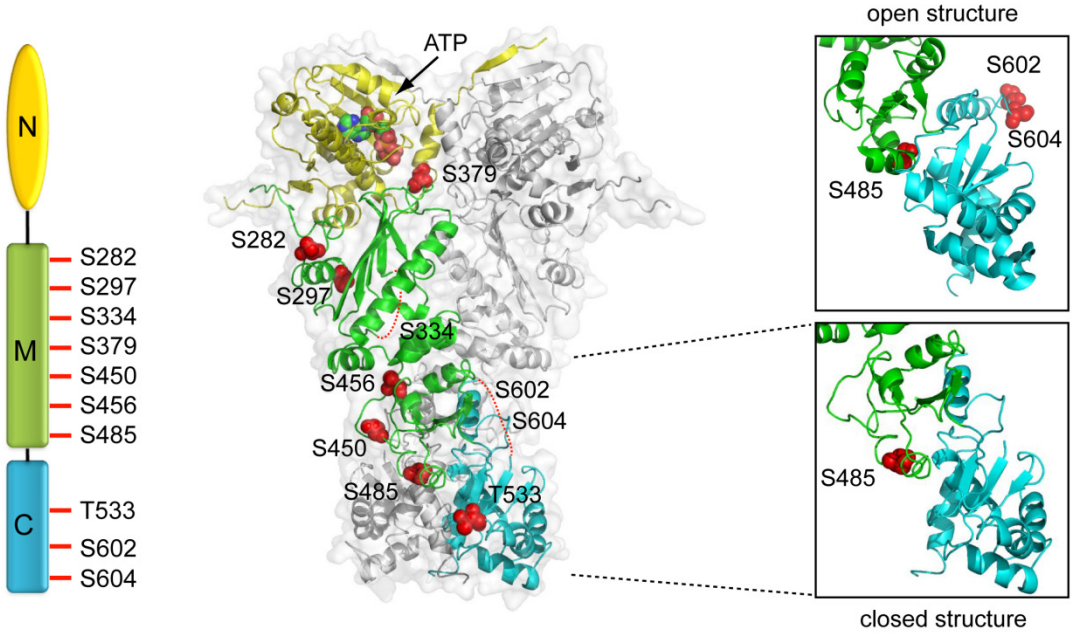

Figure 10. Identification of yeast Hsp90 phosphorylation sites
Schematic domain organization of Hsp90 indicating the identified phosphorylation sites in the structure of yeast Hsp90 in the closed conformation (Ali et al., 2006) (PDB 2CG9). In the two boxes on the right a segment of Hsp90 is shown in the open and closed conformation, respectively. The open structure is from the yeast M-C domain crystal structure (PDB 2CGE). The phosphorylation sites are marked in red.

In yeast, the Ser/Thr phosphatase Ppt1 is physically associated with Hsp90 and mediates its dephosphorylation *in vivo* (Wandinger et al., 2006). To identify the Hsp90 phosphorylation sites specifically regulated by Ppt1, Hsp90 phosphorylation patterns in wt and *ppt1*-deletion yeast cells after SILAC treatment were compared. With this approach, a marked increase in the phosphorylation of S485 and S604 in Ppt1-deficient yeast cells was observed demonstrating that these two residues in the M- and the C-domain are regulated by Ppt1 *in vivo* (Table 1).

Hsp90 phospho-site	Exp.1 ration *Δppt1*/wt yeast	Exp.2 ration *Δppt1*/wt yeast	Exp.3 ration *Δppt1*/wt yeast	Exp.4 ration *Δppt1*/wt yeast	Average ration *Δppt1*/wt yeast
S282	1.25	1.23	1.33	1.27	1.27 ± 0.05
S297	1.50	1.09		1.26	1.28 ± 0.21
S334	1.07	1.77			1.42 ± 0.49
S379	1.24		1.18	1.03	1.15 ± 0.11
S450	1.53		1.29	0.98	1.26 ± 0.27
S456	1.13	1.49		0.96	1.20 ± 0.27
S485	2.81	2.95	5.34	4.71	3.95 ± 1.27
T533	n.d.				
S602	n.d.				
S604	1.90	3.16	10.54	9.98	6.39 ± 4.50

Table 1. Quantitative analysis of yeast Hsp90 phosphorylation sites
MS identification of Hsp90 phospho-sites and SILAC-based quantification in wt versus Ppt1-deficient yeast cells. In experiments 1 and 3 wt cells were labeled with Arg^0/Lys^0 and Δ*ppt1* cells were encoded with Arg^{10}/Lys^8, whereas a reciprocal SILAC scheme was used in experiments 2 and 4. The ratios shown represent the respective phospho-site ratios normalized for Hsp90 protein abundance.

6.1.2 Conservation of Hsp90 phospho-regulation

Hsp90 was phosphorylated predominantly on serine residues and only one threonine was found to be a phospho-acceptor site in this study. A comparison of Hsp90 sequences from different species shows a strong conservation of the identified amino acids or a replacement by negatively charged 'phospho-mimetic' residues (Figure 11).

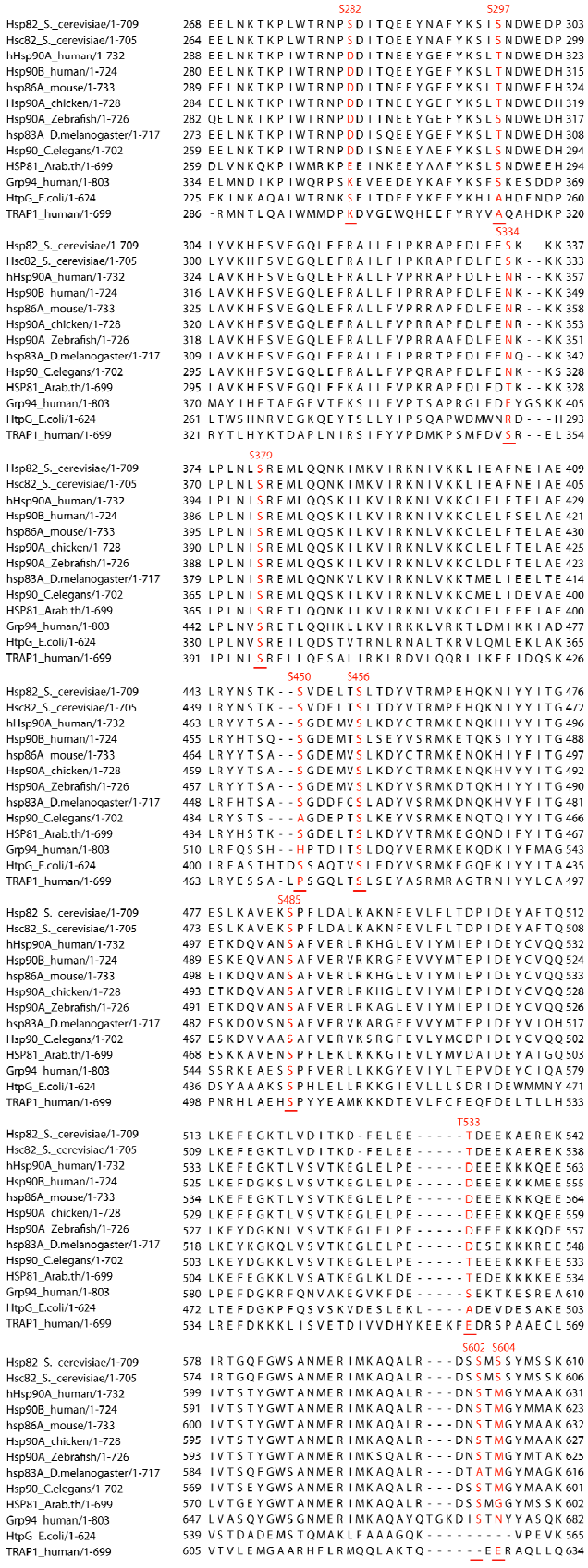

Figure 11. Sequence alignment of Hsp90 homologues
Alignment of representatives of Hsp90 showing identified Hsp90 phosphorylation sites with the respective position in yeast Hsp90 highlighted in red.

Intriguingly, unlike in yeast Hsp90, the majority of the phospho-sites known for human Hsp90 are located in the N–domain and the linker region (Lees-Miller and Anderson, 1989a; Lees-Miller and Anderson, 1989b; Lei et al., 2007; Ogiso et al., 2004; Rose et al., 1987). Of note, human and yeast Hsp90s share over 60% of sequence identity. To interrogate whether the identified phosphorylation sites are conserved between man and yeast, phosphorylation of human Hsp90 was tested in HeLa cells using mass spectrometry (Table 2). These experiments revealed two phosphorylation sites shared between both human isoforms (S226, S255 and S231, S263 in human Hsp90β and α, respectively), previously reported in the literature (Figure 8) (Kurokawa et al., 2008; Lees-Miller and Anderson, 1989b). Importantly, none of these two sites was detected at the corresponding positions in yeast Hsp90. Of note, this analysis was limited to one human cell line and one growth condition only. Since phosphorylation can be cell-type-dependent and different cells may harbor unique Hsp90 phosphorylation sites, a detailed investigation of other large-scale phospho-proteomic studies was performed. This revealed that these two sites identified in HeLa cells were present in all studies analyzed indicating their general function. Further literature inspection showed that out of all phospho-sites identified in human Hsp90 only two sites S297 and S379 (T317/T309 and S399/S391 in human Hsp90α/Hsp90β, respectively) were reported to be common phospho-sites. Thus, the Hsp90 phosphorylation pattern in yeast and man is not conserved.

6.1.3 Regulation of Hsp90 phosphorylation by CKII

The notion of rather different phosphorylation characteristics of yeast and human Hsp90 was further reinforced by distinct *in vitro* phosphorylation patterns, which were recorded in MS analysis of recombinant proteins phosphorylated by CKII. To this point, Hsp90 from man and yeast were phosphorylated *in vitro* using CKII in the presence of ATP and the proteins were subjected to MS analysis. To monitor phosphate incorporation radioactively labeled ATP was used (Figure 12). For yeast Hsp90, sites were detected predominantly in the M- and the C-domain consistent with the *in vivo* inspection (Table 2). The majority of the Hsp90 sites identified by SILAC screens could be phosphorylated by CKII *in vitro* suggesting that CKII is a potential kinase regulating Hsp90 phosphorylation status in yeast. Nevertheless, a few sites remain (S297, S450, T533), which may be targeted by different kinases.

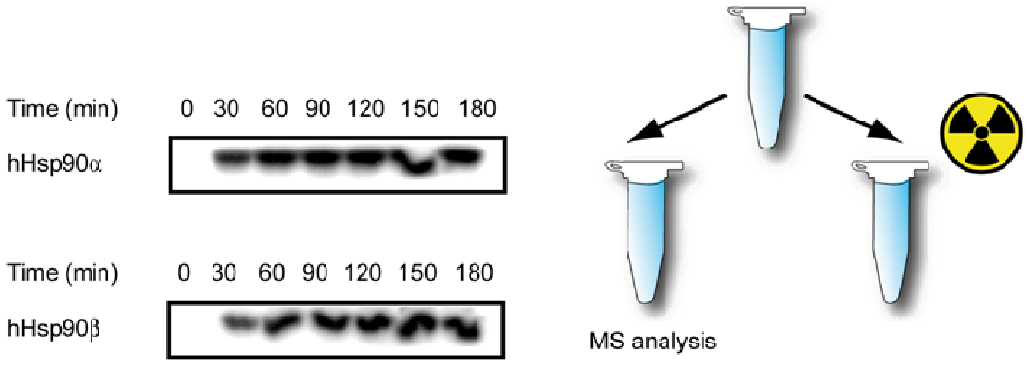

Figure 12. *In vitro* phosphorylation of human Hsp90 α and β by CKII
Both human Hsp90 isoforms were phosphorylated *in vitro* by CKII. To visualize phosphate incorporation, radioactively labeled ATP was used and samples were analyzed by autoradiography. The same experiment was performed in the presence of non-radioactively labeled ATP and these samples were used for MS analysis and phospho-site detection.

Yeast Hsp90		Human Hsp90				Proteomic studies	
in vivo	*in vitro*	*in vivo* HeLa		*in vitro*			
		α	β	α	β	α	β
	S36	S231	S226	S231	S226	T5	S45
	T95	S263	S255	S263	S255	T7	S48
S282	S282			S453	S445	Y61	Y56
	Y293			T624	S615	S63	S58
S297	S295					T88	T89
S334	S334					T90	Y192
S379	S379					Y197	S226
S450	S411					S231	S255
S456	S456					S252	S261
	Y472					S263	Y276
	S478					Y284	T285
S485	S485					T293	T297
T533	S586					Y313	Y301
	S601					S315	Y305
S602	S602					T317	S307
S604	S604					S391	T309
	S605					S399	S391
	Y606					S453	S445
	S608					Y466	S452
						Y492	S482
						Y493	Y484
						T566	Y485
						S589	Y520
						Y604	S532
						T624	Y596
						Y627	Y619
						Y689	S718
						S726	

Table 2. Summary of yeast and human Hsp90 phosphorylation sites
Human Hsp90 phosphorylation according to the PhosphoSitePlus database (kindly provided by Dr. H. Daub).

In vitro phosphorylation analysis of human Hsp90s revealed that only one site (S615 in human Hsp90β corresponding to S602 in yeast) was common in both organisms. In summary, this data confirmed the notion that yeast and human Hsp90 proteins are differentially targeted by phosphorylation.

6.1.4 Quantitative analysis of Hsp90 phosphorylation in yeast

To estimate which fraction of total Hsp90 phosphorylation in yeast the ten identified sites represent, 2D gel electrophoresis was exploited. All ten sites were simultaneously substituted by alanines or glutamates (All-A10 and All-E10 Hsp90, respectively). These two Hsp90 variants were expressed in yeast and tested for their *in vivo* function. The mutant Hsp90s were introduced in a yeast strain in which both genomic *hsp90* isoforms were replaced by a plasmid-borne form of Hsp90 (Nathan and Lindquist, 1995). Expression of the All-E10 mutant caused lethality, whereas cells expressing All-A10 were viable (data not shown and Figure 13A and B).

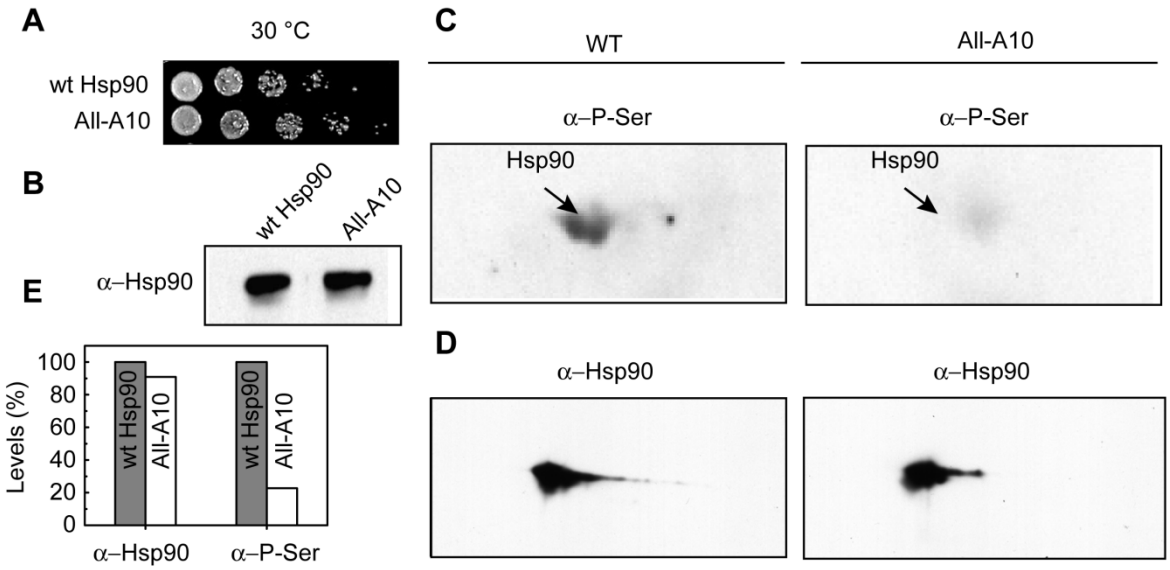

Figure 13. Quantitative analysis of yeast Hsp90 phosphorylation
(A) Growth of wt and All-A10 Hsp90-expressing yeast cells at 30 °C. **(B)** Immunoblot analysis of Hsp90 levels in yeast cells expressing only wt or All-A10 Hsp90. **(C-D)** Hsp90 protein levels and Hsp90 phosphorylation levels in wt and All-A10 Hsp90-expressing yeast cells. The proteins were separated on 2D gels and detected by Hsp90- and phospho-serine-specific antibodies. **(E)** The signal intensity of the spots was quantified using ImageJ and the data are displayed as a percentage of the wt cell.

Inspection of Hsp90 protein and phosphorylation levels in wt versus All-A10-expressing cells revealed several important details. While protein levels were unchanged, blotting with a phospho-serine-specific antibody demonstrated strongly

reduced phosphorylation in All-A10 compared to the wt cells (Figure 13C-E). Unlike in cells carrying All-A10 Hsp90, in wt yeast several phosphorylated Hsp90 isoforms were observed (Figure 13D). These data reveals that the ten phosphorylation sites identified by MS screens constitute a predominant fraction of Hsp90 phosphorylation occurring in yeast.

6.2 Analysis of globally phospho-mimicking Hsp90 variants

6.2.1 Thermotolerance and chaperone function *in vivo*

Having identified various phosphorylation sites in yeast Hsp90, eight out of the ten identified amino acids (S282, S297, S379, S450, S456, T533, S602, S604) were simultaneously replaced by alanines (All-A8) or glutamates (All-E8) to mimic the globally unphosphorylated and phosphorylated state of Hsp90, respectively. This phospho-site selection was based on the finding that phosphorylation of S334 was detected in only one experiment and therefore not included in further analysis and the mutation S485E was lethal.

The All-A8 and All-E8 mutants were viable at 30 °C showing that they support the essential function of Hsp90 (Figure 14A). To further investigate the role of the mutant proteins, cell growth at higher temperatures was monitored (Figure 14A and B). Cells expressing wt Hsp90 grew up to 39.5 °C. All-A8 and All-E8 Hsp90 showed a slightly decreased maximum growth temperature. Furthermore, All-E8 grew poorly over the entire temperature range. Yeast cells harboring the All-E8 mutation of Hsp90 exhibited a rough cell surface in comparison to the rather smooth surface of wt Hsp90 and All-A8-expressing cells (Figure 14D). Notably, Hsp90 protein levels were comparable for wt and the variants (Figure 14C).

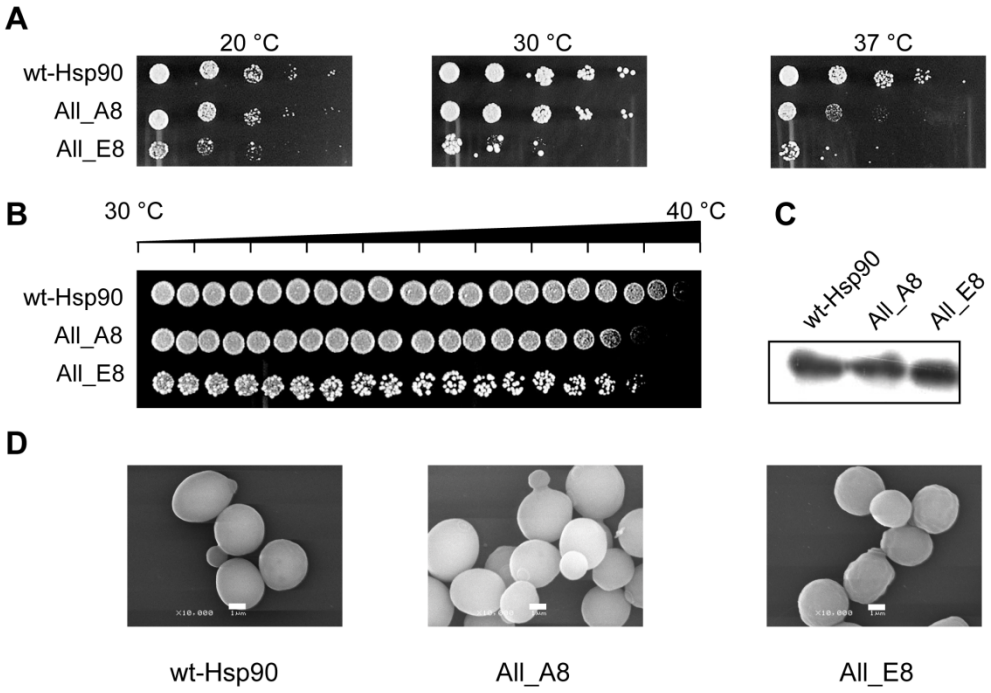

Figure 14. Effects of All-A8 and All-E8 mutations on yeast Hsp90 functions *in vivo*
(A) Wt, All-A8 or All-E8 Hsp90-expressing yeast cells were grown at 30 °C. Cultures were adjusted to the same cell density (10^7 cells/mL), spotted in 5-fold serial dilutions and incubated for 2 days at the indicated temperatures. **(B)** Yeast strains with both genomic copies of *hsp90* deleted but carrying either wt, All-A8 or All-E8 yeast Hsp90 variants were tested for their temperature-sensitive phenotypes. Cells adjusted to the same cell density (10^7 cells/mL) were spotted on selective media and incubated for 30 h in a temperature gradient. **(C)** Immunoblot analysis of yeast cells expressing wt, All-A8 or All-E8 Hsp90 variants as the sole Hsp90. Yeast cells were grown at 30 °C. Cell lysates were tested for Hsp90 expression using a rabbit anit-Hsp90 antiserum. **(D)** Scanning electron micrographic images of wt, All-A8 or All-E8 Hsp90-expressing yeast cells incubated at 30 °C (scale bar, 1 µm).

6.2.2 Client protein maturation *in vivo*

In addition to the general effects of Hsp90 on the viability of yeast cells, the effect on specific Hsp90 client proteins was examined *in vivo*. These included firefly luciferase (FFL) (Nathan et al., 1997), glucocorticoid receptor (GR) (Pratt et al., 1996) and viral Src kinase (v-Src kinase) (Nathan and Lindquist, 1995) (Figure 15). Yeast cells expressing either wt, All-A8 or All-E8 were transformed with a plasmid for expression of the respective client gene. In cells expressing All-E8, FFL activity was reduced to ~ 75% of the wt activity. No changes in FFL activity were detected for cells expressing All-A8 Hsp90. To test GR activity, a hormone-dependent reporter assay was used (Nathan and Lindquist, 1995). Expression of All-E8, but not All-A8, resulted in a markedly decreased GR activity of ~ 50% showing that All-E8 is impaired in

maintaining the receptor in a transcriptionally competent state. v-Src activity, as detected with an antibody specific for phospho-tyrosines, was comparable in the wt and All-A8 Hsp90 strains, but it was reduced to ~ 20% in All-E8. Moreover, in sharp contrast to wt or All-A8 yeast cells, expression of v-Src did not cause lethality in All-E8-expressing yeast. To test if All-E8 Hsp90 impairs general protein folding processes, maturation of the green fluorescent protein (eGFP), whose folding is Hsp90-independent (Coxon and Bestor, 1995; Wandinger et al., 2006), was analyzed. eGFP activity was unaltered in All-A8 and All-E8-expressing cells confirming that the decreased activation of the client proteins in the presence of All-E8 is specific to changes in Hsp90 potential. Thus, phospho-mimicking mutations negatively regulate Hsp90 chaperone activity *in vivo*.

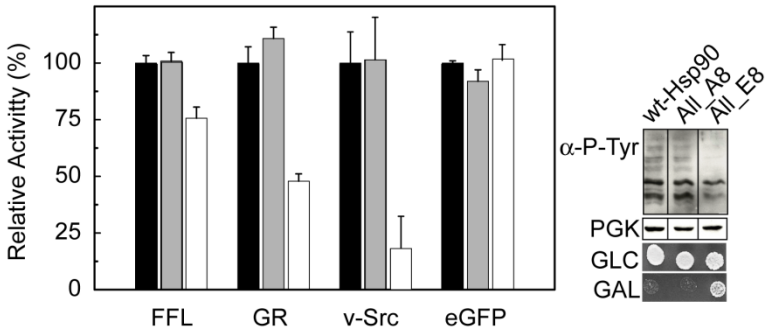

Figure 15. Client protein maturation of globally phospho-mimicking mutants
Processing of Hsp90-specific substrates by wt (black bars) All-A8 (gray bars) and All-E8 (white bars) Hsp90 variants expressed in yeast. These yeast cells were co-transformed with plasmids for the constitutive expression of FFL, GR, galactose-inducible expression of v-Src or eGFP as a control. The phosphorylation activity of v-Src was analyzed by Western blot with a phospho-tyrosine antibody (4G10). As a control, PGK was used. Yeast cells expressing v-Src under the control of the galactose promoter were spotted on glucose or galactose-containing selective media.

6.2.3 ATPase activity and modulation by co-chaperones

The modified client protein maturation described above suggests that the phospho-mimetic mutations influence the structural and/or biochemical properties of Hsp90. To test these, the All-A8 and All-E8 proteins were recombinantly expressed in *E. coli* and purified. CD spectroscopy revealed that their secondary and tertiary structures, as well as the stability of the proteins are identical to wt Hsp90 (Figure 16, Table 3 and data not shown). Furthermore, both variants formed functional dimers, as probed by SEC-HPLC and analytical ultracentrifugation (aUC) (data not shown).

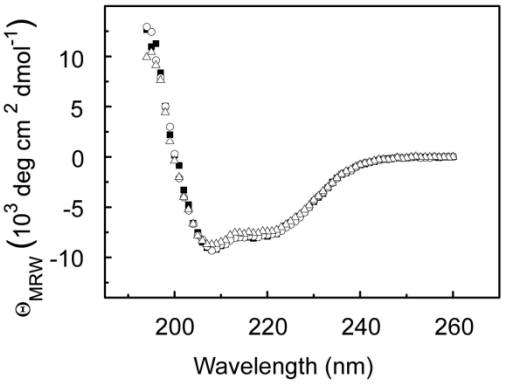

Figure 16. Far-UV CD Spectra of Hsp90 phospho-mutants
CD spectra of 0.1 mg/mL wt (■), All-A8 (∇) and All-E8 (○) were recorded at 30 °C in 5 mM sodium phosphate buffer, pH 7.5.

	Melting Temperature (°C)
wt Hsp90	65 ± 0.4
All-A8	62 ± 0.5
All-E8	68 ± 0.8

Table 3. Melting Temperatures of wt, All-A8 and All-E8 Hsp90 variants
Temperature transition of 0.1 mg/mL Hsp90 variants was monitored at wavelength 205 nm in 5 mM sodium phosphate buffer, pH 7.5. To determine the transition midpoints the forward transitions were fit to a Bolzmann equation.

Since the ATPase activity of Hsp90 can be regulated by posttranslational modifications (Mollapour et al., 2010a; Mollapour et al., 2011b; Retzlaff et al., 2009), the effect of the phospho-mimicking mutations on the catalytic activity of Hsp90 was determined (Table 4). All-A8 had an ATPase activity corresponding to that of the wt protein. However, All-E8 showed a decreased turnover rate of 0.22 min^{-1}. The apparent K_M values for ATP were not altered, indicating that nucleotide binding is not regulated by phosphorylation states.

ATPase Activity		
Construct	k_{cat} at 30 °C (min^{-1})	K_M at 30 °C (µM)
wt Hsp90	0.55 ± 0.03	373 ± 24
All-A10	0.20 ± 0.01	320 ± 93
All-A8	0.47 ± 0.06	308 ± 39
All-E8	0.22 ± 0.03	324 ± 49
S282E	0.52 ± 0.12	350 ± 40
S297E	0.69 ± 0.12	323 ± 67
S334E	0.56 ± 0.04	312 ± 52
S379E	0.19 ± 0.03	325 ±61
S450E	0.55 ± 0.12	353 ± 20
S456E	0.51 ± 0.12	408 ± 57
S485E	0.24 ± 0.06	345 ± 99
S485Y	0.22 ± 0.10	347 ± 57
S485A	0.22 ± 0.09	370 ± 85
T533E	0.47 ± 0.09	398 ± 10
S602E	0.28 ± 0.03	377 ± 46
S604E	0.35 ± 0.06	310 ± 40

Table 4. Comparison of k_{cat} and K_M values
ATPase assays were performed using a regenerative ATPase assay in buffer containing 40 mM HEPES/KOH pH 7.5, 150 mM KCl, 5 mM $MgCl_2$ at 30 °C in triplicates at a protein concentration of 2 µM and 0-4 mM ATP. The K_M and k_{cat} values were determined as described in Materials and methods.

Since the rate-limiting step in the ATPase of Hsp90 is the conformational transition leading to the hydrolysis-active state (Richter et al., 2008), it is plausible that these steps were affected by phosphorylation. To test this, the binding of those co-chaperones which interact with specific conformations of Hsp90, was assessed. First, the effect of Hop/Sti1, an inhibitor of the Hsp90 ATPase stabilizing the open conformation of Hsp90, was tested (Prodromou et al., 1999; Richter et al., 2003). Hop/Sti1 inhibited the All-A8 and All-E8 variants similar to the wt protein and with comparable K_D values (Figure 17A). Thus, the inhibitory effect of Hop/Sti1 is not affected by mutations which mimic global phosphorylation states. Aha1 is an Hsp90 ATPase activator accelerating rate limiting conformational changes (Hessling et al., 2009; Koulov et al., 2010; Retzlaff et al., 2010). Aha1 stimulation of the intrinsic ATPase activity was less pronounced in both the All-A8 and All-E8 variants compared to wt Hsp90 (Table 5).

A further inhibitory co-chaperone of Hsp90, which targets the ATP-bound closed conformation and reduces the ATP hydrolysis rate, is p23/Sba1 (Sullivan et al., 2002). Binding of p23/Sba1 to Hsp90 was monitored by SPR with p23/Sba1 attached to the sensor chip. In the presence of the non-hydrolysable ATP analogue AMP-PNP, which populates an N-terminally dimerized Hsp90 species, p23/Sba1 binding to All-

E8, but not All-A8, was diminished (Figure 17B). Taken together, these findings demonstrate that the functions of co-chaperones influencing conformations at later stages of the chaperone cycle are specifically impaired by Hsp90 phosphorylation, while Hop/Sti1 binding and its inhibitory potential appear to be unaffected by phosphorylation.

Effect of Aha1			
Construct	k_{cat} at 30 °C (min^{-1})	K_D at 30 °C (µM)	Stimulation factor
Wt-Hsp90	9.3 ± 1.5	1.3 ± 0.3	16.9
All-A10	3.3 ± 0.3	1.9 ± 0.4	16.5
All-A8	4.2 ± 0.3	0.93 ± 0.1	8.9
All-E8	1.3 ± 0.3	0.94 ± 0.2	5.9
S282E	7.5 ± 2.1	0.6 ± 0.2	14.4
S297E	11.5 ± 3.9	0.9 ± 0.4	16.7
S334E	9.8 ± 1.2	1.2 ± 0.2	17.5
S379E	1.3 ± 0.3	1.0 ± 0.1	6.8
S450E	11.6 ± 2.7	1.1 ± 0.3	21.1
S456E	7.9 ± 1.8	1.4 ± 0.3	15.5
S485E	0.82 ± 0.9	1.6 ± 0.5	3.3
S485Y	5.6 ± 1.6	> 17	25
S485A	13.2 ± 0.8	4.2 ± 0.6	60
T533E	7.0 ± 1.5	0.9 ± 0.2	14.9
S602E	8.0 ± 1.8	3.1 ± 0.6	28.6
S604E	7.6 ± 0.9	2.5 ± 0.3	20

Table 5. Stimulatory effect of Aha1 for wt and Hsp90 phospho-mutants
Aha1 stimulation was measured in 40 mM HEPES/KOH pH 7.5, 20 mM KCl, 5 mM $MgCl_2$, and 2 mM ATP at 30 °C in a regenerative ATPase assay. Hsp90 concentration was 1 µM. Different concentrations of Aha1 were used to obtain the binding affinities for the stimulated ATPase turnover rates.

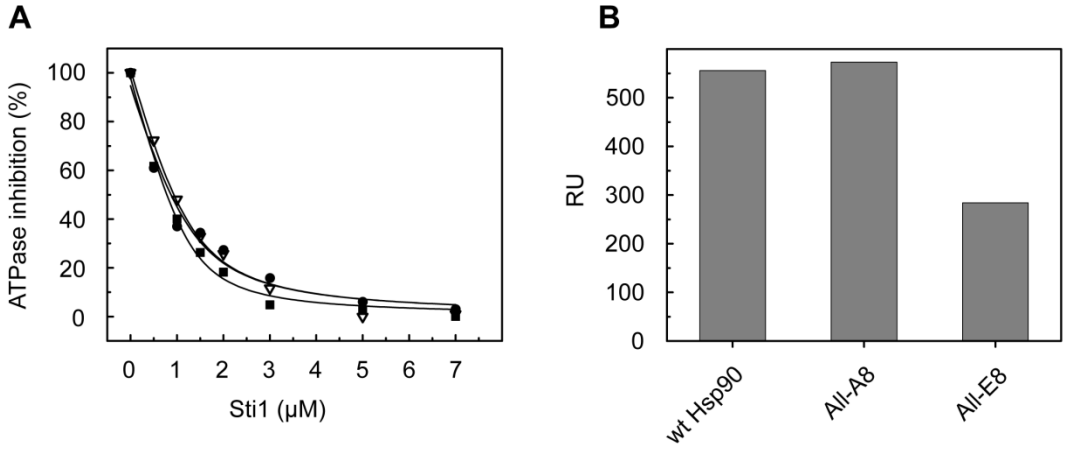

Figure 17. Effects of the co-chaperones Hop/Sti1 and p23/Sba1
(A) Effects of Hop/Sti1 on the ATPase activity of Hsp90 mutants. Hsp90 wt (■), All-A8 (∇) and All-E8 (●) at the concentration of 2.5 µM were incubated with 0-7 µM Sti1 in the presence of 2 mM ATP. The individual activities of wt and the variants were set to 100%. **(B)** Binding of p23/Sba1 to wt, All-A8 and All-E8 variants was tested by SPR. AMP-PNP concentration was 2 mM and Hsp90 concentration was 1 µM.

6.3 Analysis of the individual phosphorylation sites

6.3.1 Cell viability and effect on yeast growth

The simultaneous mutation of the phospho-sites in the Hsp90 variants All-A8 and All-E8 provided an overview of the global impact of phosphorylation *in vivo* and *in vitro*. To assess the effects of individual phospho-sites on Hsp90 function in detail, single phospho-site mutants were introduced into yeast as the only source of Hsp90. Most of the variants tested supported growth of yeast cells similar to wt Hsp90 (data not shown). However, three mutants (S379E, S485E and S604E) behaved differently. The most profound effects were observed for the Ppt1-regulated site S485 where the glutamate substitution was unable to support yeast viability (Figure 18A). The lethality suggests a strong influence of S485 phosphorylation on the essential aspects of the Hsp90 chaperone machinery. Previous studies identified S485 as an important site and its mutation to tyrosine has been described (Fang et al., 1998; Hawle et al., 2006). Although S485E was not functional *in vivo*, the tyrosine exchange was able to sustain growth, but cells were sensitive to elevated temperatures (Figure 18B). Similarly, expression of S379E resulted in a slow growth and *ts* phenotype. Cells expressing S604E exhibited growth properties similar to wt under physiological conditions but increased sensitivity was observed at higher temperatures. Unlike the Ppt1-regulated S604 phospho-mimicking variant, the S602E mutant behaved like wt, despite these two sites reside in close proximity, suggesting an important role of S604 under non-permissive conditions.

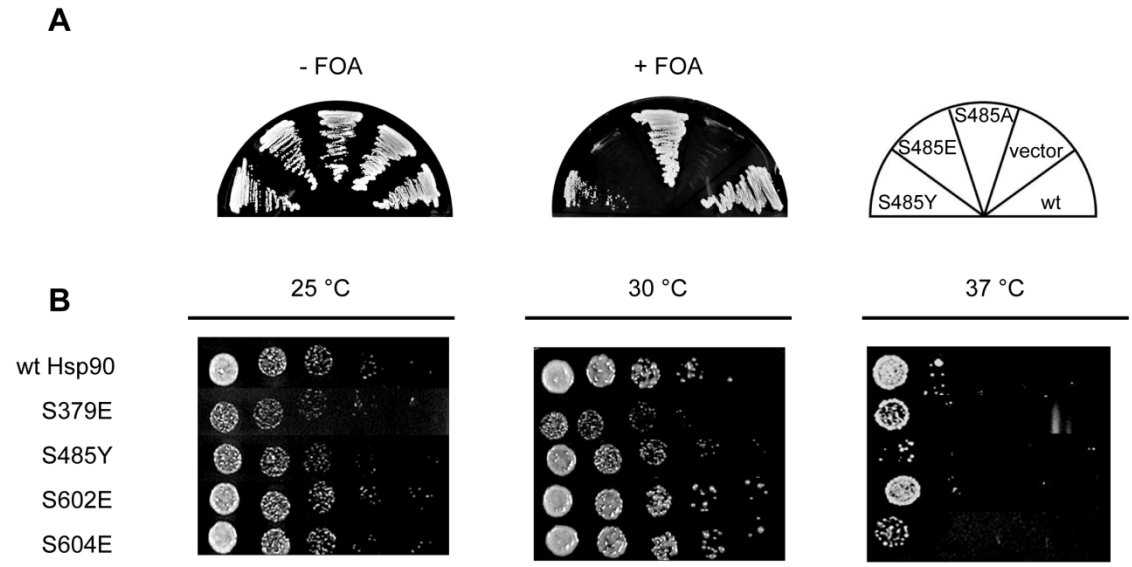

Figure 18. Effects of Hsp90 single phospho-site mutations on yeast growth
(A) Viability of Hsp90 mutants at position S485. The S485E mutation is lethal for yeast cells, whereas S485A and S485Y support growth. **(B)** Yeast cells with both genomic copies of *hsp90* deleted but carrying either wt or Hsp90 phospho-mutants were tested for their temperature sensitivity. Cultures were adjusted to the same cell density (10^7 cells/mL), spotted in 5-fold serial dilutions and incubated at the indicated temperatures.

6.3.2 Client protein maturation *in vivo*

In a next step, the influence of individual phospho-mimicking variants on the activity of Hsp90-specific client proteins was examined *in vivo*. Again, the Hsp90 model clients FFL, GR and v-Src kinase were utilized. Most variants tested supported the activation of client proteins similar to wt Hsp90 (data not shown). Mutation of S604E only minimally affected FFL and v-Src activation and the S602E variant showed wt-like client activation (Figure 19A and B). For S379E, GR and FFL maturation was significantly diminished and v-Src drastically decreased. Similarly, S485Y impaired activation of all three clients but the strongest influence was observed for GR. Importantly, Hsp90 protein levels were not altered (Figure 19C). As the alanine mutants did not alter Hsp90 chaperone function (data not shown), the effects can be specifically attributed to the influence of phosphorylation. Thus, phosphorylation of S379 and S485 has a general impact on Hsp90 chaperone function.

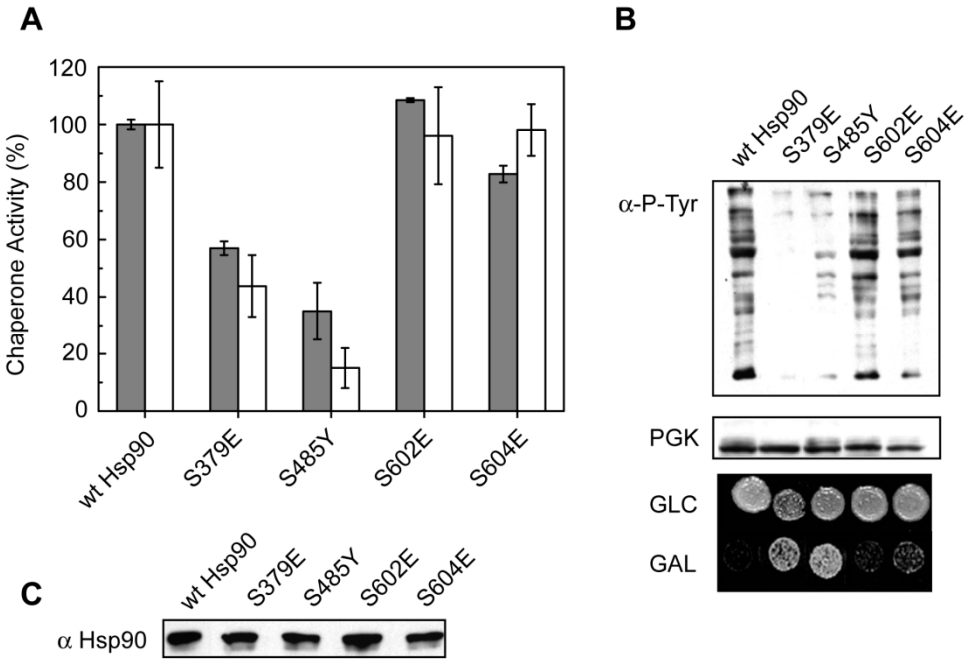

Figure 19. *In vivo* chaperone function of Hsp90 single phospho-site variants
(A) Influence of Hsp90 phospho-mutants on the activation of the client proteins FFL (gray) and GR (white). Data represent a percentage of the activity observed in wt Hsp90-expressing cells. **(B)** Effect of Hsp90 phospho-mutants on the activity of v-Src. v-Src activity was analyzed by Western blot with a phospho-tyrosine antibody (4G10). As a control PGK was used. Yeast cells expressing v-Src under control of galactose promoter were spotted on the glucose or galactose-containing selective media. **(C)** Immunoblot analysis of yeast cells expressing wt and Hsp90 phospho-variants. Cell lysates were tested for Hsp90 expression using a rabbit anti-Hsp90 antiserum.

6.3.3 Sensitivity to Hsp90 inhibition and DNA repair processes

It has been recently shown that Hsp90 phosphorylation contributes to inhibitor sensitivity (Mollapour et al., 2010a; Mollapour et al., 2011b). To test this possibility, *in vivo* effects of the Hsp90-specific inhibitor radicicol (RD) was tested in yeast cells expressing the phospho-sites mutants. Upon RD treatment, the silent sites did not show any effects (data not shown), however growth of yeast expressing the 'active' phospho-sites S379E, S485Y and S604E was affected. The sensitivity for the inhibitor was unaltered in the S602E variant in respect to wt cells (Figure 20A).

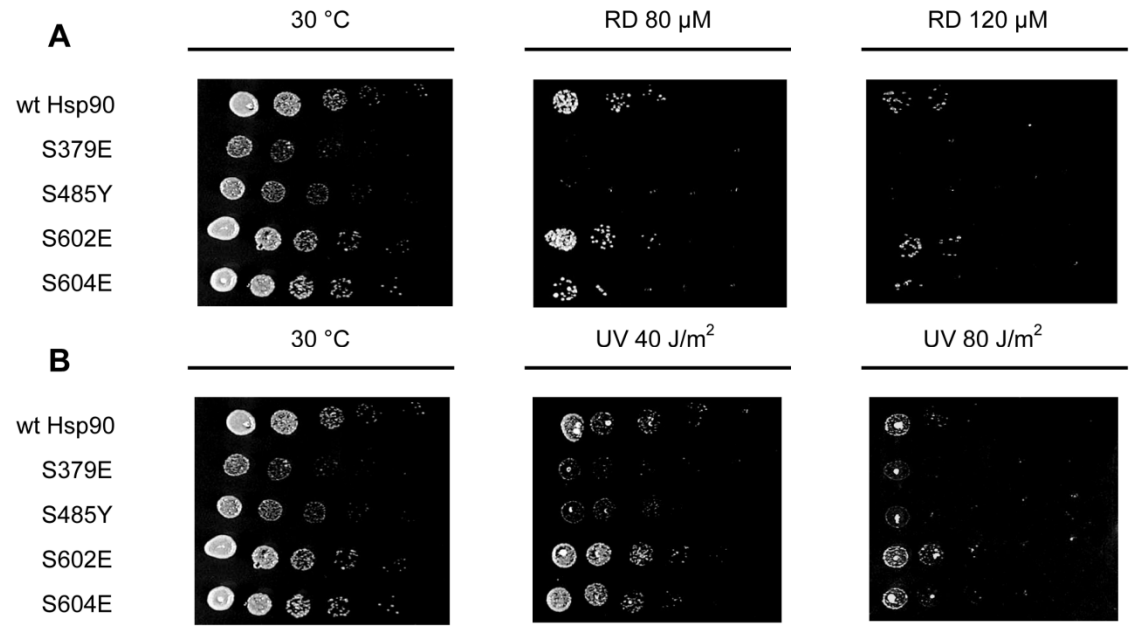

Figure 20. Resistance to Hsp90 inhibition and DNA repair processes in Hsp90 phospho-mutants
(A) Resistance of Hsp90 phospho-mutants to RD treatment. Yeast cells expressing Hsp90 phospho-mutants were incubated in media lacking or supplemented with RD at the indicated concentrations overnight at 30 °C, spotted on selective media and incubated at 30 °C. **(B)** DNA repair activity of Hsp90 phospho-mutants. Yeast cells expressing Hsp90 phospho-mutants spotted on selective media were exposed to UV light (40 and 80 J/m^2) and then incubated at 30 °C.

Hsp90 action has been associated with nuclear processes such as transcription, DNA repair activity or telomere DNA length maintenance (Echtenkamp et al., 2011; Toogun et al., 2008). An independent study showed that phosphorylation may also affect Hsp90 shuttling between the nucleus and the cytoplasm (Mollapour et al., 2010a). To determine how the active phospho-sites contribute to the DNA damage response, yeast cells expressing Hsp90 phospho-mutants were subjected to UV irradiation. The survival of cells after irradiation was affected in S379E and S485Y (Figure 20B). Growth defects were also observed in S604E, but not in the S602E variant. Importantly, no changes compared to wt were detected in alanine mutants, which mimic the constitutively dephosphorylated state confirming the specificity of these effects (data not shown). These observations show that S379, S485 and S604 alter inhibitor potency and interfere with the endogenous DNA repair activity.

6.3.4 ATPase activity

To gain insight into the functional consequences of Hsp90 phosphorylation, the effect of the all single-site mutations on the Hsp90 ATPase activity was determined (Table 4). Four active phospho-mutants, S379E, S485E, S602E and S604E showed decreased ATP hydrolysis rates. These included the two sites specifically regulated by Ppt1 confirming relevance of this phosphatase in Hsp90 phospho-regulation. The enzymatic defects of glutamate substitutions were compensated when the sites were mutated to alanine, the mimic of a dephosphorylated state. The only exception was S485. Reduced ATPase rates were detected in both alanine and tyrosine substitutions of this serine residue indicating the functional importance and structural sensitivity of this region. Binding of ATP, as judged by the K_M values, was not disturbed in both alanine and glutamate substitutions. Thus, the active Hsp90 phospho-mutants with defects in growth exhibit also defects in the inherent ATPase activities.

6.3.5 Co-chaperones regulation of the Hsp90 conformational cycle

6.3.5.1 Hop/Sti1

Since conformational changes accompanying ATP hydrolysis by Hsp90 are strictly regulated by co-chaperones, it could be reasoned that the ATPase cycle might be distinctly affected in Hsp90 phospho-mutants with diminished ATPase activity. First, the effect of Hop/Sti1, an inhibitor of the Hsp90 ATPase stabilizing the open conformation of Hsp90 (Prodromou et al., 1999; Richter et al., 2003), was assessed. Hop/Sti1 inhibited the ATPase activity of the individual active phospho-mimetic mutants similar to the wt protein (Figure 21). Thus, the inhibitory effect of Hop/Sti1 is not affected by phospho-site mutations.

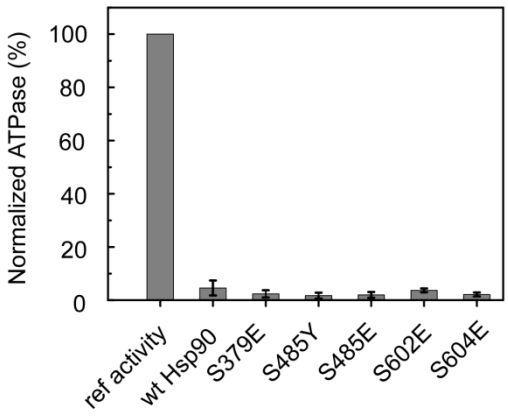

Figure 21. Inhibition of the ATPase activity mediated by Hop/Sti1
ATPase assays were performed in the presence of 2.5 µM Hsp90 variants and 7 µM Hop/Sti1. The individual Hsp90 activity was set to 100% and indicated as 'reference activity'.

6.3.5.2 Aha1

Aha1 is an Hsp90 ATPase activator accelerating rate-limiting conformational changes leading to the closed conformation of Hsp90 (Hessling et al., 2009; Koulov et al., 2010; Retzlaff et al., 2010). The ATPase experiments in the presence of Aha1 gave strikingly different results for individual active phospho-sites (Table 5, Figure 22A). While the ATPase activities of the S602E and S604E proteins were activated to a similar degree as the wt protein, S485E was susceptible to Aha1 stimulation up to the level of the non-stimulated wild-type protein and S485Y could restore activation by Aha1. Furthermore, mutation at the positions S485, S602 and S604 reduced the affinity for Aha1. In addition, Aha1-mediated stimulation was significantly reduced in S379E. This indicates that either Aha1 binding or the closing reaction induced by Aha1 are affected by the active phospho-site mutations. The effects observed for the phospho-mimicking mutants suggest that phosphorylation at the active sites S379, S485, S602 and S604 may influence the conformational dynamics of Hsp90.

The inability of the co-chaperone Aha1 to regulate the ATPase cycle of the active phospho-site mutants may be an intrinsic property of the respective mutations affecting the co-chaperone activation mechanism or it could be a consequence of conformational alterations resulting in altered interaction. To solve this conundrum, the ability of co-chaperones to bind to Hsp90 mutants was examined. First, complex formation between Aha1 and Hsp90 variants was assessed using analytical ultracentrifugation (aUC) (Li et al., 2011). None of the mutations completely

abrogated interaction with Aha1, albeit differences in binding properties were observed. Interestingly, S379E interacted with Aha1 comparable to the wt protein (Figure 22B). The S485 mutants exhibited slightly reduced binding capacity and the complex sedimented slower than that involving wt Hsp90. When the interaction of Aha1 with S602E and S604E Hsp90 was examined, reduced s values in complex with Aha1 were observed. Additionally, the fraction of Hsp90 associated with Aha1 was diminished. These results show that the phospho-sites can affect the mechanism of ATPase stimulation without affecting association with Aha1 (S379E), modulate binding of Aha1 and still retain significant stimulation potential (S602E and S604E) or affect both binding and activation (S485E and S485Y).

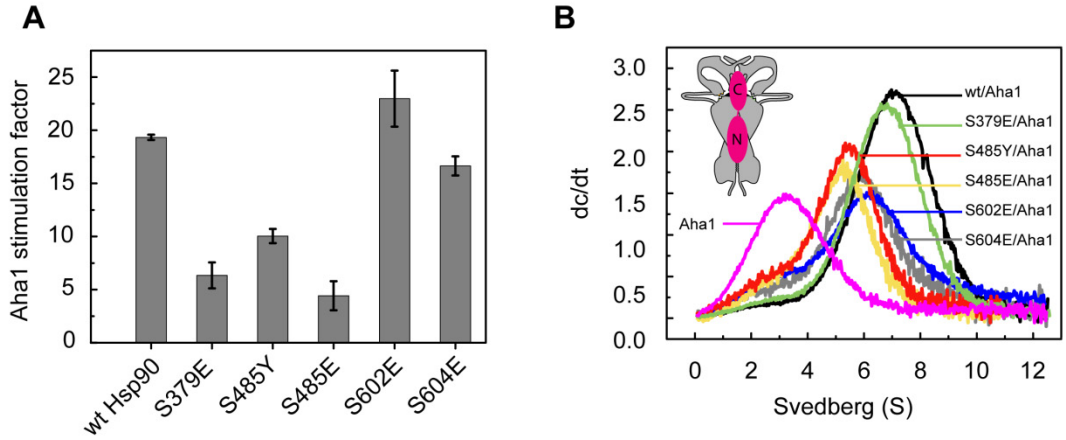

Figure 22. Regulation of the Hsp90 ATPase activity and association with Aha1
(A) Stimulation of the ATPase activity by Aha1. Data represent the 'fold' increase of the Hsp90 ATPase activity (1 µM) in the presence of Aha1 (10 µM) versus to activity of the same Hsp90 variant in the absence of this co-chaperone. **(B)** Analysis of the interaction of Aha1 with Hsp90 phospho-variants. Complex formation between Aha1 and Hsp90 phospho-mutants was monitored by fluorescence using aUC in the presence of 1 µM Alexa Fluor488-labeled Aha1 and 3 µM Hsp90 phospho-mutants.

6.3.5.3 p23/Sba1

A further inhibitory co-chaperone of Hsp90, which targets the ATP-bound closed conformation and reduces the ATP hydrolysis rate at a late stage of the cycle, is p23/Sba1. To analyze the impact of Hsp90 phosphorylation on the interaction with p23/Sba1 SPR spectroscopy was used. p23/Sba1 was immobilized and its interaction with Hsp90 mutants was probed in the presence of the non-hydrolysable ATP analogue AMP-PNP. S485 variants completely abrogated the association with p23/Sba1 (Figure 23A). Compared to wt Hsp90, binding was about half for the

S379E mutant and for the C-domain mutants, S602E and S604E, it was comparable to that of the wt protein. Overall, the influence on the association with p23/Sba1 is not uniformly affected by the S379, S485, S602 and S604 phospho-mimicking variants of Hsp90. Thus, the different conformational states recognized by the co-chaperones are altered by the active phospho-site mutants suggesting that phosphorylation may influence the conformational dynamics of Hsp90.

p23/Sba1 is a weak inhibitor of the ATPase activity. Further effects of the active phospho-sites on the p23/Sba1-mediated ATPase arrest were detected. p23/Sba1 inhibited the basal ATPase activity of wt Hsp90 and both C-domain phospho-mutants (S602E and S604E) to approximately 60% of its initial value (Figure 23B). Suppression of the ATPase activity was partly compromised in the S379E variant. The S485E and Y mutations completely abolished p23/Sba1-mediated ATPase arrest.

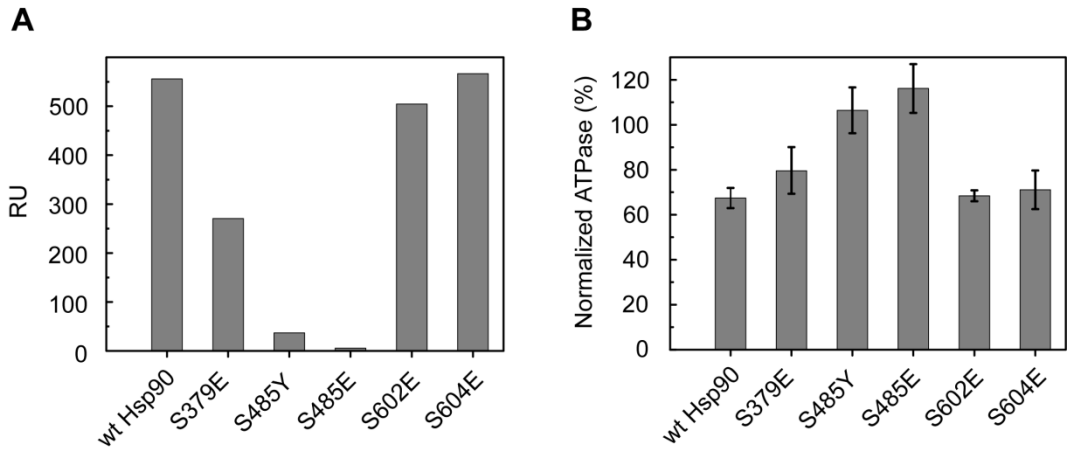

Figure 23. Binding and regulation of the ATPase activity by p23/Sba1
(A) Binding of Hsp90 phospho-mutants to p23/Sba1. Interaction of Hsp90 phospho-mutants with p23/Sba1 was determined by SPR analysis. AMP-PNP concentration was 2 mM and Hsp90 concentration was 1 µM. **(B)** Effects of the co-chaperone p23/Sba1 on the ATPase activity of Hsp90 phospho-mutants. 2.5 µM Hsp90 phospho-variants were incubated with 35 µM p23/Sba1. Data are expressed as the percentage of the ATPase activity in the presence of p23/Sba1 versus the ATPase activity without p23/Sba1.

In summary, the functions of co-chaperones influencing conformations at later stages of the chaperone cycle are specifically down-regulated in the active Hsp90 phospho-mutants, while the inhibitory potential of Hop/Sti1 appears to be unaffected. It is noteworthy that neither of the phospho-sites exhibiting compromised co-chaperone regulation localizes to the ATP binding N-domain nor is located at the known interaction interfaces with the co-chaperones Aha1 and p23/Sba1. This strongly

suggests that phosphorylation alters the Hsp90 conformation and allosterically influences the ATPase cycle.

6.4 Mechanisms of the active phosphorylation sites

6.4.1 Conformational transitions in S485 phospho-site

To test the effects of Hsp90 phosphorylation on the N-domain interactions during the ATPase cycle, a variant of Hsp90 was used, in which the ATP-lid (residues 98 to 121) was deleted (lidless-Hsp90). Lidless-Hsp90 is an inactive ATPase. However, Hsp90 heterodimers consisting of one wt and one lidless monomer show significantly increased ATP turnover compared to wt Hsp90 alone, as the lidless protomer strongly stimulates ATP hydrolysis in the neighboring wt subunit (Richter et al., 2006). When these heterodimers were formed at saturating concentrations of lidless-Hsp90, the ATP turnover increased around 10-fold for wt, while the activation was impaired in S485E (Figure 24).

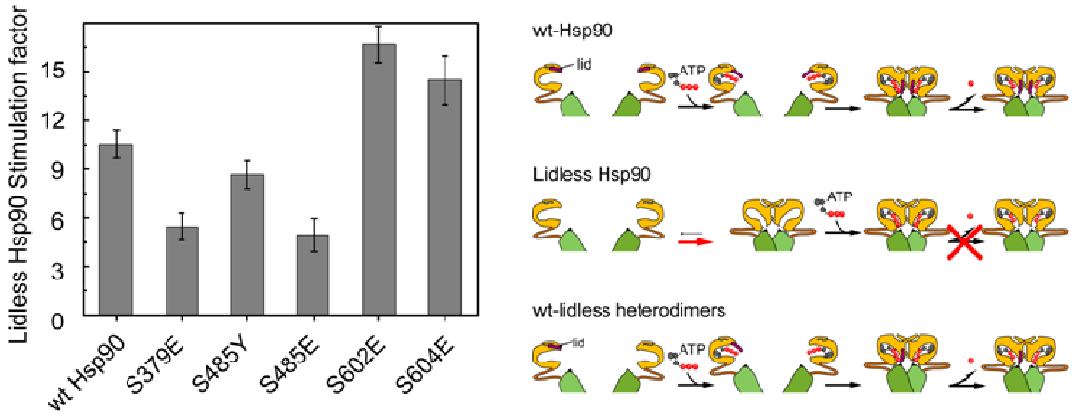

Figure 24. Stimulation of the ATPase activity by lidless-Hsp90
ATPase activity of heterodimers with lidless-Hsp90. The N-terminal association properties of 1 µM Hsp90 variants were investigated after formation of heterodimers with 10 µM lidless-Hsp90.

Also for S485Y partly reduced stimulation by the lidless variant was observed. Thus the potential of lidless to stimulate the intrinsic ATPase activity was affected in all S485 mutants tested. To further analyze the conformational consequences of phosphorylation, the structural transitions induced by the ATP analogue AMP-PNP in wt Hsp90 and S485 variants were compared by aUC. Addition of AMP-PNP promotes the N-domain contact and results in the structural compaction of Hsp90.

This process can be monitored as a change in the s value of the sedimenting protein (Hessling et al., 2009). Upon addition of AMP-PNP, the sedimentation velocity of S485 mutants was significantly decreased compared to wt protein indicating that AMP-PNP was not effective in inducing structural transitions to the fully closed conformation (Table 6).

Hsp90 variant	s value (S)		
	w/o nucleotide	AMP-PNP	ATPγS
wt Hsp90	6.1	6.9	6.8
S379E	6.1	6.3	6.7
S485Y	5.2	5.4	5.4
S485E	5.4	5.4	5.6
S602E	6.1	6.9	n.d.
S604E	6.1	6.8	n.d.

Table 6. s values for wt and Hsp90 phospho-mutants (6 µM) in the presence and absence of nucleotides

Unexpectedly, the S485 mutants showed also a reduced sedimentation coefficient in the absence of nucleotide. As the sedimentation coefficient depends on the molecular weight and molecular shape of the molecule, thus either dissociation of the dimers or changes in the open conformation of S485 mutants could contribute to these effects. The titration experiment revealed no changes in the s values in S485 mutants at several protein concentrations tested implying that the monomer-dimer equilibrium was not affected by the mutations (Table 7).

	s value (S)		
	2 µM	6µM	18 µM
S485E	5.2	5.2	5.4
S485Y	5.2	5.3	5.4

Table 7. s values for S485 variants at different protein concentrations

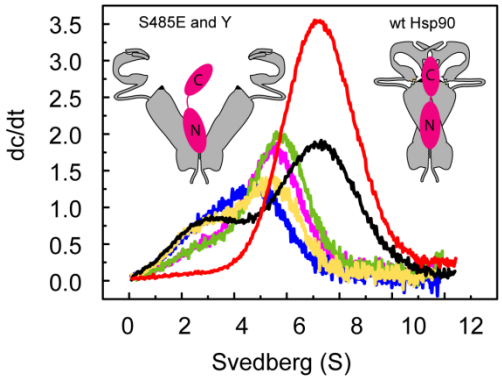

Figure 25. Analysis of the interaction of Aha1 with S485 variants
Complex formation between Aha1 and Hsp90 phospho-mutants was monitored by fluorescence using aUC in the presence of 1 µM Alexa Fluor-labeled Aha1 and 7 µM wt (red), 0.75 µM wt (black), 7 µM S485Y (green) 1.5 µM S485Y (yellow), 7 µM S485E (magenta), 1.5 µM S485E (blue).

In agreement with this notion is the finding that the complex of Aha1 with S485 mutants sedimented slower than that with wt Hsp90 (Figure 25). This can be explained by alterations of the complex shape, which seems to result in differences in the stimulation of the Hsp90 ATPase. To exclude any perturbations in the C-domain dimerization properties, a cross-linking experiment was performed. Similar ratios of Hsp90 in the monomeric and dimeric forms were found for wt and S485 mutants confirming that the C-domain contacts and the ability to exchange subunits are not altered by S485 mutations (Figure 26).

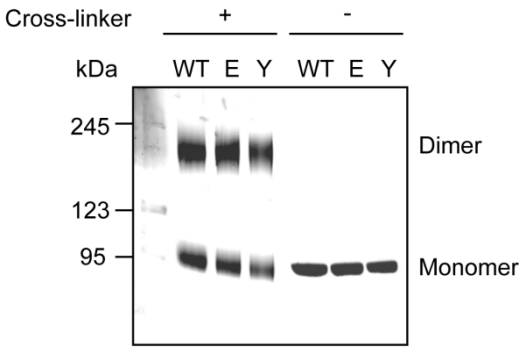

Figure 26. Dimerization properties of S485 mutants
Ability to form dimers by S485 mutants was assessed by a cross-linking of wt Hsp90 (WT), S485E (E) and S485Y (Y) mutants. Cross-linked Hsp90 variants form both monomeric and dimeric forms. As a control, Hsp90 variants in the absence of cross-linker were loaded corresponding to the monomeric species.

The cross-linking and aUC experiments consistently showed that the primary dimerization interface was unaltered in S485 variants. Collectively, the different sedimentation behavior and reduced stimulatory effect of the lidless mutant imply that S485 mutants adopt a more open, elongated shape in the apo state. The proposed model of altered open conformations of S485 mutants and their inability to form nucleotide-induced N-terminal contacts are also in line with an impaired p23/Sba1

and Aha1 binding described above (Figure 22 and 23). This shows that S485 phosphorylation contributes to the communication between remote regions in Hsp90.

6.4.2 S379 phospho-site impairs the active site formation

The S379E mutant showed impaired lidless-Hsp90 stimulation (Figure 24). aUC experiments further revealed that upon addition of AMP-PNP, the shift of the S379E-Hsp90 peak to higher s values was significantly reduced indicating that the formation of the N-contacts is impaired (Table 6). Importantly, sedimentation of S379E was not affected when the nucleotide was absent. This shows that at least the open conformations of S379E and wt Hsp90 are similar. To investigate in more detail whether the S379 and S485 mutants act by comparable mechanisms, the slowly hydrolyzing ATP analogue ATPγS was used. Addition of ATPγS induced conformational transitions in S379E similar to wt Hsp90 revealing that the S379E mutant can sense different types of nucleotide (Table 6). ATPγS also restored the ability of the S379E mutant to interact with p23/Sba1 like wt Hsp90 (data not shown).

The kinetics of conformational changes between the N- and the M-domains were monitored by fluorescence resonance energy transfer (FRET) (Hessling et al., 2009). After equilibrating donor- and acceptor-labeled Hsp90 with nucleotides, the FRET complex was chased by addition of unlabeled wt Hsp90 (Figure 27A). If nucleotide was omitted or ATP was used, the wt Hsp90 FRET complex dissociated rapidly, since the open state was populated. However, when the complex was preincubated in the presence of ATPγS or AMP-PNP, a very slow or no chase, respectively, was detected. Different effects were observed for the S379E mutant (Figure 27B). For the S379E FRET complex, a slower chase with unlabeled wt Hsp90 was observed when ATP or ATPγS was added, consistent with the slower ATP hydrolysis of this mutant. In line with aUC, in the presence of AMP-PNP, the S379E FRET complex could still dissociate. This confirms the observation that in the presence of this nucleotide S379E does not achieve a fully closed conformation.

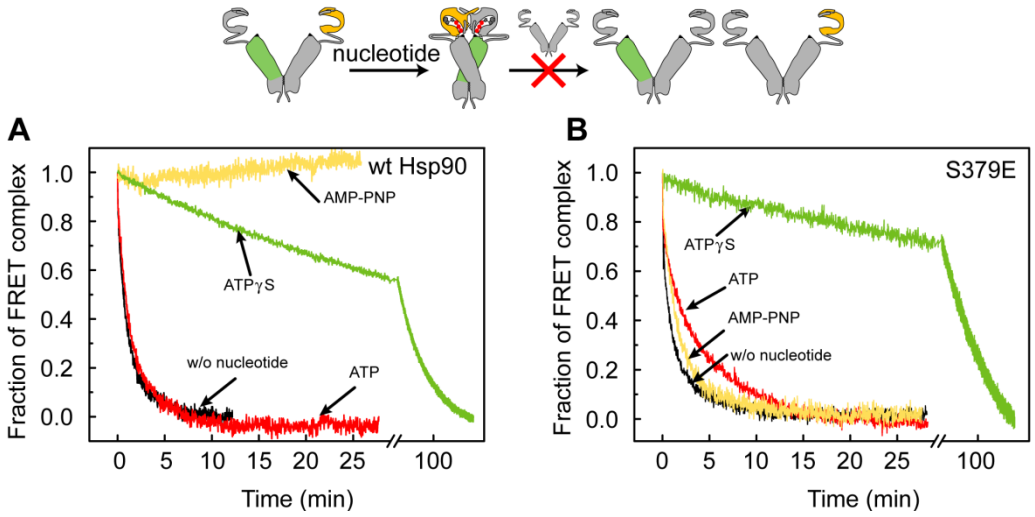

Figure 27. FRET analysis of the N-terminal dimerization
Donor- and acceptor-labeled **(A)** wt Hsp90 or **(B)** S379E were preincubated to enable formation of heterodimers. 2 mM of ATPγS (green), AMP-PNP (yellow) or ATP (red) were added or the heterodimers were preincubated in the absence of nucleotide (black). The chase reaction was initiated by addition of an excess of unlabeled wt Hsp90.

It appears that the late steps of the conformational cycle are altered by the S379E variant, in particular the active site formation after the nucleotide is bound. As S485 mutations interfere with conformational rearrangements independent of the nucleotide used, S485 mutants disrupt the conformational flexibility of Hsp90 in a more global way. Hence, both phospho-site mutants affect structural transitions, albeit by different molecular mechanisms.

6.4.3 Inter-subunit communication in the phospho-sites S602/S604

Both the C-domain phospho-site mutants S602E and S604E had no influence on the nucleotide-induced N-domain association and could be strongly stimulated by the lidless-Hsp90 variant (Table 6, Figure 24). However, these mutants exhibited indirect effects on the ATPase activity and activation by Aha1 suggesting that the phosphorylation in the C-domain either altered the primary dimerization sites or inter-domain communication processes. Since the dimerization properties were similar for wt and the C-domain phospho-site mutants, the first hypothesis was excluded (data not shown). This suggested that the mechanism of ATPase activation by Aha1 was impaired. In the Aha1 binding study, the fractions of S602E and S604E found in a complex with Aha1 was decreased confirming that phosphorylation in the C-domain contributes to the altered interaction (Figure 22B). To further test this, a titration experiment was performed. This study revealed increasing amounts of Aha1 in the wt

Hsp90 protein complexes at 7.5 S (Figure 28). When the same experiment was performed with the S602E mutant, two effects were obvious. First, the affinity was reduced compared to wt Hsp90 by at least a factor of three. Further, even at a high concentration of S602E Hsp90, the protein complex fraction never sedimented at 7.5 S, but consistently at 6.4 S. This can only be explained by alterations of the complex shape and by a failure of Aha1 to induce the ATPase-stimulated conformation in this mutant.

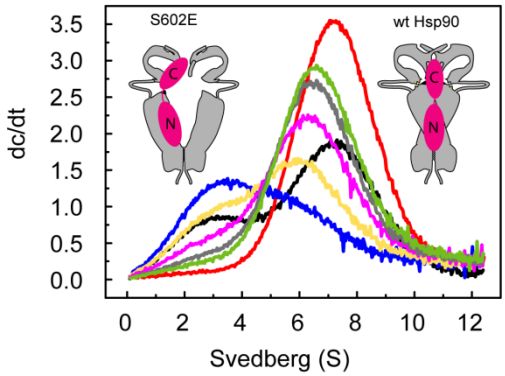

Figure 28. Influence of S602E mutation on Aha1 binding
1 µM Alexa Fluor-labeled Aha1 was mixed with 7 µM wt (red), 0.75 µM wt (black), 7 µM S602E (green), 5 µM S602E (gray), 3 µM S602E (magenta), 1.5 µM S602E (yellow), 0.75 µM S602E (blue) Hsp90.

Aha1 binding to Hsp90 is known to involve the N-terminal and the M-domain of Hsp90, but not the C-terminus (Retzlaff et al., 2010). It was therefore enigmatic how the C-domain mutations affect the association with Aha1. Given the effects of the mutation on the ATP turnover rate, it is plausible that these effects are coupled and thus the alterations in the C-domain of Hsp90 induced by the mutations may affect the domain organization in a way that the ATPase rate is reduced and the potential of Aha1 to stimulate the ATPase rate is affected. In order to support this notion, the ability of Aha1 to induce the closing reaction (as it had been shown for wt Hsp90) was tested in the C-domain mutant S602E. To study the effects of Aha1 on the subunit exchange of the Hsp90 dimer, the stability of each of the Aha1-Hsp90 FRET complexes was tested by a chase with an excess of unlabeled wt or S602E (Figure 29A). The disassembly of the FRET complex was monitored by a decrease in the Hsp90 acceptor fluorescence. To determine the apparent half-life of the reaction, data were analyzed by single exponentials (Figure 29B). The half-life for subunit exchange was unaltered in both wt and the S602E mutant when Aha1 was absent, confirming unaltered primary dimerization contacts. Upon addition of Aha1, the half-

life of the Hsp90 subunit exchange reaction in S602E mutant was decreased 6-fold compared to its half-life of wt Hsp90. Thus, Aha1 failed to stabilize the Hsp90 dimer in the S602E mutant. In summary, phosphorylation affects Hsp90 by different mechanisms. Depending on the site, the nucleotide-dependent N-terminal association or C-terminal conformational properties can be modulated.

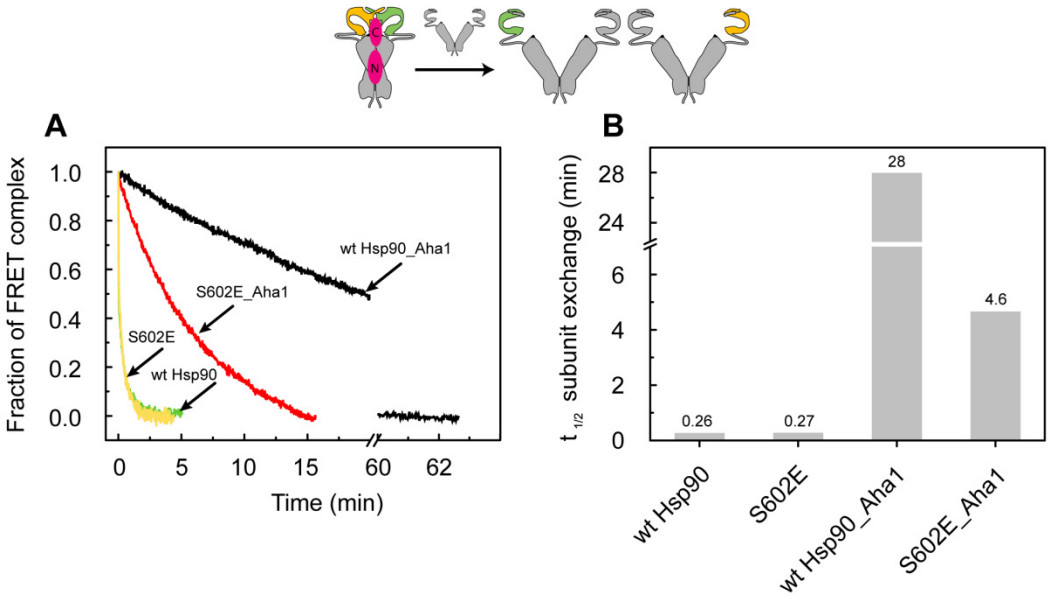

Figure 29. FRET analysis of conformational transitions induced by Aha1
(A) Subunit exchange of 100 nM Hsp90 heterodimers in the absence or presence of Aha1 upon addition of 2 µM unlabeled wt or S602E Hsp90. The normalized decrease of Hsp90 acceptor fluorescence over time is shown for wt Hsp90 (green), S602E (yellow), wt Hsp90 in complex with Aha1 (black) and S602E in complex with Aha1 (red). **(B)** The apparent half-life of subunit exchange ($t_{1/2}$) is estimated using equation 3 in Materials and Methods.

7 Discussion

Hsp90 is a highly regulated molecular chaperone which modulates the activity of hundreds of clients, many of which are important regulatory proteins (McClellan et al., 2007). Thus Hsp90 can be seen as a hub for the conformational regulation of proteins in the eukaryotic cell (Whitesell and Lindquist, 2005). Hsp90 function is modified by phosphorylation on multiple sites and it has been proposed that cycling of phosphorylation and dephosphorylation might be coupled to the binding and release of client proteins (Zhao et al., 2001). Though it has been known for long time that Hsp90 is a phospho-protein (Lees-Miller and Anderson, 1989a), it remained unclear how global control of Hsp90 function is achieved by phosphorylation. The starting point for this study was the analysis of a phosphatase (Pp5/Ppt1) which has a TPR domain via which it specifically associates with the C-terminal end of Hsp90. Though its deletion had a negative impact on Hsp90-dependent activity in yeast (Wandinger et al., 2006), the mechanism of phospho-regulation was unsolved.

7.1 Yeast Hsp90 phosphorylation and specific role of Ppt1

To identify yeast Hsp90 phosphorylation sites, a SILAC approach in combination with mass spectrometry was applied. This analysis revealed in total ten sites modified *in vivo*. Seven of these phosphorylation sites are in the M-domain and three are located in a flexible loop in the C-domain. This is in line with the observation that phospho-sites are more frequently located in flexible regions and the functional consequences of phosphorylation often depend on the flexibility of the phosphorylated sequence (Gnad et al., 2009). Prior bioinformatics analyses also revealed that serine and threonine phosphorylation sites tend to occur on fast evolving loops and hinge regions (Gnad et al., 2010).

This analysis did not cover all possible phosphorylation events in yeast Hsp90. In particular, no modifications in the N-domain were detected, although recent reports described two important phospho-sites Y24 and T22 in this region (Mollapour et al., 2010a; Mollapour et al., 2011b). These sites were also not identified in any previous

MS study (Albuquerque et al., 2008; Holt et al., 2009). It is conceivable that the phospho-Y24 and T22-containing tryptic peptides from yeast Hsp90 have either weak ionization properties and/or are of low abundance which would preclude their detection by LC-ESI-MS approaches.

Importantly, the quantitative analysis revealed that the ten identified sites constitute a major fraction of Hsp90 phosphorylation in yeast under non-stress conditions. It was also possible to address a direct role of Ppt1. Two sites (S485/S604) were specifically dephosphorylated by this phosphatase confirming its importance in the Hsp90 chaperone cycle. *In vitro* phosphorylation studies further suggest that one of the potential kinase regulating the phosphorylation status of these sites is CKII. This would point to a general rather than client-specific regulation mechanism *in vivo*.

It seems that the phosphorylation patterns in yeast and man are quite different, although the majority of yeast phospho-sites are conserved residues also in the human proteins. Experiments presented here suggest that conserved Ser/Thr residues are differentially targeted for phosphorylation in yeast and man. This observation is in accordance with the notion that yeast phosphorylation sites show low conservation with respect to higher eukaryotes (Gnad et al., 2010). This is due to the fact that many of the known human kinases evolved after the divergence of higher eukaryotes from yeast. Therefore, there are a number of specific kinases present in yeast and not in higher eukaryotes and vice versa. In higher organisms, phosphorylation is involved in a wide range of important cellular processes such as cellular signaling and cell-cell communication. This explains the low phospho-site conservation between the multicellular and single cell organisms (Gnad et al., 2010). These findings point to a considerable functional diversity of Hsp90 mediated by phosphorylation in different organisms allowing adjusting its chaperone function to a specific clientele and cellular environment.

7.2 Global Hsp90 phosphorylation

To determine the effects of the identified phosphorylation sites on Hsp90 activity, glutamate and alanine mutations mimicking phosphorylated and non-phosphorylated states, respectively, were engineered. The combined phospho-mimicking mutation of all the identified sites was lethal (All-E10). Furthermore, a phosphorylation-mimicking

variant (All-E8) where most of the identified sites were modified (except for S334 and S485) resulted in significantly impaired ATPase activity of Hsp90 and changes in its co-chaperone interactions. A weaker association with co-chaperones, whose binding is restricted to the closed conformation of Hsp90 was observed suggesting that phosphorylation affects later stages of the ATPase cycle. Underlying these effects are phosphorylation-induced alterations in the conformational dynamics leading to a reduced chaperone activity towards its client proteins. In contrast, the combined alanine variant (All-A8) exhibited only a minor influence on Hsp90-dependent functions *in vivo*. Thus, the effects observed for the All-E8 variant reflect the effects of phosphorylation, and do not derive just from the mutation of these sites.

7.3 Effects of the individual phosphorylation sites

Inspection of the individual phosphorylation sites revealed that four of the ten positions influence the properties of Hsp90 *in vivo* and/or *in vitro* (S379/S485/S602/S604). In general, cells expressing the active phospho-mutants were hypersensitive to elevated temperatures, impaired Hsp90 inhibition and showed defects in DNA repair pathways. This indicates that phosphorylation-mediated regulation of Hsp90 chaperone function is not only restricted to its cytoplasmic pool, but may also involve nuclear processes. These effects collectively show that various aspects of the Hsp90 chaperone machinery are affected by these important phosphorylation events. For the remaining six identified phospho-sites no specific functions could be attributed. It could well be that they are a part of non-functional phosphorylation occurring in the cell which only enhances the solubility of the protein without affecting the enzymatic activity (Lienhard, 2008). This does not eliminate the possibility, however, that these phospho-sites are potentially involved in other cellular processes including protein translocation, degradation, cell apoptosis, etc which were not a scope of this study. Thus, these sites may have other yet undiscovered functions.

7.4 Enzymatic activity and conformational cycle

In all active phospho-site mutants, decreased ATP hydrolysis rates were observed. Hsp90 acts via an 'active' ATP-dependent mechanism and its ATPase activity is absolutely essential for its chaperone function *in vivo.* The dynamics of ATP binding and hydrolysis coupled with large conformational shifts regulates the interaction with client proteins and is correlated with the cycling of Hsp90 complexes *in vivo*. This high degree of conformational flexibility has to be strictly fine-tuned to promote client maturation. It appears that too long or too short association with the Hsp90 chaperone machinery is deleterious as both increased and decreased ATP hydrolysis rates negatively impact client activation. It is also possible that certain clients need a fast Hsp90 ATPase cycle for their folding, while other clients, whose folding pathways are more complex, require a slower ATPase cycle to productively associate with Hsp90. In this study, phospho-mimicking mutants affected the intrinsic ATPase activity by different molecular mechanisms. Hence, Hsp90 phosphorylation could serve as the timing mechanism of the client activation process by regulating various aspects of the conformational cycle.

Under non-stress conditions, only 5% of Hsp90 wt activity is sufficient for yeast growth (Borkovich et al., 1989). This would suggest that the chaperoning capacity of Hsp90 largely exceeds its cellular requirements. What could be the reason for keeping such a high Hsp90 protein levels without any obvious need? This abundant chaperone reservoir seems to be critical for a quick response to environmental perturbations. Under non-permissive conditions, the chaperone reservoir can be readily used to sustain proteostasis. It is possible that reversible phosphorylation attenuates a pool of Hsp90 allowing its rapid activation according to cellular demands. The finding that Ppt1 dephosphorylates Hsp90 at two active phospho-sites and its phosphatase activity is regulated by stress stimuli further supports this hypothesis (Gasch et al., 2000).

It has been estimated that around 20% of all yeast proteins are influenced by Hsp90, which makes Hsp90 a highly connected protein in the yeast genome (Breitkreutz et al., 2008). However, the great unknown remains how Hsp90 associates with and mediates client protein folding. Biochemical studies revealed that in the open conformation, Hsp90 exposes hydrophobic regions that promote association with the

unfolded client. ATP binding is accompanied by conformational changes to the state with a low affinity to the client. Phosphorylation-based structural alterations in Hsp90 detected in this study may impact the accessible hydrophobic surfaces and influence binding and/or dissociation with certain client proteins. For two phosphorylation sites, S379 and S485, client-specific effects were observed indicating that phosphorylation could specifically direct Hsp90 to certain cellular pathways.

7.5 Hsp90 phosphorylation and client protein activation

It seems there is not one general mechanism of Hsp90 phospho-regulation. Instead, individual sites may target different aspects of the conformational cycle and with different consequences. This is in line with the observation that phosphorylation completely attenuates (S485) or partly decreases Hsp90 activity (S379), becomes important only under certain environmental conditions (S604) or is non-functional. It is highly unlikely that the regulation of Hsp90 activity is uniform for such a diverse Hsp90 clientele. Various clients require specific co-chaperones for their delivery to the Hsp90 system and co-chaperones can recognize different conformational states of Hsp90. Finally, both clients and co-chaperones were shown to promote conformational transitions providing directionality to the Hsp90 chaperone cycle. It can be envisioned that by affecting important aspects of the conformational cycle, phosphorylation can influence the equilibrium between the different conformational states, thus adjusting the structural shifts to the need of the particular client.

The results presented here predict that phosphorylation provides additional and/or parallel level of regulation of distinct stages of the chaperone cycle and activation of specific Hsp90 clients *in vivo*. Consequently, this quick and reversible protein modification would enable Hsp90 to adjust its activity to environmental requirements. Of note, the Hsp90 mutants analyzed in this study mimic constitutively phosphorylated or non phosphorylated states. In fact, the dynamics of phosphorylation may be critical and influence binding and release of Hsp90 clients. Thus, the effects of Hsp90 phosphorylation/dephosphorylation *in vivo*, which depend on the interplay between kinases and phosphatases, could directly affect the activation of specific clients. Although it is still to be verified if Hsp90 phosphorylation influences its chaperone function in a similar manner as the phospho-mimicking

mutations, these results suggest that phosphorylation can selectively regulate the interaction of Hsp90 with its clientele.

7.6 Mechanisms of the active Hsp90 phosphorylation sites

7.6.1 Phospho-site S379

S379E sustained viability but was defective in chaperoning Hsp90-specific clients with most prominent effects observed for v-Src activation. This could indicate that S379 phosphorylation is specifically involved in kinase maturation. This variant was susceptible to DNA damage showing that not only cytoplasmic, but also nuclear processes are affected by this phospho-mimicking mutation. The finding that S379E showed decreased resistance to the Hsp90 inhibitor RD suggests that the phosphorylation status may contribute to drug sensitivity *in vivo*. How the S379E mutant causes a substantial drop in catalytic activity and modulation by co-chaperones has not yet been determined, but it is likely that S379E disturbs the conformational cycle at the stage of the ATPase active site formation and contributes to the altered M-N domain interactions. Structurally, S379 is located in the M-domain catalytic loop (amino acids 370-390) harboring key residues that are essential for ATP hydrolysis (Ali et al., 2006). The assembly of the active site requires correct positioning of the middle segment catalytic residue R380, which interacts with the γ-phosphate of the nucleotide to promote ATP hydrolysis reaction. S379 phosphorylation would affect this interaction locally, most probably by the electrostatic interference with R380. This would prevent the formation of the catalytically active conformation of R380 and consequently severely impact ATP hydrolysis, as observed. Thus phospho-mimicking mutation S379E will likely influence the conformational transitions at the late stage of the formation of the closed active conformation when the catalytic site is formed (Figure 30).

7.6.2 Phospho-site S485

The MS data identified S485 as a Ppt1 target. Cells harbouring the phospho-mimicking mutant S485E were not viable, thus it was not possible to determine the

consequences of this mutation *in vivo*. This suggested that the key aspects of the Hsp90 chaperone activity were disturbed by the mutation. It was however possible to query the influence of a tyrosine substitution, whose functional importance was already uncovered by prior mutagenesis studies (Fang et al., 1998; Hawle et al., 2006). *In vivo* inspection revealed that GR maturation was most sensitive to S485Y. Furthermore, this variant impaired DNA repair processes and increased yeast sensitivity again RD treatment. Both the E and Y mutants had reduced ATPase activities and affected association with co-chaperones. However, there is no quantitative correlation between the reduction of the ATP hydrolysis rates and the effects of the S485 variants *in vivo*. The interaction of E and Y mutations with p23/Sba1 was lost and with Aha1 it was moderately reduced. Although the binding with Aha1 was uniformly reduced by S485 variants, the degree to which Aha1 could stimulate their inherent ATPase activity varied significantly between the mutations. For S485E, the Aha1 activation was significantly compromised while for S485Y it was only partly reduced. This could explain the different effects of the E and Y mutations on cell viability. The co-chaperone binding study suggested an influence of these variants on the Hsp90 conformational dynamics. The impaired activity of the S485 mutants results from an increased stability of the open conformation and an inability to undergo structural compaction in the presence of nucleotides (Figure 30). Thus, the functionally important phospho-site S485 located in a region distant from the catalytic site is involved in signal propagation and inter-domain communication pathways in Hsp90 dimer.

7.6.3 Phospho-sites S602 and S604

The two active phosphorylation sites S602 and Ppt1-regulated S604 were identified in the C-domain. Cells expressing the phospho-mimicking variants showed no visible effect on yeast growth and client protein activation under normal temperatures implying no alterations in the general chaperone function mediated by Hsp90. It appears however that in particularly S604 serves as a switch point allowing regulating Hsp90 action under non-permissive conditions, such as elevated temperatures, Hsp90 inhibition or DNA damage caused by UV treatment. This shows how certain ‘silent’ phosphorylation sites may be activated by environmental fluctuations acting as molecular sensors. Phospho-mimicking variants mildly affected

the ATPase activity and had no impact on the nucleotide-driven conformational cycle. Nevertheless, certain conformational transitions, specifically facilitated by Aha1 necessary to achieve ATPase competence, were influenced by the C-domain phospho-site mutations (Figure 30). Under non-optimum conditions, when Hsp90 levels become limiting, Aha1 increases the efficiency of the Hsp90 system. These steps are apparently influenced by the C-domain phosphorylation. This explains why S604 phosphorylation becomes critical only under certain circumstances. Structural analysis of the M-C domain revealed that the two phospho-sites reside in the surface-exposed C-domain flexible loop (Ali et al., 2006). The exact position of these two sites in the closed conformation of the full length Hsp90 is yet unknown as the region containing these two sites is not resolved (Ali et al., 2006). The C-domain phospho-sites represent a conformational switch region that propagates long-range communication and transmits structural information along the dimeric Hsp90 protein.

The data presented here reveal that phosphorylation can modulate Hsp90 function in a number of ways: the modifications can regulate the enzymatic activity by influencing the conformational transitions either locally or globally, alter co-chaperone interaction and/or their mechanism of action thereby regulating distinct facets of the chaperone cycle. The fact that Ppt1 activity is associated with the regulation of the two active phosphorylation sites shows important contribution of this phosphatase to the Hsp90 phospho-regulation.

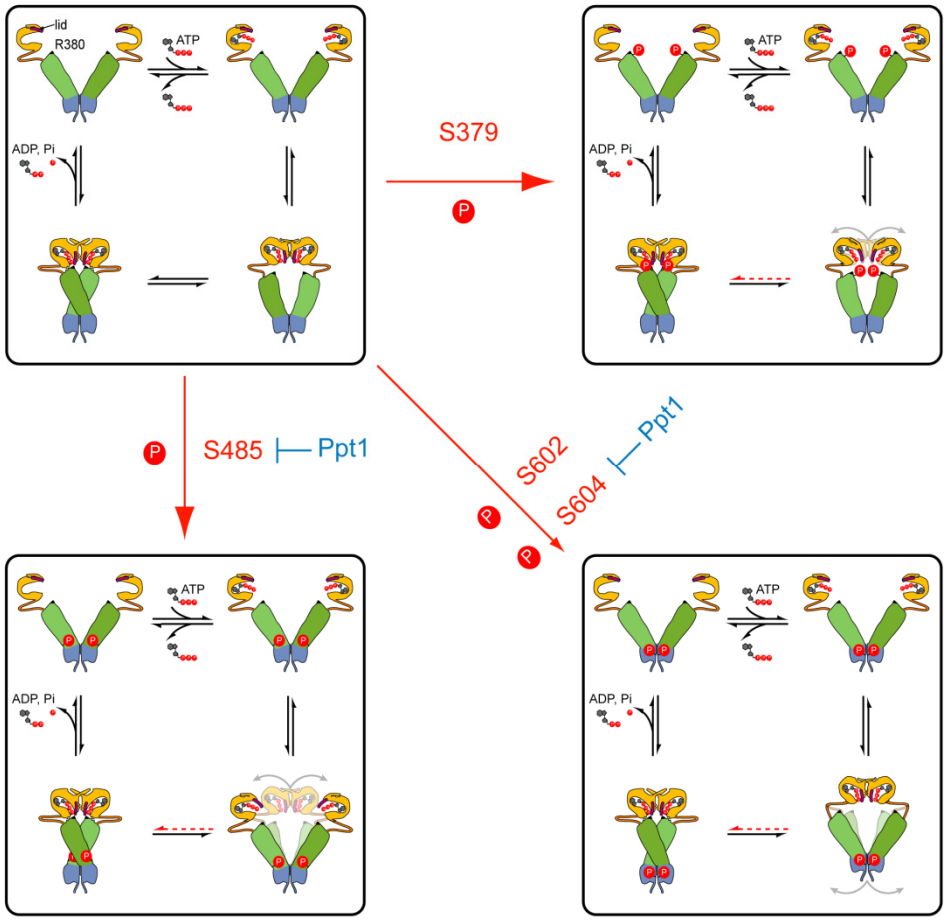

Figure 30. Mechanism of the Hsp90 phospho-regulation
The four phosphorylation sites acting on the conformational dynamics of Hsp90 employ different mechanisms to regulate Hsp90 function. Phosphorylation at S379, located in a catalytic loop involved in ATP hydrolysis, affects conformational rearrangements during the ATPase cycle by interfering with the formation of the active site. Mutation of S485 located in a contact region between the C-terminal and the M-domain modulates conformational flexibility essential in the communication within dimeric Hsp90. Modification of S602 and S604 in the C-terminal domain influences the inter-subunit communication required for efficient ATP hydrolysis.

7.7 Different Hsp90 phosphorylation scenarios

Although in this study several phosphorylation sites were identified, the data do not provide information about Hsp90 phosphorylation pattern in yeast. It is not sure whether certain phosphorylations are highly abundant and others are restricted to only a small subpopulation of Hsp90. It can be anticipated that Hsp90 occurs in different phospho-isoforms (i.e. small fraction of Hsp90 highly phosphorylated versus larger fraction of Hsp90 pool with only few phosphorylation sites being modified). Thus, the strong inhibitory influence of S379 and S485 phosphorylation discovered in this study can be limited to only a small amount of Hsp90 molecules in the cell. It

could well be that certain phosphorylations are specific for subcellular compartments (i.e. nuclear or cytoplasmic forms). In agreement, three phosphorylation sites S379, S485 and S604 affected the nuclear processes suggesting that their phosphorylation may alter Hsp90 translocation. It seems plausible that different Hsp90 phospho-variants are populated in response to various stimuli. It is supported by the notion that Ppt1 levels are highest during periods of rapid growth and drop off when cells enter stationary phase or are exposed to stress conditions. Thus, depending on the physiological state of the cell, different Hsp90 phosphorylation scenarios can be suggested (Figure 31). One foresees that Hsp90 in a fully phosphorylated form is silenced. Next, Ppt1 activation keeps S485 and S604 in the dephosphorylated form while other two active sites are being phosphorylated. In this incompletely phosphorylated state Hsp90 restores partly its chaperone activity. Third possibility envisions that Hsp90 is fully dephosphorylated and active. Thus, when environmental conditions change suddenly, the cell must respond rapidly and adjust Hsp90 potential to provide an adaptation to the new conditions. This could be a mechanism to ensure an optimal internal milieu.

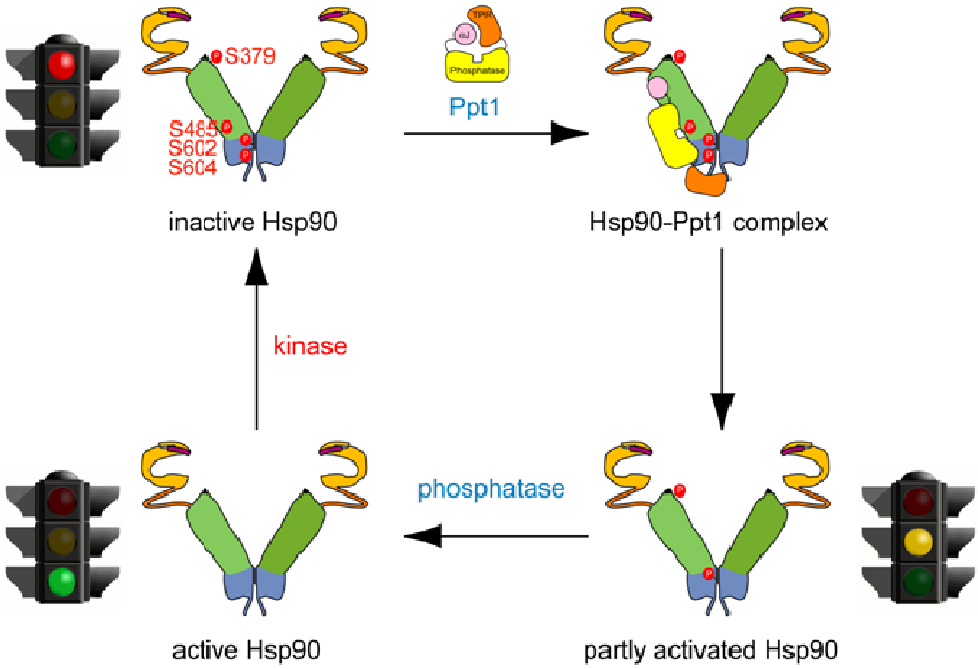

Figure 31. Hsp90 phosphorylation scenarios
Hsp90 can be phosphorylated at four active phosphorylation sites (S379, S485, S602, S604) which attenuates its chaperone activity. Ppt1 can associate with Hsp90 and dephosphorylate S485 and S604 while S379 and S602 are still phosphorylated. In this form Hsp90 restores partly its chaperone function. Finally, yet unknown phosphatase(s) can dephosphorylate Hsp90 at S379 and S602 resulting in its full activation. For simplicity, the phosphorylation of one Hsp90 protomer only is presented.

8 Materials and Methods

8.1 *E. coli* strains

Strain	Genotype	Origin
E. coli DH10B	F⁻*ara*D 139Δ(*ara leu*) 7697*Δlac*X74 *gal*U *gal*K *mcr*A Δ(*mrr- hsd*RMS-*mcr*BC) *rps*L *dec*R 380 Δ*lac*Z ΔM15 *end*A1 *nup*G *rec*A1	Berthesda Research Laboratories (Berthesda, USA)
E. coli XL1 Blue	*rec*A1 *end*A1 *gyr*A96 *thi*-1 *hsd*R17 *sup*E44 *rel*A1 *lac* [F'proAB *lac*IqZDM15 Tn10 (*Tet*R)]	Stratagene (La Jolla, USA)
E. coli BL21 (DE3) Codon Plus	F⁻*omp*T *hsdS*$_B$ ($r_B^-m_B^-$) gal *endA* The [argU ileY leuW Cam^R]	Stratagene (La Jolla, USA)

8.2 *S. cerevisiae* strains

Strain	Genotype	Origin
YAL6B	MATa; *his3Δ leu2Δ met15Δ ura3Δ lys1::KanMX6 arg4::KanMX4*	Henrik Daub
YAL6B-*Δppt1*	MATa; *his3Δ leu2Δ met15Δ ura3Δ lys1::KanMX6 arg4::KanMX4* YGR123c:: NatMX4	Sebastian Wandinger
ECU82α	MATα; can1-100 *ade2*-1 *his3*-11,15 *leu2*-3,12 trp1-1 *ura3*-1 hsc82::LEU2 hsp82::LEU2 (pKAT6)	Debbie Nathan

8.3 Plasmids

Name	Vector	Cloning site	Origin
Wt-Hsp90	pET28b	NdeI/SalI	GeneArt (Regensburg, Germany)
S282E-Hsp90	pET28b	NdeI/BamHI	This work
S297E-Hsp90	pET28b	NdeI/BamHI	This work
S334E-Hsp90	pET28b	NdeI/BamHI	This work
S379E-Hsp90	pET28b	NdeI/BamHI	This work
S450E-Hsp90	pET28b	NdeI/BamHI	This work
S456E-Hsp90	pET28b	NdeI/BamHI	This work
S485E-Hsp90	pET28b	NdeI/BamHI	This work
S485Y-Hsp90	pET28b	NdeI/BamHI	This work
S485A-Hsp90	pET28b	NdeI/BamHI	This work
T533E-Hsp90	pET28b	NdeI/BamHI	This work
S602E-Hsp90	pET28b	NdeI/BamHI	This work
S604E-Hsp90	pET28b	NdeI/BamHI	This work
All-A10-Hsp90	pET28b	NdeI/SalI	This work
All-E10-Hsp90	pET28b	NdeI/SalI	This work
All-A8-Hsp90	pET28b	NdeI/SalI	This work
All-E8-Hsp90	pET28b	NdeI/SalI	This work
Lidless-Hsp90	pET28b		Klaus Richter (TUM)
D61C-Hsp90	pET28b		Martin Hessling (TUM)
Q385C-Hsp90	pET28b		Martin Hessling (TUM)
D61C_S379E-Hsp90	pET28b	NdeI/BamHI	This work
Q385C_S379E-Hsp90	pET28b	NdeI/BamHI	This work
D61C_S602E-Hsp90	pET28b	NdeI/BamHI	This work
Aha1	pET28b		Klaus Richter (TUM)
Sti1	pET28b		Andreas Schmidt (TUM)
Sba1	pET28b		Martin Hessling (TUM)
Wt-Hsp90	P423GPD	BamHI/SalI	GeneArt (Regensburg, Germany)
S282E-Hsp90	P423GPD	BamHI/SalI	This work
S297E-Hsp90	P423GPD	BamHI/SalI	This work
S334E-Hsp90	P423GPD	BamHI/SalI	This work
S379E-Hsp90	P423GPD	BamHI/SalI	This work
S450E-Hsp90	P423GPD	BamHI/SalI	This work
S456E-Hsp90	P423GPD	BamHI/SalI	This work
S485E-Hsp90	P423GPD	BamHI/SalI	This work
S485Y-Hsp90	P423GPD	BamHI/SalI	This work
S485A-Hsp90	P423GPD	BamHI/SalI	This work
T533E-Hsp90	P423GPD	BamHI/SalI	This work
S602E-Hsp90	P423GPD	BamHI/SalI	This work

S604E-Hsp90	P423GPD	BamHI/SalI	This work
All-A10-Hsp90	P423GPD	BamHI/SalI	This work
All-E10-Hsp90	P423GPD	BamHI/SalI	This work
All-A8-Hsp90	P423GPD	BamHI/SalI	This work
All-E8-Hsp90	P423GPD	BamHI/SalI	This work

8.4 Chemicals

Name	Origin
Acrylamide solution (38% with 2% bisacrylamide)	Roth (Karlsruhe, Germany)
Adenosyl-imidodiphosphate (AMP-PNP)	Roche (Mannheim, Germany)
Adenosine 5′-O-(3-thiotriphosphate) ATPγS	Roche (Mannheim, Germany)
Adenosine-5´-diphosphate (ADP), disodium salt	Roche (Mannheim, Germany)
Adenosine-5´-triphosphate (ATP), disodium salt	Roche (Mannheim, Germany)
[^{32}P]ATP	Hartmann Analytics (Darmstadt, Germany)
Agarose, ultra pure	Roth (Karlsruhe, Germany)
Albumin from bovine serum	Sigma (St. Louis, USA)
Ammoniumperoxodisulfate (APS)	Roche (Mannheim, Germany)
Ammoniumsulfate	Merck (Darmstadt, Germany)
Ampicillin	Roth (Karlsruhe, Germany)
Bacto Agar	Difco (Detroit, USA)
Bacto Peptone	Difco (Detroit, USA)
Bacto Trypthone	Difco (Detroit, USA)
Bacto Yeast Extract	Difco (Detroit, USA)
Bromephenolblue S	Serva (Heidelberg, Germany)
CHAPS	Sigma (St. Louis, USA)
Complete Protease Inhibitor Cocktail Tablets	Roche (Mannheim, Germany)
Coomassie Brilliant Blue R-250	Serva (Heidelberg, Germany)
Coomassie Protein Assay Reagent	Pierce (Rockford, USA)
Desoxynucleotidetriphosphates (dNTPs)	Roche (Mannheim, Germany)
5,5’ Dithio-bis-Nitrobenzoic acid (DTNB)	Sigma (St. Louis, USA)
1,4-Dithiothreithol (DTT)	Roth (Karlsruhe, Germany)
Ethanol, p.a.	Roth (Karlsruhe, Germany)
Ethylendiamintetraacidic acid (EDTA)	Merck (Darmstadt, Germany)
Ethidiumbromide	Sigma (St. Louis, USA)
Glutaraldehyd, 25% in water	Serva (Heidelberg, Germany)
Glycerol, 99 %	ICN, (Costa Mesa, USA)

Guanidine hydrochloride, p.a.	ICN, (Costa Mesa, USA)
N-(2-Hydroxyethyl)-piperazine-N'-2-Ethanesulfonic acid (HEPES)	ICN, (Costa Mesa, USA)
Isopropanol	Roth (Karlsruhe, Germany)
Isopropyl-β-D-thiogalaktopyranosid (IPTG)	Roth (Karlsruhe, Germany)
Kanamycin	Roth (Karlsruhe, Germany)
β-Mercaptoethanol, pure	Merck (Darmstadt, Germany)
Nourseothricin	Werner Bioagents (Jena, Germany)
Pharmalyte 3 – 10	GE Healthcare (Freiburg, Germany)
Phosphatase inhibitor cocktail 1	Sigma (St. Louis, USA)
Phosphatase inhibitor cocktail 2	Sigma (St. Louis, USA)
Salmon sperm DNA	Sigma (St. Louis, USA)
Serdolit MB-1	Serva (Heidelberg, Germany)
Sodiumdodecylsulfate (SDS)	Roth (Karlsruhe, Germany)
Sodium fluoride	Sigma (St. Louis, USA)
Sodium orthovanadate	Sigma (St. Louis, USA)
N,N,N',N'-Tetramethylethylendiamin (TEMED)	Roth (Karlsruhe, Germany)
Thiourea	Sigma (St. Louis, USA)
Tris-(hydroxymethyl)-aminomethan (Tris)	ICN, (Costa Mesa, USA)
Urea, p.a.	Roth (Karlsruhe, Germany)
Polyoxyethylen-sorbitan-monolaurat (Tween-20)	Merck (Darmstadt, Germany)
Yeast Nitrogene Base	Difco (Detroit ,USA)

All other reagents were from Merck (Darmstadt, Germany) except of fluorescence labels and were of grade p.a. if not stated otherwise. For the preparation of buffers double distillate water was used.

8.5 Fluorescence label

Name	**Origin**
Atto 488 maleimide	AttoTec (Germany)
Atto 550 maleimide	AttoTec (Germany)
Alexa Fluor-488 succinimidyl ester	Invitrogen (Karlsruhe, Germany)

8.6 Markers and kits

Name	Origin
BiaCore amine coupling kit	BiaCore Inc. (Uppsala, Sweden)
Roti-Mark prestained (SDS-PAGE and Western blot)	Roth (Karlsruhe, Germany)
ECL+ plus Western Blotting Detection System	Amersham Pharmacia (Uppsala, Sweden)
1 kb DNA ladder molecular weight standard	New England Biolabs (Beverly, USA)
Wizard® Plus SV Mini-Preps DNA purification kit	Promega (Madison, USA)
High Pure PCR Product Purification Kit	Promega (Madison, USA)
High-Range-molecular weight marker (HMW for SDS-PAGE)	BioRad (Munich, Germany)
Low-Range-molecular weight marker (LMW for SDS-PAGE)	BioRad (Munich, Germany)
Luciferase assay reagent	Promega (Madison, USA)
Tropix Galacto-LightPlus Kit	Applied Biosystems (Foster City, USA)

8.7 Proteins and antibodies

Name	Origin
Alkaline phosphatase	Roche (Mannheim, Germany)
Apyrase	Sigma (St. Louis, USA)
Casein kinase II	Roche (Mannheim, Germany)
Amino acids for SILAC labeling	Cambridge Isotope Laboratories (Andover, USA) and Sigma-Isotec (Miamisburg, USA)
Polynucleotide kinase PNK	Roche (Mannheim, Germany)
Pfu DNA polymerase	Roche (Mannheim, Germany)
Pfu-Turbo DNA polymerase	Roche (Mannheim, Germany)
Restriction enzymes	New England Biolabs (Beverly, USA)
T4-Ligase	Promega (Madison, USA)
Monoclonal IgG-POD conjugate against rabbit-IgG (sheep)	Sigma (St. Louis, USA)
Monoclonal IgG-POD conjugate against mouse-IgG (sheep)	Sigma (St. Louis, USA)
Polyclonal serum against Hsp90 (rabbit)	Pineda (Berlin, Germany)
Polyclonal serum against Ppt1 (rabbit)	Pineda (Berlin, Germany)
human Hsp90-specific antibody sc-13119	Santa Cruz Biotechnology (Santa Cruz, USA)

phospho-tyrosine specific antibody 4G10	Upstate (Hamburg, Germany)
phospho-serine antibody Q5	Qiagen (Valencia, CA, USA)
phosphoglycerate kinase antibody 22C5	Invitrogen (Karlsruhe, Germany)

8.8 Chromatography material

Name	Origin
HiLoad FF Ni-NTA (5 mL)	GE Healthcare (Freiburg, Germany)
Resource-Q (6 mL)	GE Healthcare (Freiburg, Germany)
Superdex 75 Prep Grade (26/60)	GE Healthcare (Freiburg, Germany)
Superdex 200 Prep Grade (26/60)	GE Healthcare (Freiburg, Germany)
Superdex 200 10/300GL (HPLC)	GE Healthcare (Freiburg, Germany)

8.9 Buffers

Molecular biology		
TAE (50x)	2 M	Tris/acetate pH 8.0
	50 mM	EDTA pH 8.0
BJ (10x)	50% (v/v)	Glycerol
	10 mM	EDTA pH 8.0
	0.2% (w/v)	Bromphenolblue
	0.2% (w/v)	Xylencyanol
1 % Agarose-Solution:	1 g	Agarose
	100 mL	TAE (1x)
	1 µL	Ethidiumbromide-Solution
Solution A	13 mL	3 M NaAc (pH 5.5)
	100 mL	1 M $CaCl_2$
	25 mL	2.8 M $MnCl_2$
	862 mL	H_2O
Solution A + Glycerol	69 mL	Glycerol (87%)
	331 mL	Solution A
Protein chemical buffers		
SDS running buffer (10x)	250 mM	Tris/HCl pH 6.8
	2 M	Glycine
	1% (w/v)	SDS
Laemmli sample buffer	312.5 mM	Tris/HCl pH 6.8
(5x)	10% (w/v)	SDS
	50% (v/v)	Glycerol
	2.5% (v/v)	β-mercaptoethanol
	0.05% (w/v)	bromphenolblue
separating gel buffer (4x)	250 mM	Tris/HCl pH 8.8

	0.8% (w/v)	SDS
stacking gel buffer (2x)	250 mM	Tris/HCl pH 6.8
	0.4% (w/v)	SDS
Fairbanks A	2.5 g	Coomassie Brilliant Blue R-250
	250 mL	Ethanol
	80 mL	Acetic acid
	adjust to 1 L	H_2O
Fairbanks D	250 mL	Ethanol
	80 mL	Acetic acid
	adjust to 1 L	H_2O
Western Blotting	36 g	Glycine
Transfer Buffer	7.6 g	Tris
	500 mL	Methanol
	adjust to 2.5 L	H_2O
PBS-T	5.84 g	NaCl
	11.5 g	Na_2HPO_4
	2.96 g	NaH_2PO_4
	adjust to 1 L	H_2O
	1 mL	Tween-20
Buffers for protein purification		
Ni-NTA buffer A	40 mM	Sodium Phosphate pH 7.5
	150 mM	KCl
	6 mM	Imidazol
Ni-NTA buffer B	40 mM	Sodium Phosphate pH 7.5
	150 mM	KCl
	300 mM	Imidazol
Resource-Q buffer A	40 mM	HEPES/KOH pH 7.5
	20 mM	KCl
	1 mM	DTT
	1 mM	EDTA
Resource-Q buffer B	40 mM	HEPES/KOH pH 7.5
	1 M	KCl
	1 mM	DTT
	1 mM	EDTA
GF buffer	40 mM	HEPES/KOH pH 7.5
	300 mM	KCl
	1 mM	DTT
	1 mM	EDTA
Dialysis buffer	40 mM	HEPES/KOH pH 7.5
	20 mM	KCl

8.10 Equipment and programs

Equipment	
Absorption Spectrophotometers	
Varian Cary 50 Bio UV-VIS-Spectrophotometer	Varian (Darmstadt, Germany)
Circular dichroism spectropolarimeter	
Jasco J715 with PTC 343 Peltier temperature device	Jasco (Groß-Umstadt, Germany)
Fluorescence Spectrophotometer	
Spex FluoroMaxIII spectrofluorimeter (with autopolarizers) with temperature adjustable cuvette holder	Jobin Yvon (Munich, Germany)
Surface plasmon resonance instrument	
BiaCore X	BiaCore (Uppsala, Sweden)
Analytical ultracentrifuge	
XL-I equipped with absorbance and interference detection systems	BeckmanCoulter (Krefeld, Germany)
XL-A equipped with absorbance and fluorescence detection systems	BeckmanCoulter (Krefeld, Germany) and AVIV Biomedical (Lakewood, USA)
Chromatography devices	
ÄKTA FPLC	GE Healthcare (Freiburg, Germany)
Super-loop 150 mL	GE Healthcare (Freiburg, Germany)
HPLC devices	
Shimadzu HPLC system equipped with autosampler	Shimadzu (Munich, Germany)
Gel electrophoresis and blotting devices	
Hoefer Mighty Small II	GE Healthcare (Freiburg, Germany)
Fast Blot B44 Apparatus	Biometra (Göttingen, Germany)
Power amplifier	
LKB-GPS 200/400	Amersham (Uppsala, Sweden)
EPS 3500, 301 and EPS 1001	GE Healthcare (Freiburg, Germany)
Analytical Balance	
BP 121 S	Satorius (Göttingen, Germany)
BL 310	Satorius (Göttingen, Germany)
Centrifuges	
Rotina 46 R Centrifuge	Hettich (Tuttlingen, Germany)
Eppendorf-Centrifuge 5415 C	Eppendorf (Hamburg, Germany)
Avanti J25, JA-10 and JA-25.50 Rotor	Beckmann (Vienna, Austria)
Plate reader	
Genios SpectraFluor plus	Tecan (Creilsheim, Germany)
Phosphoimager	
Typhoon 9200 and Storage	Amersham (Uppsala, Sweden)

Phosphoscreen	
Additional Equipment	
Cell disruption machine Basic Z	Constant Systems (Warwick, England)
Eppendorf-Thermomixer	Eppendorf (Hamburg, Germany)
Ice machine	Ziegra (Isernhagen, Germany)
Magnetic stirrer Heidolph MR2000	Heidolph (Kehlheim, Germany)
Metal thermo block TB 1	Biometra (Göttingen, Germany)
Mixer Mill MM 400	Retsch (Haan, Germany)
pH-Meter	WTW (Weilheim, Germany)
Thermocycler MWG	MWG, Ebersberg, Germany
Incubator	New Brunswick Scientific (Nürtingen, Germany)
Water bath Haake F6-K	Haake (Karlsruhe, Germany)
Centricon 10/30 microconcentrators	Millipore (Bedford, USA)
Dialysis tubes Spectra/Por (6-8 kDa)	Spectrum (Houston, USA)
Cuvettes	Zefa (Munich, Germany)
Computer Programs and Web Tools	
Adobe CS	Adobe Systems (San Jose, USA)
Microsoft Office 2007	Microsoft (Unterschleißheim, Germany)
Origin 8	OriginLab (Nothhampton, USA)
ClustalW sequence alignment	http://www.genome.jp/tools/clustalw/
PhosphoSitePlus	http://www.phosphosite.org/
ProtParamTool	ExPasy (http://www.expasy.ch)
Reference Manager 12	ISI (Philadelphia, USA)
ImageJ	NIH (Bethesda, USA)

8.11 Media

Media	
Media for *E. coli* growth	
LB_0	
LB powder	20 g/L
Bacto Agar (for plates)	20 g/L
Antibiotic concentrations used for *E. coli* growth:	
Ampicillin	100 µg/mL
Kanamycin	35 µg/mL
Chloramphenicol	35 µg/mL
Media for yeast growth	
YPD	
Yeast Extract	5 g
Bacto Pepton	10 g
Glucose	20 g
H_2O	adjust to 1 L

Bacto Agar (for plates)	20 g
CSM	
YNB	6.7 g
Selektive-Amino acid-Mix	1.0 g
Glucose	20 g
1 M NaOH	1 mL
H_2O	adjust to 1 L
Bacto Agar (for plates)	20 g
Selective amino acid mix	
Adenine	0.5 g
Alanine	2.0 g
Arginine	2.0 g
Asparagine	2.0 g
Aspartate	2.0 g
Cysteine	2.0 g
Glutamine	2.0 g
Glutamate	2.0 g
Glycine	2.0 g
Histidine	2.0 g
Inositole	2.0 g
Isoleucine	2.0 g
Leucine	10.0 g
Lysine	2.0 g
Methionine	2.0 g
Phenylalanine	2.0 g
Proline	2.0 g
Serine	2.0 g
Threonine	2.0 g
Tryptophane	2.0 g
Uracil	2.0 g
Valine	2.0 g

8.12 Molecular methods

8.12.1 Cultivation and storage of *E. coli*

E. coli cells were incubated at 37 °C either on LB plates or in LB liquid media. To select cells harboring the corresponding resistance genes either on the plasmid or in the genome, strains were selected by supplementing medium with appropriate antibiotics. Liquid cultures were inoculated 1:100 with fresh overnight cultures or by transferring single colony from a plate. Growth of *E. coli* cells was monitored

photometrically at 600 nm where OD_{600} of 1 equals approximately $8x10^8$ cells/mL (Sambrook et al., 1989). For long-term storage, 300 µL 50% glycerol were added to 700 µL of an exponentially growing bacterial culture, shock-frozen in liquid nitrogen and stored at -80 °C.

8.12.2 Cultivation and storage of *S. cerevisiae*

S. cerevisiae was cultivated at 30 °C if not indicated otherwise, either on YPD, on CSM plates or in liquid media. Strains were selected by omission of the appropriate amino acids or nucleotides in the media or by addition of an antibiotic (120 µg/mL Nourseothricin). Small liquid cultures were inoculated by transferring a single colony from a plate and larger liquid cultures were inoculated with stationary overnight cultures. Growth of yeast cells was monitored photometrically at 600 nm, where OD_{600} of 1 equals approximately $2x10^7$ cells/mL (Sambrook et al., 1989). For long-term storage, 300 µL 50 % glycerol were added to 700 µL of an exponentially growing yeast culture, shock-frozen in liquid nitrogen and stored at -80 °C.

8.12.3 PCR amplification

PCR was used to selectively amplify the desired DNA fragment from coding regions of plasmids and/or to subclone the DNA fragments in various other plasmids. Pfu polymerase was used with the buffer containing $MgCl_2$ and the reaction was performed as stated below. PCR products were analyzed by a 1% agarose gel electrophoresis supplemented with 0.001% ethidiumbromide solution.

Amplification of DNA fragments

Standard reaction mix:

sterile H_2O	84 µL
dNTPs (10 mM)	2 µL
Pfu polymerase (3 U/µL)	1 µL
Each primer (100 pmol/µL)	1 µL
Pfu 10x buffer	10 µL
Template DNA	1µL

Standard reaction protocol:

1 melting	95 °C	2 min
Repeat 2-4 25x		
2 melting	95 °C	1 min
3 annealing	52-55 °C	1 min
4 elongation	72 °C	6 min
5 elongation of short ends	72 °C	10 min
6 storage	4 °C	forever

Site-directed mutagenesis

Cloning of Hsp90 single phospho-site variants was performed using wt Hsp90-pET28b or wt Hsp90-p423GPD as templates. Pfu-Turbo polymerase was used with the buffer containing $MgCl_2$ and the reaction was performed as stated below. To introduce specific mutation, primer carrying the corresponding modified codon was used to amplify the entire plasmid. PCR products were analyzed by a 1% agarose gel electrophoresis supplemented with 0.001% ethidiumbromide solution.

Standard reaction protocol:

sterile H_2O	42 µL
dNTPs (10 mM)	1 µL
Pfu-Turbo polymerase (2.5 U/µL)	1 µL
Each primer (10 pmol/µL)	1 µL
Pfu 10x buffer	5 µL
Template DNA	1µL

Standard reaction protocol:

1 melting	95 °C	2 min
Repeat 2-4 35x		
2 melting	95 °C	1 min
3 annealing	52-55 °C	1 min
4 elongation	68 °C	12 min
5 storage	4 °C	forever

8.12.4 Purification and storage of DNA

Amplified DNA was purified with the Wizard Plus SV Miniprep DNA kit. DNA was stored at -20 °C in sterile H_2O.

8.12.5 DNA digestion, phosphorylation, dephosphorylation and ligation

DNA was digested, dephosphorylated and ligated using the following protocols.

DNA digestion protocol:

sterile H_2O	4 µL
Buffer 10x	5 µL
DNA	40 µL
Restriction enzyme (10 U/µL)	1 µL

Mixture with each restriction enzyme was incubated at 37 °C for 4 h.

DNA dephosphorylation

After digestion with restriction enzymes, the vector DNA was treated with alkaline phosphatase to prevent its religation. To this end, 10 µl of 10x reaction buffer and 2 µl of alkaline phosphatase (1 U/µL) were added to 88 µL of a cut vector DNA and the mixture was incubated at 37 °C for 2 h.

DNA ligation protocol:

sterile H_2O	7 µL
Ligase (3 U/µL)	1 µL
Ligase buffer 10x	2 µL
Digested PCR products (insert)	7 µL
Digested plasmid DNA (vector)	3 µL

Mixture was incubated at 4 °C overnight.

DNA phosphorylation

After site-directed mutagenesis, PCR products were phosphorylated by PNK according to the protocol below:

DNA phosphorylation protocol:

DNA	23 µL
ATP (100 mM)	3 µL

Ligase buffer 10x	3 µL
PNK (10 U/µL)	1 µL

The mixture was incubated at 37 °C for 2 h.

8.12.6 Sequencing of DNA

All constructs were sequenced to confirm their correct sequence. Purified plasmid DNA was sent to GATC Biotech (Konstanz, Germany) for sequencing.

8.12.7 Preparation of chemical competent *E. coli* cells

Competent *E. coli* cells were prepared according to the protocol provided by (Sambrook et al., 1989). To 100 mL of fresh *E. coli* liquid cultures with OD_{600} between 0.5 and 1, 2 mL of 1M $MgCl_2$ was added and the cells were incubated for 10 min at 37 °C with agitation. The cells were next incubated for 1 h on ice, harvested by centrifugation at 4500 rpm for 5 min, resuspended in Solution A and incubated for 1 h on ice. The cell were again harvested by centrifugation and resuspended in 2 mL of Solution B, aliquoted and stored at -80 °C.

8.12.8 Transformation of *E. coli* cells

To 50 µL of chemical competent *E. coli* cells 1 µL of plasmid DNA was added. The mixture was first incubated on ice for 5 min, followed by a heat step at 42 °C for 60 sec. Subsequently, the cells were incubated on ice for 5 min. After addition of 800 µL of LB_0, the cells were incubated at 37 °C for 30 min in a shaking incubator. The cells were harvested by centrifugation at 14000 rpm for 1 min, the supernatant was discarded, cell pellet was resuspended in the remaining media and plated on the respective selection plates followed by incubation at 37 °C.

8.12.9 Transformation of *S. cerevisiae*

Yeast cultures were grown overnight at 30 °C to saturation. 1 mL of the cell culture was spun down, supernatant was decanted and the cells were left in 100 µL remaining media. 2µL of DNA carrier at the concentration of 10 mg/mL and 1 µL of a

plasmid DNA were added to the mixture and resuspended. Next, 0.5 mL of the plate mixture and 20 µL of 1 M DTT were added, the mixture was again resuspended and incubated at RT for 8-12 h. The cells were-heat stressed for 10 min at 42 °C, spun down for 1 min at 14000 rpm, the supernatant was decanted, cell pellet was resuspended in the remaining media, plated on the respective selective plates and incubated at 30 °C.

Plate mix:

Sterile 45% PEG	90 mL
1 M LiOAc	10 mL
1 M Tris/HCl (pH 7.5)	1 mL
0.5 M EDTA	0.2 mL

8.12.10 Metabolic yeast cell labeling and Hsp90 precipitation

YAL6B yeast cells that either expressed or were deficient for Ppt1, were differentially labeled with either 100 µg/mL of normal L-arginine (Arg^0) and L-lysine (Lys^0) or the isotopic variants L-arginine-U-$^{13}C_6$-$^{15}N_4$ (Arg^{10}) and L-lysine-U-$^{13}C_6$-$^{15}N_2$ (Lys^8) or L-lysine-U-$^{13}C_6$ (Lys^6). Wt and *Δppt1* YAL6B cells were grown for 17 h at 30 °C for full metabolic incorporation of the labeled arginine and lysine. Cells were harvested by centrifugation for 5 min at 4500 rpm at 4 °C, resuspended in the lysis buffer (40 mM HEPES/KOH pH 7.5, 150 mM KCl, 2 mM EDTA, 2 mM EGTA, 20 mM NaF, 5 mM Na_3VO_4, protease inhibitor cocktail with AEBSF, aprotinin, leupeptin, E-64/EDTA, phosphatase inhibitor cocktail 1, phosphatase inhibitor cocktail 2) and lysed. To identify phosphorylation sites regulated by Ppt1 activity, the lysates from cells expressing Ppt1 and cells deficient for Ppt1 were separated. The lysis buffer was additionally supplemented with 100 nM MEEVD-containing peptide and 100 nM okadaic acid to prevent Ppt1 association with Hsp90 and inhibit its phosphatase activity, respectively. In total, four biological replicate experiments were performed that included two with reciprocal SILAC encoding to quantify the effect of cellular Ppt1 deficiency on yeast Hsp90 phosphorylation. The total protein concentration was determined by a Bradford assay prior to immunoprecipitation. Hsp90 was isolated from 400 µL lysates by immunoprecipitation for 3 h at 4 °C on a rotating wheel using 40 µL polyclonal anti-Hsp90 antiserum and 60 µL protein A Sepharose (GE

Bioscience, Munich, Germany). The mixture was washed three times with 750 µL buffer containing 40 mM HEPES/KOH pH 7.5, 150 mM KCl.

8.13 Protein chemical methods

8.13.1 SDS polyacrylamid gel electrophoresis

SDS-PAGE was performed according to the protocol provided by Laemmli (Laemmli, 1970).

12.5% Separation gel:

40% Acrylamide (40% w/v, Acrylamide/Bisacrylamide 38:2)	3.125 mL
4 x SDS-Buffer (0.8% SDS, 1.5 M Tris/HCl, pH 8.8)	2.5 mL
H_2O	4.375 mL

5% Stacking gel:

40% Acrylamide (40% w/v, Acrylamide/Bisacrylamide 38:2)	0.625 mL
2 x SDS-Buffer (0.4% SDS, 0.25 M Tris/HCl, pH 6.8)	2.5 mL
H_2O	1.875 mL

Addition of TEMED and APS induced the polymerization of the solution. Electrophoresis was performed at a constant current of 35 mA per gel for 45 min. Gels were stained with Coomassie according to the protocol provided by Fairbanks (Fairbanks et al., 1971). Protein solution was mixed with 5x Laemmli buffer and cooked at 95 °C for 5 min prior loading on the gel. The molecular weight of the analyzed proteins was compared with LMW or HMW marker standards.

8.13.2 2D gel electrophoresis

Sample preparation and 2D gel electrophoresis were performed as described (Hiniker and Bardwell, 2004). To 1 mL overnight yeast cultures 400 µL of 50% TCA was added, the mixture was incubated on ice for 1 h, harvested by centrifugation at 14000 rpm for 45 min at 4 °C at and the supernatant was decanted. Cell pellet was resuspended in 500 µL acetone, vortexed, harvested by centrifugation for 5 min at 4 °C at 14000 rpm and again the supernatant was decanted. Cell pellet was let dry on the bench for 15 min. 1 mL of 2D-lysis buffer was added and the mixture was

incubated with agitation at 1000 rpm, at 20 °C for 1 h. 450 µL of the sample was applied to pH gradient 4-7 strips (Imobiline DryStrip pH 4 – 7, GE Healthcare) followed by separation on 10% gel by SDS-PAGE. Protein spots corresponding to Hsp90 were excised from 2D gels, digested with trypsin, and identified by Maldi ToF/ToF MS. Hsp90 was detected by Western blot using Hsp90- and phospho-serine-specific antibodies and both Hsp90 protein and phosphorylation levels were quantified by ImageJ. 2D-PAGE and staining was performed by Bettina Richter.

2D-lysis buffer:

7 M	Urea
2 M	Thiourea
65 mM	DTT
32,5 mM	CHAPS
1 % (w/v)	Serdolit MB-1
2 % (v/v)	Pharmalyte 3-10

8.13.3 Western blotting

Proteins were first separated on a gel by SDS-PAGE and subsequently electrophoretically transferred on a nitrocellulose membrane in a Semi-Dry blotting apparatus (Biometra, Göttingen, Germany) at a constant current of 75 mA per SDS-PAGE gel for 1 h. After the transfer, membranes were incubated in a PBS-T buffer supplemented with 5% milk powder with agitation at 4 °C overnight to block free binding sites. The primary antibody was diluted in PBS-T buffer supplemented with 5% milk powder (dilution depended on the individual antibody) and incubated for 1 h at RT. The membrane was washed 3x for 20 min with PBS-T buffer and incubated for 1 h with a peroxidase-conjugated secondary antibody (dilution 1:40000) at RT followed by three washing steps with PBS-T buffer, 20 min each. Detection was performed with the ECL detection kit according to the protocol provided by supplier.

8.13.4 Protein expression and purification

All recombinant proteins were expressed in *E.coli* BL21 (DE3) codon plus cells from pET28b vector. The expression was performed in 10 L LB medium supplemented with an antibiotic. Flasks were inoculated with fresh overnight cultures with 1:100

dilutions. Cells were grown at 37 °C and growth was monitored at OD_{600}. When the OD_{600} reached 0.6-0.8 the protein expression was induced by addition of 1 mM IPTG for 4 h at 37 °C. Cells where harvested by centrifugation for 10 min at 8000 rpm at 8 °C (JA 10 rotor), resuspended in the Ni-NTA buffer A supplemented with protease inhibitor mix HP and lysed using a cell disruption apparatus (Basic Z Constant System) at a pressure of 1.8 kbar. The lysate was centrifuged for 45 min at 18000 rpm at 8 °C (JA 25.50 rotor) and the supernatant was applied on the 5 mL HisTrap FastFlow Ni-NTA affinity chromatography column. Hsp90 variants and co-chaperones were purified using the following purification steps: Ni-NTA affinity chromatography followed by Resource-Q anion exchange chromatography and finally Superdex200 or Superdex75 pre-grade size exclusion chromatography. Proteins were dialyzed against 40 mM HEPES/KOH pH 7.5, 20 mM KCl, concentrated to 5-20 mg/mL and stored at -80 °C.

8.13.5 Protein concentration determination by Bradford assay

The Bradford assay is a colorimetric protein assay used to determine the protein concentration. The assay is based on the observation that the absorbance maximum of the dye Coomassie Brilliant Blue G-250 shifts from 465 nm (red form) to 595 nm (blue form) upon binding of a chromophore to particularly basic and aromatic amino acids in proteins (Bradford, 1976). To this end, the commercially available chromophore solution (Coomassie Protein Assay Reagent, Pierce, Rockford, USA) was first diluted 1:1 with water. 995 or 990 µL of the solution was mixed with 5 or 10 µL of protein solution, respectively, incubated for 5 min at RT and the absorption at 595 nm was measured. The standard curve was calculated on a BSA standard.

8.13.6 Protein labeling

Hsp90 variants were labeled at the engineered cysteine residues using Atto-488 or Atto-550 maleimide (AttoTec, Germany).Proteins were first incubated with 0.1 M DTT on ice for 2 h and separated from DTT by SEC-HPLC on a Superdex 200 10/300 in buffer containing 40 mM HEPES/KOH pH 7.5, 150 mM KCl. Hsp90 cysteine labeling was achieved by incubating the protein with the label at RT for 1 h followed by quenching the reaction by the addition of an excess of DTT. Protein was again

separated from the label and DTT by SEC-HPLC. Aha1 was labeled with Alexa Fluor-488 succinimidyl ester according to the protocol provided by the manufacturer. The labeling efficiency was determined using UV spectroscopy and the extinction coefficients provided by the manufacturer.

8.13.7 MS analysis

The MS experiments were performed in collaboration with Dr. Henrik Daub from the MPI of Biochemistry in Martinsried. Immunoprecipitated Hsp90 was eluted with buffer containing 7 M urea, 2 M thio-urea and 50 mM HEPES/KOH, pH 7.5 for 10 min at 37 °C on a shaker and subjected to in-solution digestion as described elsewhere (Olsen et al., 2006). Briefly, Hsp90 protein samples were supplemented with 1% n-octylglucoside, reduced, alkylated and then sequentially digested with 1.15 µg Lys-C (Wako, Neuss, Germany) for 4 h and by trypsin (sequencing grade, Promega, Mannheim, Germany) overnight. Phosphorylated peptides were purified by two consecutive incubations with 2.5 µg TiO_2 beads (GL Sciences Inc., Mainz, Germany) and analysed by liquid chromatography (LC)-MS analysis on LTQ-Orbitrap and LTQ-Orbitrap-Velos instruments (Thermo Fisher Scientific, Schwerte, Germany) as described previously (Daub et al., 2008; Olsen et al., 2006). For quantitative yeast Hsp90 analysis, 20% of the peptide sample were removed prior to phospho-peptide enrichment and then desalted by StageTip extraction for parallel assessment of yeast Hsp90 protein abundance by LC-MS analysis (Rappsilber et al., 2007). Raw MS data were processed using the software MaxQuant (v. 1.0.13.13) (Cox and Mann, 2008). MS data were searched against an in-house curated decoy yeast ORF SGD database (6,719 entries) (Gnad et al., 2009). MaxQuant searches were performed using previously described settings and filtering criteria (Schreiber et al., 2010). Identified peptides were automatically quantified and phosphorylation sites assigned by posttranslational modification (PTM) score-based localization in MaxQuant (Cox and Mann, 2008; Olsen et al., 2006). For phosphorylation site analysis, only class I sites with a localization probability of at least 0.75 (Olsen et al., 2006) were considered. Phosphorylation site assignments were further verified by manual inspection of MS/MS spectra. Yeast Hsp90 phosphorylation site ratios were computed by MaxQuant based on the identified and quantified phospho-peptides. Moreover, ratios were further normalized for Hsp82 and Hsc82 abundance based on

the quantification of unique non-phosphorylated peptides detected in StageTip-purified peptide samples.

8.13.8 Cross-linking experiment

Cross-linking was performed using 7 µg of wt Hsp90 or S485 mutants in a buffer containing 40 mM HEPES/KOH pH 7.5, 150 mM KCl, 5 mM $MgCl_2$. Hsp90 variants were preincubated for 15 min at RT. Cross-linking was initiated by addition of 2 µL 2.5% glutardialdehyde to a 15 µL final reaction volume and incubated for 3 min. The reaction was stopped by addition of 10 µL of 1 M Tris (pH 8.0). Samples were separated on a 4–12% (w/v) Tris–glycine precast polyacrylamide gel (Invitrogen, Karlsruhe, Germany) and visualized by Coomassie staining.

8.13.9 *In vitro* phosphorylation with CKII

6 µM Hsp90 in 200 µl final reaction volume was incubated in 20 mM Tris/HCl pH 7.8, 130 mM KCl, 10 mM $MgCl_2$ in the presence of 20 µL CKII (4 µmol Pi in 20 min at 37 °C) and 100 µM ATP for 3 h at 37 °C. As a control, 0.4 µM radioactively labeled ATP was added and Hsp90 phosphorylation was visualized by autoradiography using a Typhoon 9200 Variable Mode Imager (GE Bioscience, Munich, Germany).

8.13.10 Analytical ultracentrifugation

Experiments were performed in a Beckman XL instrument (Beckman Coulter, Brea, USA) equipped with either a fluorescence detection system (Aviv Biomedical, Lakewood, NJ) or with a standard interferometer attached to a UV/VIS detection system (Beckman Coulter, Brea, USA). Runs were performed at 35000 rpm for the analysis of conformational states in a standard buffer (40 mM HEPES/KOH pH 7.5, 150 mM KCl, 5 mM $MgCl_2$). To determine conformational changes in Hsp90 phospho-variants, the protein concentration was 0.5 mg/mL and nucleotides were added as indicated. Generally, the observed s values matched well with those determined with the UV-detection system. In cases were 2 mM nucleotides were present, the interference optics was used. Boundary analysis was performed

according to the dc/dt method (Stafford W.F., 1992). Data was fit to a Gaussian function in Origin.

To determine the affinity of Hsp90 to Aha1, Alexa Fluor-488-labeled Aha1 was used. Sedimentation properties were monitored by the fluorescence detection system. Data analysis was performed using a dc/dt approach. The resulting differentials of the sedimentation boundary were fitted using bi-Gaussian functions. This allowed determining s values of the uncomplexed and complexed proportion of the co-factors. The resulting s values and the amplitudes were used to estimate the binding affinity and the ability of the corresponding Hsp90 mutants to undergo conformational changes.

8.14 Spectroscopic methods

8.14.1 Absorption spectroscopy (UV-VIS)

Proteins in solution absorb UV light with maximum absorbance at around 280 and 200 nm. Amino acids containing aromatic side chains contribute to the absorbance at 280 nm, while the peptide bond to the absorbance at 190-230 nm.

	λ_{max}	ε_{max} (M^{-1} cm^{-1})
tryptophan	280	5700
tyrosine	274	1400
phenylalanine	257	200
disulphide bond	250	300

The protein concentration in solution can be determined directly from its absorbance at 280 nm according to the Lambert–Beer law:

Equation 1: $$A = \varepsilon * l * c$$

where A is absorbance, c is the protein concentration (M), l is the path length in cm, and ε (M^{-1} cm^{-1}) is the molar extinction coefficient which was calculated based on its amino acid composition using the program ProtParam.
(http://web.expasy.org/protparam/).

All UV absorption experiments were performed in UV Quartz cuvettes with a thickness of 1 cm in a final volume of 150 µL. All proteins were diluted to A between

0.5 and 1 to ensure the linearity of Lambert-Beer's law. Spectra were recorded from 220 to 400 nm and were buffer-corrected.

8.14.2 Circular dichroism spectroscopy

Circular dichroism (CD) spectroscopy measures the difference in the absorption of left and right circularly polarized light by optically active molecules. Proteins consist of a large number of optically active amino acids and form a secondary structure. CD spectroscopy in the far-UV (190-250 nm) allows determining the secondary structure of a protein. Within this region the chromophore is the peptide bond and the signal arises when it is placed in a regular, folded environment. α-helix exhibits two characteristic minima at 222 and 208 nm and β-sheet at 218 nm. Certain aspects of protein tertiary structure can be determined by the CD spectrum in the near-UV (250-350 nm). Within this region the chromophores are the aromatic amino acids and disulfide bonds and the CD signal depends on the asymmetric environment within the native structure of the protein. Signals in the region from 250-270 nm correspond to phenylalanines, 270-290 nm to tyrosines, and 280-300 nm to tryptophans. Disulfide bonds give rise to broad weak signals throughout the near-UV spectrum.

All recorded spectra were buffer-corrected and normalized to the mean residual weight ellipticity θ_{MRW} using the following equation:

Equation 2:
$$\theta_{MRW} = \frac{\theta * 100}{l * c * N_{aa}}$$

Where θ is the ellipticity (mdeg), l cell length (cm), c concentration (mM) and N_{aa} is the number of amino acids.

The experiments were performed with the following conditions:

Parameter	**Far-UV**
Wavelength (nm)	260-190
Scan speed (nm/min)	20
Band width (nm)	1
Path length (cm)	0.1
Concentration (mg/mL)	0.1
Response time (s)	8
Data pitch (s)	0.2

Temperature (°C)	30
Accumulations	10

To assess the thermal stability, 0.1 mg/mL protein samples were heated with 20 °C/h in a 1 mm Quartz cuvette followed by monitoring changes in the CD signal at 205 nm. The midpoint of the equation was determined by a Boltzmann fit.

8.14.3 Fluorescence spectroscopy

After excitation, the electronic state of the molecule changes from the ground state to one of the excited electronic states. The excited electronic state is usually the first excited singlet state, S1. Fluorescence occurs when electrons go back from a singlet excited state to the ground state. Proteins contain three aromatic amino acid residues with the delocalized π-electron ring systems (tryptophan, tyrosine, phenylalanine) which contribute to their intrinsic fluorescence.

FRET measurements

For FRET measurements fluorophores were attached to the cysteine residues of Hsp90 proteins following maleimide chemistry. The excitation and emission parameters of the dyes are listed below:

	Excitation wavelength (nm)	**Emission wavelength (nm)**	**ε_{max} (M^{-1} cm^{-1})**
Atto-488	501	523	90000
Atto-550	554	576	120000

The experiments were performed as described elsewhere (Hessling et al., 2009). To probe the conformational changes induced by nucleotide, heterodimers containing 100 nM M-domain donor- and 100 nM N-domain acceptor-labeled Hsp90 were preincubated at 20 °C in the buffer containing 40 mM HEPES/KOH pH 7.5, 150 mM KCl, 5 mM $MgCl_2$ in the presence of 2 mM AMP-PNP, ATPγS, ATP or without nucleotide. After the addition of 2 µM unmodified wt Hsp90, the decrease in the FRET signal was recorded.

To test the conformational rearrangements induced by Aha1 binding, 100 nM of N-domain donor-labeled S602E or wt Hsp90 were incubated at 20 °C for 15 min with 100 nM N-domain acceptor-labeled S602E or wt Hsp90, respectively, and the change

in FRET signal was recorded. 15 µM Aha1 was added to the mixed Hsp90 heterodimers and the effect on FRET efficiencies was monitored. To determine subunit exchange in the Hsp90 dimer in the presence and absence of Aha1, 2 µM unlabeled Hsp90 wt or S602E, respectively, were added to the solution and the reduction of the FRET signal was measured. The qualitative apparent half-life time of the subunit exchange was estimated using equation 3:

Equation 3:
$$y = y_0 + A * \exp\left(-x * \left(\frac{\ln(2)}{t_{1/2}}\right)\right)$$

where y_0 is the offset, A the amplitude of fluorescence change, $t_{1/2}$ is the apparent half-life time of the reaction.

8.14.4 Surface Plasmon Resonance

Surface plasmon resonance (SPR) spectroscopy can be applied to analyze protein-protein interaction. SPR is an optical technique that allows measuring label-free binding of two molecules in real time where one is mobile (analyte) and the other one is fixed on a thin gold film (ligand). The SPR effect is sensitive to binding of analyte because the associated increase in mass causes a proportional increase in refractive index, which is observed as a shift in the resonance angle.

In this work, proteins were immobilized by an amine-coupling reaction on a sensor chip. Experiments were performed as described before (Hainzl et al., 2004). For all SPR measurements, p23/Sba1 was coupled to the CM5 sensor chip (BiaCore, Uppsala, Sweden). p23/Sba1 coupling gave a signal of 750 RU. The instrument was equilibrated at 25 °C. The running buffer contained 40 mM HEPES/KOH pH 7.5, 150 mM KCl, 5 mM $MgCl_2$ and 2 mM AMP-PNP or ATPγS. 50 µL of protein was injected with the flow rate of 20 µL/min. Data analysis for direct binding was performed as described earlier (Richter et al., 2004).

8.15 Activity test for proteins *in vitro*

8.15.1 Regenerative ATPase assay

To determine the ATPase activity, a spectrophotometric assay based on an enzymatic ATP regeneration system was used (Richter et al., 2001). This assay uses a coupled-enzymatic approach that rapidly converts produced ADP to ATP in the presence of phosphoenolpyruvate, pyruvate kinase, NADH and lactate dehydrogenase. The ATPase activity is determined by the NADH consumption monitored by absorbance spectroscopy at 340 nm. The hydrolysis rates were calculated using the differential molar extinction coefficient of NADH and NAD^+ of 6200 $cm^{-1}M^{-1}$ at 340 nm.

Equation 4:

$$v_{spec} = \frac{m}{d * \left(-6200 \frac{1}{cm * M} \right) * c_{ATPase}}$$

m is the slope of the resulting lines, d is the thickness of the cuvette in cm and c_{ATPase} is the concentration of the respective ATPase in µM.

The assay buffer was 40 mM HEPES/KOH, pH 7.5, 150 mM KCl, 5 mM $MgCl_2$, the temperature was 30 °C. The experiments were performed in 200 µl final reaction volume. The reaction mix included 75 µL of 2x Premix, assay buffer, protein, ATP. 2 µM of Hsp90 wt or variants were used in the presence of 0 to 4 mM ATP. The reaction was inhibited by adding 50 µM radicicol (Sigma, St Louis, USA).

2x Premix:

Assay buffer	4156 µL
100 mM Phosphoenolpyruvate	240 µL
50 mM NADH	48 µL
Pyruvate kinase suspension	12 µL
Lactate dehydrogenase suspension	44 µL

The K_M and k_{cat} values were derived from the ATPase activities using standard Michaelis-Menten kinetics according to equation 5:

Equation 5:

$$v_{spec} = k_{cat} * \frac{x}{K_M + x}$$

where x is the concentration of ATP in the assay.

To investigate the influence of co-chaperones, 1 or 2.5 µM Hsp90 was preincubated with different concentrations of Aha1 or Hop/Sti1 and p23/Sba1, respectively, at 30 °C and 2 mM ATP. To enhance the binding affinity between Aha1 and Hsp90, the assay buffer contained 20 mM KCl, whereas for Hop/Sti1 and p23/Sba1 the assay buffer contained 150 mM KCl. Data for Aha1 activation were fitted according to equation 6:

Equation 6:

$$v_{spec} = \frac{(V_{\max} - V_0) * x}{K_D + x} + V_0$$

where x is the concentration of Aha1 in the assay and K_D is the apparent binding affinity. Data for Sti1 inhibition were fitted as described before (Li et al., 2011).

For heterodimer formation, 1 µM Hsp90 and 10 µM lidless-Hsp90 were mixed and preincubated at 30 °C for 20 min in standard assay buffer before 2 mM ATP was added (Richter et al., 2006).

8.16 Activity assays for proteins *in vivo*

8.16.1 5'FOA shuffling

To test the *in vivo* functionality of Hsp90 phospho-mutants, a plasmid shuffling approach was applied, as described previously (Nathan and Lindquist, 1995). A yeast strain deficient for both genomic copies of *hsp90* was used that contains a plasmid coding for *hsp90* under the control of a constitutive glyceraldehyde-3-phosphate dehydrogenase gene promoter (GPD promotor). This plasmid also carries an URA selection marker, which enables a selection for cells that had lost the wt Hsp90 plasmid in the medium supplemented with 5'FOA.

8.16.2 Nuclear Hsp90 chaperone activity assay

Exponentially growing yeast cells expressing Hsp90 phospho-mutants were adjusted to an OD_{600} of 0.5 (corresponding to 10^7 cells/mL), spotted in 1:5 dilution series on selective media, exposed to UV light (40 and 80 J/m^2) at RT and incubated at 30 °C.

8.16.3 Hsp90 inhibitor assay

Yeast cells expressing Hsp90 phospho-mutants were incubated overnight in liquid media supplemented with the indicated concentrations of radicicol. Cells were adjusted to an OD_{600} of 0.5 (corresponding to 10^7 cells/mL), spotted in 1:5 dilution series into selective media and incubated at 30 °C.

8.16.4 v-Src activity assay

To analyze v-Src activity in yeast cells, the phospho-tyrosine activity of the heterologously-expressed v-Src was assessed by Western blot (Nathan and Lindquist, 1995). Yeast cells were transformed with v-Src expression plasmid (URA marker). Due to v-Src toxicity, its expression was under the control of the galactose-inducible promoter. Cells were first grown in the glucose-containing media overnight, then transferred to the raffinose-containing media and incubated overnight. Finally, yeast cells were incubated in the galactose-containing media for 6 h at 30 °C to induce v-Src expression. Cells were harvested by centrifugation at 14000 rpm for 5 min, lysed using glass beads in the buffer containing 40 mM HEPES/KOH pH 7.5, 150 mM KCl at 4 °C. Protein concentration was determined by Bradford assay and normalized. Samples were analyzed by Western blot with monoclonal phospho-tyrosine antibody 4G10 (dilution 1:1000, incubation overnight at 4 °C) followed by incubation with POD-conjugated α-mouse IgG (dilution 1:40000, incubation for 1 h at RT) according to the standard protocol. Growth of wt and the Hsp90 phospho-variants was examined on the glucose- and galactose-containing media.

8.16.5 GR activity assay

To analyze GR activity, GR receptor assay was employed. Cells were transformed with plasmid for constitutive expression of GR and β-galactosidase under the control of GR response element (ADE marker). To analyze GR expression, cells were grown in the glucose-containing media. To induce the expression of β-galactosidase, cells were incubated with 20 μM desoxycorticosterone (DOC) for 6 h at 30 °C. Cells were harvested by centrifugation at 14000 rpm for 5 min, lysed using glass beads in the buffer containing 40 mM HEPES/KOH pH 7.5, 150 mM KCl, at 4 °C. β-galactosidase activity was assessed by Galacto-LightPlus Kit and the activity was normalized for protein concentration determined by Bradford assay. As a control, β-galactosidase background activity in the cells without the induction was measured.

8.16.6 Luciferase activity assay

To determine luciferase activity, yeast cells were transformed with plasmid for constitutive expression of FFL (URA marker). FFL expression was assessed by incubating yeast cells at 30 °C for 6 h. Cells were harvested by centrifugation at 14000 rpm for 5 min, lysed in buffer A using glass beads. Next, 100 μL of the lysate was mixed with 100 μL buffer B and the luminescence was immediately measured in a plate reader. The activity was normalized for protein concentration determined by Bradford assay.

Buffer A:
40 mM HEPES/KOH, pH 7.5
100 mM KCl
5 mM $MgCl_2$

Buffer B:
Buffer A supplemented with 2 mM ATP and 0.2 mM luciferin.

8.16.7 eGFP activity assay

To compare protein biosynthesis and protein folding in the yeast cells, eGFP activity was measured. Cells were transformed with plasmid for constitutive expression of

eGFP and its expression was assessed by incubating yeast cells at 30 °C for 6 h. Cells were harvested by centrifugation at 14000 rpm for 5 min, lysed in the buffer A (see 8.16.6) using glass beads. To enable eGFP chromophore oxidation, lysates were incubated at 4 °C for 1 h with agitation. After second centrifugation step, the lysates were normalized for the protein concentration and the fluorescence intensity was measured. The activity was normalized for protein concentration determined by Bradford assay.

8.17 Scanning Electron Microscopy

Electron microscopy study of yeast cells was performed with JOEL 5900 LV Microscope (JEOL, Eching, Germany). Yeast cells were prepared and analyzed as described (Haslbeck et al., 2004).

9 Abbreviations

A - Ampere

Å - Angström = 0.1 nm (10^{-10}m)

All-A - Hsp90 variant with the identified phosphorylation sites simultaneously mutated to alanine

All-E - Hsp90 variant with the identified phosphorylation sites simultaneously mutated to glutamate

AMP-PNP – Adenosine 5'-(β,γ-imidodiphosphate)

APS - ammoniumpersulfate

ATPγS - Adenosine 5′-O-(3-thiotriphosphate)

[γ-^{32}P]ATP - Adenosine 5'-triphosphate (γ-^{32}P)

aUC - analytical ultracentrifugation

BSA - bovine serum albumin

CD - circular dichroism

CKII – casein kinase 2

Da - dalton

DOC – desoxycorticosterone

E. coli - *Escherichia coli*

FFL – firefly luciferase

g - gram

GFP - green fluorescent protein

GR - glucocorticoid receptor

h – hour

Hsp - heat shock protein

kDa – kilo Dalton

λ - wavelength

Lidless-Hsp90 - Hsp90 variant with a deletion of amino acids 98 - 121 corresponding to the ATP lid

min - minute

mL - milliliter

mM - millimolar

µM – micromolar

nm – nanometer

OD - optical density

PAGE - polyacrylamide gel electrophoresis

PGK – phosphoglycerate kinase

pH - potentia hydrogenii

PNK – polynucleotide kinase

PPIase - peptidylprolyl isomerase

RD – radicicol

RT – room temperature

rpm - rounds per minute

UV - ultraviolet

S. cerevisiae - *Saccharomyces cerevisiae*

SDS - sodium dodecylsulfate

SEM - scanning electron microscopy

SHR - steroid hormone receptor

SILAC - stable isotope labeling with amino acids in cell culture

SPR – surface plasmon resonance

TPR domain - tetratricopeptide repeat domain

v-Src kinase - viral Src kinase

v/v - volume per volume

w/v - weight per volume

w/o - without

wt - wild type

10 References

Abbas-Terki,T., Briand,P.A., Donze,O., and Picard,D. (2002). The Hsp90 co-chaperones Cdc37 and Sti1 interact physically and genetically. Biol Chem. *383*, 1335-1342.

Albuquerque,C.P., Smolka,M.B., Payne,S.H., Bafna,V., Eng,J., and Zhou,H. (2008). A multidimensional chromatography technology for in-depth phosphoproteome analysis. Mol Cell Proteomics. *7*, 1389-1396.

Ali,M.M., Roe,S.M., Vaughan,C.K., Meyer,P., Panaretou,B., Piper,P.W., Prodromou,C., and Pearl,L.H. (2006). Crystal structure of an Hsp90-nucleotide-p23/Sba1 closed chaperone complex. Nature *440*, 1013-1017.

Andreeva,A.V. and Kutuzov,M.A. (1999). RdgC/PP5-related phosphatases: novel components in signal transduction. Cell Signal. *11*, 555-562.

Austin,M.J., Muskett,P., Kahn,K., Feys,B.J., Jones,J.D., and Parker,J.E. (2002). Regulatory role of SGT1 in early R gene-mediated plant defenses. Science *295*, 2077-2080.

Bagatell,R. and Whitesell,L. (2004). Altered Hsp90 function in cancer: a unique therapeutic opportunity. Mol Cancer Ther. *3*, 1021-1030.

Bali,P., Pranpat,M., Bradner,J., Balasis,M., Fiskus,W., Guo,F., Rocha,K., Kumaraswamy,S., Boyapalle,S., Atadja,P., Seto,E., and Bhalla,K. (2005). Inhibition of histone deacetylase 6 acetylates and disrupts the chaperone function of heat shock protein 90: a novel basis for antileukemia activity of histone deacetylase inhibitors. J Biol Chem. *280*, 26729-26734.

Bardwell,J.C. and Craig,E.A. (1988). Ancient heat shock gene is dispensable. J Bacteriol. *170*, 2977-2983.

Barral,J.M., Hutagalung,A.H., Brinker,A., Hartl,F.U., and Epstein,H.F. (2002). Role of the myosin assembly protein UNC-45 as a molecular chaperone for myosin. Science *295*, 669-671.

Becker,W., Kentrup,H., Klumpp,S., Schultz,J.E., and Joost,H.G. (1994). Molecular cloning of a protein serine/threonine phosphatase containing a putative regulatory tetratricopeptide repeat domain. J Biol Chem. *269*, 22586-22592.

Blank,M., Mandel,M., Keisari,Y., Meruelo,D., and Lavie,G. (2003). Enhanced ubiquitinylation of heat shock protein 90 as a potential mechanism for mitotic cell death in cancer cells induced with hypericin. Cancer Res. *63*, 8241-8247.

Borkovich,K.A., Farrelly,F.W., Finkelstein,D.B., Taulien,J., and Lindquist,S. (1989). hsp82 is an essential protein that is required in higher concentrations for growth of cells at higher temperatures. Mol Cell Biol *9*, 3919-3930.

Bradford,M.M. (1976). A rapid and sensitive method for the quantitation of microgram quantities of protein utilizing the principle of protein-dye binding. Anal. Biochem *72*, 248-254.

Breitkreutz,B.J., Stark,C., Reguly,T., Boucher,L., Breitkreutz,A., Livstone,M., Oughtred,R., Lackner,D.H., Bahler,J., Wood,V., Dolinski,K., and Tyers,M. (2008). The BioGRID Interaction Database: 2008 update. Nucleic Acids Res. *36*, D637-D640.

Brinker,A., Scheufler,C., Von Der,M.F., Fleckenstein,B., Herrmann,C., Jung,G., Moarefi,I., and Hartl,F.U. (2002). Ligand discrimination by TPR domains. Relevance and selectivity of EEVD-recognition in Hsp70 x Hop x Hsp90 complexes. J Biol Chem. *277*, 19265-19275.

Buchner,J. (2010). Bacterial Hsp90--desperately seeking clients. Mol Microbiol. *76*, 540-544.

Carbone,D.L., Doorn,J.A., Kiebler,Z., Ickes,B.R., and Petersen,D.R. (2005). Modification of heat shock protein 90 by 4-hydroxynonenal in a rat model of chronic alcoholic liver disease. J Pharmacol. Exp. Ther. *315*, 8-15.

Carbone,D.L., Doorn,J.A., Kiebler,Z., Sampey,B.P., and Petersen,D.R. (2004). Inhibition of Hsp72-mediated protein refolding by 4-hydroxy-2-nonenal. Chem. Res. Toxicol. *17*, 1459-1467.

Chen,M.S., Silverstein,A.M., Pratt,W.B., and Chinkers,M. (1996). The tetratricopeptide repeat domain of protein phosphatase 5 mediates binding to glucocorticoid receptor heterocomplexes and acts as a dominant negative mutant. J Biol Chem. *271*, 32315-32320.

Chen,M.X., McPartlin,A.E., Brown,L., Chen,Y.H., Barker,H.M., and Cohen,P.T. (1994). A novel human protein serine/threonine phosphatase, which possesses four tetratricopeptide repeat motifs and localizes to the nucleus. EMBO J *13*, 4278-4290.

Chen,S. and Smith,D.F. (1998). Hop as an adaptor in the heat shock protein 70 (Hsp70) and hsp90 chaperone machinery. J Biol Chem. *273*, 35194-35200.

Chen,W.Y., Chang,F.R., Huang,Z.Y., Chen,J.H., Wu,Y.C., and Wu,C.C. (2008). Tubocapsenolide A, a novel withanolide, inhibits proliferation and induces apoptosis in MDA-MB-231 cells by thiol oxidation of heat shock proteins. J Biol Chem. *283*, 17184-17193.

Chinkers,M. (2001). Protein phosphatase 5 in signal transduction. Trends Endocrinol. Metab *12*, 28-32.

Cintron,N.S. and Toft,D. (2006). Defining the requirements for Hsp40 and Hsp70 in the Hsp90 chaperone pathway. J Biol Chem. *281*, 26235-26244.

Cox,J. and Mann,M. (2008). MaxQuant enables high peptide identification rates, individualized p.p.b.-range mass accuracies and proteome-wide protein quantification. Nat. Biotechnol. *26*, 1367-1372.

Coxon,A. and Bestor,T.H. (1995). Proteins that glow in green and blue. Chem. Biol *2*, 119-121.

Csermely,P., Schnaider,T., Soti,C., Prohaszka,Z., and Nardai,G. (1998). The 90-kDa molecular chaperone family: structure, function, and clinical applications. A comprehensive review. Pharmacol. Ther. *79*, 129-168.

Cutforth,T. and Rubin,G.M. (1994). Mutations in Hsp83 and cdc37 impair signaling by the sevenless receptor tyrosine kinase in Drosophila. Cell *77*, 1027-1036.

Das,A.K., Cohen,P.W., and Barford,D. (1998). The structure of the tetratricopeptide repeats of protein phosphatase 5: implications for TPR-mediated protein-protein interactions. EMBO J *17*, 1192-1199.

Daub,H., Olsen,J.V., Bairlein,M., Gnad,F., Oppermann,F.S., Korner,R., Greff,Z., Keri,G., Stemmann,O., and Mann,M. (2008). Kinase-selective enrichment enables quantitative phosphoproteomics of the kinome across the cell cycle. Mol Cell *31*, 438-448.

de Zoeten,E.F., Wang,L., Butler,K., Beier,U.H., Akimova,T., Sai,H., Bradner,J.E., Mazitschek,R., Kozikowski,A.P., Matthias,P., and Hancock,W.W. (2011). Histone deacetylase 6 and heat shock protein 90 control the functions of foxp3+ T-regulatory cells. Mol Cell Biol *31*, 2066-2078.

Deb,T.B., Zuo,A.H., Wang,Y., Barndt,R.J., Cheema,A.K., Sengupta,S., Coticchia,C.M., and Johnson,M.D. (2011). Pnck induces ligand-independent EGFR degradation by probable perturbation of the Hsp90 chaperone complex. Am. J Physiol Cell Physiol *300*, C1139-C1154.

Dutta,R. and Inouye,M. (2000). GHKL, an emergent ATPase/kinase superfamily. Trends Biochem. Sci. *25*, 24-28.

Duval,M., Le,B.F., Huot,J., and Gratton,J.P. (2007). Src-mediated phosphorylation of Hsp90 in response to vascular endothelial growth factor (VEGF) is required for VEGF receptor-2 signaling to endothelial NO synthase. Mol Biol Cell *18*, 4659-4668.

Echtenkamp,F.J., Zelin,E., Oxelmark,E., Woo,J.I., Andrews,B.J., Garabedian,M., and Freeman,B.C. (2011). Global Functional Map of the p23 Molecular Chaperone Reveals an Extensive Cellular Network. Mol Cell *43*, 229-241.

Eckert,K., Saliou,J.M., Monlezun,L., Vigouroux,A., Atmane,N., Caillat,C., Quevillon-Cheruel,S., Madiona,K., Nicaise,M., Lazereg,S., Van,D.A., Sanglier-Cianferani,S., Meyer,P., and Morera,S. (2010). The Pih1-Tah1 cochaperone complex inhibits Hsp90 molecular chaperone ATPase activity. J Biol Chem. *285*, 31304-31312.

Eustace,B.K., Sakurai,T., Stewart,J.K., Yimlamai,D., Unger,C., Zehetmeier,C., Lain,B., Torella,C., Henning,S.W., Beste,G., Scroggins,B.T., Neckers,L., Ilag,L.L., and Jay,D.G. (2004). Functional proteomic screens reveal an essential extracellular role for hsp90 alpha in cancer cell invasiveness. Nat. Cell Biol *6*, 507-514.

Fairbanks,G., Steck,T.L., and Wallach,D.F. (1971). Electrophoretic analysis of the major polypeptides of the human erythrocyte membrane. Biochemistry *10*, 2606-2617.

Fang,Y., Fliss,A.E., Rao,J., and Caplan,A.J. (1998). SBA1 encodes a yeast hsp90 cochaperone that is homologous to vertebrate p23 proteins. Mol Cell Biol *18*, 3727-3734.

Fanghanel,J. and Fischer,G. (2004). Insights into the catalytic mechanism of peptidyl prolyl cis/trans isomerases. Front Biosci. *9*, 3453-3478.

Felts,S.J., Owen,B.A., Nguyen,P., Trepel,J., Donner,D.B., and Toft,D.O. (2000). The hsp90-related protein TRAP1 is a mitochondrial protein with distinct functional properties. J Biol Chem. *275*, 3305-3312.

Flom,G., Weekes,J., Williams,J.J., and Johnson,J.L. (2006). Effect of mutation of the tetratricopeptide repeat and asparatate-proline 2 domains of Sti1 on Hsp90 signaling and interaction in Saccharomyces cerevisiae. Genetics *172*, 41-51.

Fontana,J., Fulton,D., Chen,Y., Fairchild,T.A., McCabe,T.J., Fujita,N., Tsuruo,T., and Sessa,W.C. (2002). Domain mapping studies reveal that the M domain of hsp90 serves as a molecular scaffold to regulate Akt-dependent phosphorylation of endothelial nitric oxide synthase and NO release. Circ. Res. *90*, 866-873.

Freeman,B.C. and Yamamoto,K.R. (2002). Disassembly of transcriptional regulatory complexes by molecular chaperones. Science *296*, 2232-2235.

Frey,S., Leskovar,A., Reinstein,J., and Buchner,J. (2007). The ATPase cycle of the endoplasmic chaperone Grp94. J Biol Chem. *282*, 35612-35620.

Gaiser,A.M., Kretzschmar,A., and Richter,K. (2010). Cdc37-Hsp90 complexes are responsive to nucleotide-induced conformational changes and binding of further cofactors. J Biol Chem. *285*, 40921-40932.

Gamerdinger,M., Hajieva,P., Kaya,A.M., Wolfrum,U., Hartl,F.U., and Behl,C. (2009). Protein quality control during aging involves recruitment of the macroautophagy pathway by BAG3. EMBO J *28*, 889-901.

Gangaraju,V.K., Yin,H., Weiner,M.M., Wang,J., Huang,X.A., and Lin,H. (2011). Drosophila Piwi functions in Hsp90-mediated suppression of phenotypic variation. Nat. Genet. *43*, 153-158.

Garcia-Cardena,G., Fan,R., Shah,V., Sorrentino,R., Cirino,G., Papapetropoulos,A., and Sessa,W.C. (1998). Dynamic activation of endothelial nitric oxide synthase by Hsp90. Nature *392*, 821-824.

Gasch,A.P., Spellman,P.T., Kao,C.M., Carmel-Harel,O., Eisen,M.B., Storz,G., Botstein,D., and Brown,P.O. (2000). Genomic expression programs in the response of yeast cells to environmental changes. Mol Biol Cell *11*, 4241-4257.

Gerber,M.R., Farrell,A., Deshaies,R.J., Herskowitz,I., and Morgan,D.O. (1995). Cdc37 is required for association of the protein kinase Cdc28 with G1 and mitotic cyclins. Proc. Natl. Acad. Sci U. S. A *92*, 4651-4655.

Gnad,F., de Godoy,L.M., Cox,J., Neuhauser,N., Ren,S., Olsen,J.V., and Mann,M. (2009). High-accuracy identification and bioinformatic analysis of in vivo protein phosphorylation sites in yeast. Proteomics. *9*, 4642-4652.

Gnad,F., Forner,F., Zielinska,D.F., Birney,E., Gunawardena,J., and Mann,M. (2010). Evolutionary constraints of phosphorylation in eukaryotes, prokaryotes, and mitochondria. Mol Cell Proteomics. *9*, 2642-2653.

Grad,I., McKee,T.A., Ludwig,S.M., Hoyle,G.W., Ruiz,P., Wurst,W., Floss,T., Miller,C.A., III, and Picard,D. (2006). The Hsp90 cochaperone p23 is essential for perinatal survival. Mol Cell Biol *26*, 8976-8983.

Graf,C., Stankiewicz,M., Kramer,G., and Mayer,M.P. (2009). Spatially and kinetically resolved changes in the conformational dynamics of the Hsp90 chaperone machine. EMBO J *28*, 602-613.

Grenert,J.P., Johnson,B.D., and Toft,D.O. (1999). The importance of ATP binding and hydrolysis by hsp90 in formation and function of protein heterocomplexes. J Biol Chem. *274*, 17525-17533.

Hainzl,O., Lapina,M.C., Buchner,J., and Richter,K. (2009). The charged linker region is an important regulator of Hsp90 function. J Biol Chem. *284*, 22559-22567.

Hainzl,O., Wegele,H., Richter,K., and Buchner,J. (2004). Cns1 is an activator of the Ssa1 ATPase activity. J Biol Chem. *279*, 23267-23273.

Haslbeck,M., Braun,N., Stromer,T., Richter,B., Model,N., Weinkauf,S., and Buchner,J. (2004). Hsp42 is the general small heat shock protein in the cytosol of Saccharomyces cerevisiae. EMBO J *23*, 638-649.

Hawle,P., Siepmann,M., Harst,A., Siderius,M., Reusch,H.P., and Obermann,W.M. (2006). The middle domain of Hsp90 acts as a discriminator between different types of client proteins. Mol Cell Biol *26*, 8385-8395.

Hessling,M., Richter,K., and Buchner,J. (2009). Dissection of the ATP-induced conformational cycle of the molecular chaperone Hsp90. Nat. Struct. Mol. Biol *16*, 287-293.

Hiniker,A. and Bardwell,J.C. (2004). In vivo substrate specificity of periplasmic disulfide oxidoreductases. J Biol Chem. *279*, 12967-12973.

Holt,L.J., Tuch,B.B., Villen,J., Johnson,A.D., Gygi,S.P., and Morgan,D.O. (2009). Global analysis of Cdk1 substrate phosphorylation sites provides insights into evolution. Science *325*, 1682-1686.

Huai,Q., Wang,H., Liu,Y., Kim,H.Y., Toft,D., and Ke,H. (2005). Structures of the N-terminal and middle domains of E. coli Hsp90 and conformation changes upon ADP binding. Structure. *13*, 579-590.

Jarosz,D.F. and Lindquist,S. (2010). Hsp90 and environmental stress transform the adaptive value of natural genetic variation. Science *330*, 1820-1824.

Johnson,B.D., Schumacher,R.J., Ross,E.D., and Toft,D.O. (1998). Hop modulates Hsp70/Hsp90 interactions in protein folding. J Biol Chem. *273*, 3679-3686.

Johnson,J.L. and Toft,D.O. (1994). A novel chaperone complex for steroid receptors involving heat shock proteins, immunophilins, and p23. J Biol Chem. *269*, 24989-24993.

Johnson,J.L. and Toft,D.O. (1995). Binding of p23 and hsp90 during assembly with the progesterone receptor. Mol Endocrinol. *9*, 670-678.

Kadota,Y., Amigues,B., Ducassou,L., Madaoui,H., Ochsenbein,F., Guerois,R., and Shirasu,K. (2008). Structural and functional analysis of SGT1-HSP90 core complex required for innate immunity in plants. EMBO Rep. *9*, 1209-1215.

Kamath,R.S., Fraser,A.G., Dong,Y., Poulin,G., Durbin,R., Gotta,M., Kanapin,A., Le,B.N., Moreno,S., Sohrmann,M., Welchman,D.P., Zipperlen,P., and Ahringer,J. (2003). Systematic functional analysis of the Caenorhabditis elegans genome using RNAi. Nature *421*, 231-237.

Kang,H., Sayner,S.L., Gross,K.L., Russell,L.C., and Chinkers,M. (2001). Identification of amino acids in the tetratricopeptide repeat and C-terminal domains of protein phosphatase 5 involved in autoinhibition and lipid activation. Biochemistry *40*, 10485-10490.

Kimura,Y., Rutherford,S.L., Miyata,Y., Yahara,I., Freeman,B.C., Yue,L., Morimoto,R.I., and Lindquist,S. (1997). Cdc37 is a molecular chaperone with specific functions in signal transduction. Genes Dev. *11*, 1775-1785.

Kosano,H., Stensgard,B., Charlesworth,M.C., McMahon,N., and Toft,D. (1998). The assembly of progesterone receptor-hsp90 complexes using purified proteins. J Biol Chem. *273*, 32973-32979.

Koulov,A.V., LaPointe,P., Lu,B., Razvi,A., Coppinger,J., Dong,M.Q., Matteson,J., Laister,R., Arrowsmith,C., Yates,J.R., III, and Balch,W.E. (2010). Biological and structural basis for Aha1 regulation of Hsp90 ATPase activity in maintaining proteostasis in the human disease cystic fibrosis. Mol Biol Cell *21*, 871-884.

Kovacs,J.J., Murphy,P.J., Gaillard,S., Zhao,X., Wu,J.T., Nicchitta,C.V., Yoshida,M., Toft,D.O., Pratt,W.B., and Yao,T.P. (2005). HDAC6 regulates Hsp90 acetylation and chaperone-dependent activation of glucocorticoid receptor. Mol Cell *18*, 601-607.

Krishna,P. and Gloor,G. (2001). The Hsp90 family of proteins in Arabidopsis thaliana. Cell Stress. Chaperones. *6*, 238-246.

Kundrat,L. and Regan,L. (2010). Balance between folding and degradation for Hsp90-dependent client proteins: a key role for CHIP. Biochemistry *49*, 7428-7438.

Kurokawa,M., Zhao,C., Reya,T., and Kornbluth,S. (2008). Inhibition of apoptosome formation by suppression of Hsp90beta phosphorylation in tyrosine kinase-induced leukemias. Mol Cell Biol *28*, 5494-5506.

Laemmli,U.K. (1970). Cleavage of structural proteins during the assembly of the head of bacteriophage T4. Nature *227*, 680-685.

Large,A.T., Goldberg,M.D., and Lund,P.A. (2009). Chaperones and protein folding in the archaea. Biochem Soc Trans. *37*, 46-51.

Lees-Miller,S.P. and Anderson,C.W. (1989a). The human double-stranded DNA-activated protein kinase phosphorylates the 90-kDa heat-shock protein, hsp90 alpha at two NH2-terminal threonine residues. J Biol Chem. *264*, 17275-17280.

Lees-Miller,S.P. and Anderson,C.W. (1989b). Two human 90-kDa heat shock proteins are phosphorylated in vivo at conserved serines that are phosphorylated in vitro by casein kinase II. J Biol Chem. *264*, 2431-2437.

Legagneux,V., Morange,M., and Bensaude,O. (1991). Heat shock increases turnover of 90 kDa heat shock protein phosphate groups in HeLa cells. FEBS Lett. *291*, 359-362.

Lei,H., Venkatakrishnan,A., Yu,S., and Kazlauskas,A. (2007). Protein kinase A-dependent translocation of Hsp90 alpha impairs endothelial nitric-oxide synthase activity in high glucose and diabetes. J Biol Chem. *282*, 9364-9371.

Leskovar,A., Wegele,H., Werbeck,N.D., Buchner,J., and Reinstein,J. (2008). The ATPase cycle of the mitochondrial Hsp90 analog Trap1. J Biol Chem. *283*, 11677-11688.

Li,J., Richter,K., and Buchner,J. (2011). Mixed Hsp90-cochaperone complexes are important for the progression of the reaction cycle. Nat. Struct. Mol Biol *18*, 61-66.

Li,W., Li,Y., Guan,S., Fan,J., Cheng,C.F., Bright,A.M., Chinn,C., Chen,M., and Woodley,D.T. (2007). Extracellular heat shock protein-90alpha: linking hypoxia to skin cell motility and wound healing. EMBO J *26*, 1221-1233.

Lienhard,G.E. (2008). Non-functional phosphorylations? Trends Biochem Sci *33*, 351-352.

Lotz,G.P., Lin,H., Harst,A., and Obermann,W.M. (2003). Aha1 binds to the middle domain of Hsp90, contributes to client protein activation, and stimulates the ATPase activity of the molecular chaperone. J Biol Chem. *278*, 17228-17235.

Martinez-Ruiz,A., Villanueva,L., Gonzalez de,O.C., Lopez-Ferrer,D., Higueras,M.A., Tarin,C., Rodriguez-Crespo,I., Vazquez,J., and Lamas,S. (2005). S-nitrosylation of Hsp90 promotes the inhibition of its ATPase and endothelial nitric oxide synthase regulatory activities. Proc. Natl. Acad. Sci U. S. A *102*, 8525-8530.

Mayr,C., Richter,K., Lilie,H., and Buchner,J. (2000). Cpr6 and Cpr7, two closely related Hsp90-associated immunophilins from Saccharomyces cerevisiae, differ in their functional properties. J Biol Chem. *275*, 34140-34146.

McClellan,A.J., Xia,Y., Deutschbauer,A.M., Davis,R.W., Gerstein,M., and Frydman,J. (2007). Diverse cellular functions of the Hsp90 molecular chaperone uncovered using systems approaches. Cell *131*, 121-135.

McLaughlin,S.H., Smith,H.W., and Jackson,S.E. (2002). Stimulation of the weak ATPase activity of human hsp90 by a client protein. J Mol. Biol *315*, 787-798.

McLaughlin,S.H., Sobott,F., Yao,Z.P., Zhang,W., Nielsen,P.R., Grossmann,J.G., Laue,E.D., Robinson,C.V., and Jackson,S.E. (2006). The co-chaperone p23 arrests the Hsp90 ATPase cycle to trap client proteins. J Mol Biol *356*, 746-758.

Meiri,D. and Breiman,A. (2009). Arabidopsis ROF1 (FKBP62) modulates thermotolerance by interacting with HSP90.1 and affecting the accumulation of HsfA2-regulated sHSPs. Plant J *59*, 387-399.

Meyer,P., Prodromou,C., Liao,C., Hu,B., Roe,S.M., Vaughan,C.K., Vlasic,I., Panaretou,B., Piper,P.W., and Pearl,L.H. (2004). Structural basis for recruitment of the ATPase activator Aha1 to the Hsp90 chaperone machinery. EMBO J *23*, 1402-1410.

Mickler,M., Hessling,M., Ratzke,C., Buchner,J., and Hugel,T. (2009). The large conformational changes of Hsp90 are only weakly coupled to ATP hydrolysis. Nat. Struct. Mol. Biol *16*, 281-286.

Millson,S.H., Vaughan,C.K., Zhai,C., Ali,M.M., Panaretou,B., Piper,P.W., Pearl,L.H., and Prodromou,C. (2008). Chaperone ligand-discrimination by the TPR-domain protein Tah1. Biochem J *413*, 261-268.

Miyata,Y. (2009). Protein kinase CK2 in health and disease: CK2: the kinase controlling the Hsp90 chaperone machinery. Cell Mol Life Sci *66*, 1840-1849.

Mollapour,M., Tsutsumi,S., Donnelly,A.C., Beebe,K., Tokita,M.J., Lee,M.J., Lee,S., Morra,G., Bourboulia,D., Scroggins,B.T., Colombo,G., Blagg,B.S., Panaretou,B., Stetler-Stevenson,W.G., Trepel,J.B., Piper,P.W., Prodromou,C., Pearl,L.H., and Neckers,L. (2010a). Swe1Wee1-dependent tyrosine phosphorylation of Hsp90 regulates distinct facets of chaperone function. Mol Cell *37*, 333-343.

Mollapour,M., Tsutsumi,S., Kim,Y.S., Trepel,J., and Neckers,L. (2011a). Casein kinase 2 phosphorylation of Hsp90 threonine 22 modulates chaperone function and drug sensitivity. Oncotarget. *2*, 407-417.

Mollapour,M., Tsutsumi,S., and Neckers,L. (2010b). Hsp90 phosphorylation, Wee1 and the cell cycle. Cell Cycle *9*, 2310-2316.

Mollapour,M., Tsutsumi,S., Truman,A.W., Xu,W., Vaughan,C.K., Beebe,K., Konstantinova,A., Vourganti,S., Panaretou,B., Piper,P.W., Trepel,J.B., Prodromou,C., Pearl,L.H., and Neckers,L. (2011b). Threonine 22 phosphorylation attenuates hsp90 interaction with cochaperones and affects its chaperone activity. Mol Cell *41*, 672-681.

Morishima,Y., Kanelakis,K.C., Murphy,P.J., Lowe,E.R., Jenkins,G.J., Osawa,Y., Sunahara,R.K., and Pratt,W.B. (2003). The hsp90 cochaperone p23 is the limiting

component of the multiprotein hsp90/hsp70-based chaperone system in vivo where it acts to stabilize the client protein: hsp90 complex. J Biol Chem. *278*, 48754-48763.

Nair,S.C., Rimerman,R.A., Toran,E.J., Chen,S., Prapapanich,V., Butts,R.N., and Smith,D.F. (1997). Molecular cloning of human FKBP51 and comparisons of immunophilin interactions with Hsp90 and progesterone receptor. Mol Cell Biol *17*, 594-603.

Nathan,D.F. and Lindquist,S. (1995). Mutational analysis of Hsp90 function: interactions with a steroid receptor and a protein kinase. Mol. Cell Biol *15*, 3917-3925.

Nathan,D.F., Vos,M.H., and Lindquist,S. (1997). In vivo functions of the Saccharomyces cerevisiae Hsp90 chaperone. Proc. Natl. Acad. Sci. U. S. A *94*, 12949-12956.

Neckers,L. (2007). Heat shock protein 90: the cancer chaperone. J Biosci. *32*, 517-530.

Obermann,W.M., Sondermann,H., Russo,A.A., Pavletich,N.P., and Hartl,F.U. (1998). In vivo function of Hsp90 is dependent on ATP binding and ATP hydrolysis. J Cell Biol *143*, 901-910.

Ogiso,H., Kagi,N., Matsumoto,E., Nishimoto,M., Arai,R., Shirouzu,M., Mimura,J., Fujii-Kuriyama,Y., and Yokoyama,S. (2004). Phosphorylation analysis of 90 kDa heat shock protein within the cytosolic arylhydrocarbon receptor complex. Biochemistry *43*, 15510-15519.

Olsen,J.V., Blagoev,B., Gnad,F., Macek,B., Kumar,C., Mortensen,P., and Mann,M. (2006). Global, in vivo, and site-specific phosphorylation dynamics in signaling networks. Cell *127*, 635-648.

Panaretou,B., Prodromou,C., Roe,S.M., O'Brien,R., Ladbury,J.E., Piper,P.W., and Pearl,L.H. (1998). ATP binding and hydrolysis are essential to the function of the Hsp90 molecular chaperone in vivo. EMBO J *17*, 4829-4836.

Panaretou,B., Siligardi,G., Meyer,P., Maloney,A., Sullivan,J.K., Singh,S., Millson,S.H., Clarke,P.A., Naaby-Hansen,S., Stein,R., Cramer,R., Mollapour,M., Workman,P., Piper,P.W., Pearl,L.H., and Prodromou,C. (2002). Activation of the ATPase activity of hsp90 by the stress-regulated cochaperone aha1. Mol. Cell *10*, 1307-1318.

Picard,D. (2002). Heat-shock protein 90, a chaperone for folding and regulation. Cell Mol Life Sci *59*, 1640-1648.

Picard,D., Khursheed,B., Garabedian,M.J., Fortin,M.G., Lindquist,S., and Yamamoto,K.R. (1990). Reduced levels of hsp90 compromise steroid receptor action in vivo. Nature *348*, 166-168.

Pratt,W.B. (1993). The role of heat shock proteins in regulating the function, folding, and trafficking of the glucocorticoid receptor. J Biol Chem. *268*, 21455-21458.

Pratt,W.B., Gehring,U., and Toft,D.O. (1996). Molecular chaperoning of steroid hormone receptors. EXS *77*, 79-95.

Pratt,W.B., Morishima,Y., Murphy,M., and Harrell,M. (2006). Chaperoning of glucocorticoid receptors. Handb. Exp. Pharmacol. 111-138.

Pratt,W.B., Morishima,Y., Peng,H.M., and Osawa,Y. (2010). Proposal for a role of the Hsp90/Hsp70-based chaperone machinery in making triage decisions when proteins undergo oxidative and toxic damage. Exp. Biol Med. (Maywood.) *235*, 278-289.

Pratt,W.B. and Toft,D.O. (1997). Steroid receptor interactions with heat shock protein and immunophilin chaperones. Endocr. Rev. *18*, 306-360.

Pratt,W.B. and Toft,D.O. (2003). Regulation of signaling protein function and trafficking by the hsp90/hsp70-based chaperone machinery. Exp. Biol Med. (Maywood.) *228*, 111-133.

Prodromou,C., Roe,S.M., Piper,P.W., and Pearl,L.H. (1997). A molecular clamp in the crystal structure of the N-terminal domain of the yeast Hsp90 chaperone. Nat. Struct. Biol *4*, 477-482.

Prodromou,C., Siligardi,G., O'Brien,R., Woolfson,D.N., Regan,L., Panaretou,B., Ladbury,J.E., Piper,P.W., and Pearl,L.H. (1999). Regulation of Hsp90 ATPase activity by tetratricopeptide repeat (TPR)-domain co-chaperones. EMBO J *18*, 754-762.

Qbadou,S., Becker,T., Mirus,O., Tews,I., Soll,J., and Schleiff,E. (2006). The molecular chaperone Hsp90 delivers precursor proteins to the chloroplast import receptor Toc64. EMBO J *25*, 1836-1847.

Queitsch,C., Sangster,T.A., and Lindquist,S. (2002). Hsp90 as a capacitor of phenotypic variation. Nature *417*, 618-624.

Rappsilber,J., Mann,M., and Ishihama,Y. (2007). Protocol for micro-purification, enrichment, pre-fractionation and storage of peptides for proteomics using StageTips. Nat. Protoc. *2*, 1896-1906.

Ratajczak,T. and Carrello,A. (1996). Cyclophilin 40 (CyP-40), mapping of its hsp90 binding domain and evidence that FKBP52 competes with CyP-40 for hsp90 binding. J Biol Chem. *271*, 2961-2965.

Ratzke,C., Mickler,M., Hellenkamp,B., Buchner,J., and Hugel,T. (2010). Dynamics of heat shock protein 90 C-terminal dimerization is an important part of its conformational cycle. Proc. Natl. Acad. Sci U. S. A *107*, 16101-16106.

Retzlaff,M., Hagn,F., Mitschke,L., Hessling,M., Gugel,F., Kessler,H., Richter,K., and Buchner,J. (2010). Asymmetric activation of the hsp90 dimer by its cochaperone aha1. Mol. Cell *37*, 344-354.

Retzlaff,M., Stahl,M., Eberl,H.C., Lagleder,S., Beck,J., Kessler,H., and Buchner,J. (2009). Hsp90 is regulated by a switch point in the C-terminal domain. EMBO Rep. *10*, 1147-1153.

Richter,K., Moser,S., Hagn,F., Friedrich,R., Hainzl,O., Heller,M., Schlee,S., Kessler,H., Reinstein,J., and Buchner,J. (2006). Intrinsic inhibition of the Hsp90 ATPase activity. J Biol Chem. *281*, 11301-11311.

Richter,K., Muschler,P., Hainzl,O., and Buchner,J. (2001). Coordinated ATP hydrolysis by the Hsp90 dimer. J Biol Chem. *276*, 33689-33696.

Richter,K., Muschler,P., Hainzl,O., Reinstein,J., and Buchner,J. (2003). Sti1 is a non-competitive inhibitor of the Hsp90 ATPase. Binding prevents the N-terminal dimerization reaction during the atpase cycle. J Biol Chem. *278*, 10328-10333.

Richter,K., Soroka,J., Skalniak,L., Leskovar,A., Hessling,M., Reinstein,J., and Buchner,J. (2008). Conserved conformational changes in the ATPase cycle of human Hsp90. J Biol Chem. *283*, 17757-17765.

Richter,K., Walter,S., and Buchner,J. (2004). The Co-chaperone Sba1 connects the ATPase reaction of Hsp90 to the progression of the chaperone cycle. J Mol. Biol *342*, 1403-1413.

Riggs,D.L., Roberts,P.J., Chirillo,S.C., Cheung-Flynn,J., Prapapanich,V., Ratajczak,T., Gaber,R., Picard,D., and Smith,D.F. (2003). The Hsp90-binding peptidylprolyl isomerase FKBP52 potentiates glucocorticoid signaling in vivo. EMBO J *22*, 1158-1167.

Roe,S.M., Ali,M.M., Meyer,P., Vaughan,C.K., Panaretou,B., Piper,P.W., Prodromou,C., and Pearl,L.H. (2004). The Mechanism of Hsp90 regulation by the protein kinase-specific cochaperone p50(cdc37). Cell *116*, 87-98.

Rose,D.W., Wettenhall,R.E., Kudlicki,W., Kramer,G., and Hardesty,B. (1987). The 90-kilodalton peptide of the heme-regulated eIF-2 alpha kinase has sequence similarity with the 90-kilodalton heat shock protein. Biochemistry *26*, 6583-6587.

Rutherford,S.L. and Lindquist,S. (1998). Hsp90 as a capacitor for morphological evolution. Nature *396*, 336-342.

Sambrook L, Fritsch F, Maniatis T. (1989) Molecular Cloning. Cold Spring Harbor Press, Cold Spring Harbor, New York.

Sangster,T.A., Lindquist,S., and Queitsch,C. (2004). Under cover: causes, effects and implications of Hsp90-mediated genetic capacitance. Bioessays *26*, 348-362.

Sangster,T.A. and Queitsch,C. (2005). The HSP90 chaperone complex, an emerging force in plant development and phenotypic plasticity. Curr. Opin. Plant Biol *8*, 86-92.

Sato,T., Minagawa,S., Kojima,E., Okamoto,N., and Nakamoto,H. (2010). HtpG, the prokaryotic homologue of Hsp90, stabilizes a phycobilisome protein in the cyanobacterium Synechococcus elongatus PCC 7942. Mol Microbiol. *76*, 576-589.

Scheibel,T., Weikl,T., and Buchner,J. (1998). Two chaperone sites in Hsp90 differing in substrate specificity and ATP dependence. Proc. Natl. Acad. Sci. U. S. A *95*, 1495-1499.

Scheufler,C., Brinker,A., Bourenkov,G., Pegoraro,S., Moroder,L., Bartunik,H., Hartl,F.U., and Moarefi,I. (2000). Structure of TPR domain-peptide complexes: critical elements in the assembly of the Hsp70-Hsp90 multichaperone machine. Cell *101*, 199-210.

Schreiber,T.B., Mausbacher,N., Keri,G., Cox,J., and Daub,H. (2010). An integrated phosphoproteomics work flow reveals extensive network regulation in early lysophosphatidic acid signaling. Mol Cell Proteomics. *9*, 1047-1062.

Scroggins B.T., Neckers N. (2007). Post-translational modification of heat-shock protein impact on chaperone function. Expert Opin. Drug Discov. 2.

Scroggins,B.T., Robzyk,K., Wang,D., Marcu,M.G., Tsutsumi,S., Beebe,K., Cotter,R.J., Felts,S., Toft,D., Karnitz,L., Rosen,N., and Neckers,L. (2007). An acetylation site in the middle domain of Hsp90 regulates chaperone function. Mol Cell *25*, 151-159.

Shiau,A.K., Harris,S.F., Southworth,D.R., and Agard,D.A. (2006). Structural Analysis of E. coli hsp90 reveals dramatic nucleotide-dependent conformational rearrangements. Cell *127*, 329-340.

Shiu,R.P., Pouyssegur,J., and Pastan,I. (1977). Glucose depletion accounts for the induction of two transformation-sensitive membrane proteinsin Rous sarcoma virus-transformed chick embryo fibroblasts. Proc. Natl. Acad. Sci U. S. A *74*, 3840-3844.

Sidera,K. and Patsavoudi,E. (2008). Extracellular HSP90: conquering the cell surface. Cell Cycle *7*, 1564-1568.

Sinclair,C., Borchers,C., Parker,C., Tomer,K., Charbonneau,H., and Rossie,S. (1999). The tetratricopeptide repeat domain and a C-terminal region control the activity of Ser/Thr protein phosphatase 5. J Biol Chem. *274*, 23666-23672.

Smith,D.F. (1993). Dynamics of heat shock protein 90-progesterone receptor binding and the disactivation loop model for steroid receptor complexes. Mol Endocrinol. *7*, 1418-1429.

Smith,D.F., Stensgard,B.A., Welch,W.J., and Toft,D.O. (1992). Assembly of progesterone receptor with heat shock proteins and receptor activation are ATP mediated events. J Biol Chem. *267*, 1350-1356.

Smith,D.F., Sullivan,W.P., Marion,T.N., Zaitsu,K., Madden,B., McCormick,D.J., and Toft,D.O. (1993). Identification of a 60-kilodalton stress-related protein, p60, which interacts with hsp90 and hsp70. Mol Cell Biol *13*, 869-876.

Smith,D.F. and Toft,D.O. (2008). Minireview: the intersection of steroid receptors with molecular chaperones: observations and questions. Mol Endocrinol. *22*, 2229-2240.

Smith,D.F., Whitesell,L., Nair,S.C., Chen,S., Prapapanich,V., and Rimerman,R.A. (1995). Progesterone receptor structure and function altered by geldanamycin, an hsp90-binding agent. Mol Cell Biol *15*, 6804-6812.

Southworth,D.R. and Agard,D.A. (2008). Species-dependent ensembles of conserved conformational states define the Hsp90 chaperone ATPase cycle. Mol Cell *32*, 631-640.

Stafford,W.F., III (1992). Boundary analysis in sedimentation transport experiments: a procedure for obtaining sedimentation coefficient distributions using the time derivative of the concentration profile. Anal. Biochem *203*, 295-301.

Sullivan,W.P., Owen,B.A., and Toft,D.O. (2002). The influence of ATP and p23 on the conformation of hsp90. J Biol Chem. *277*, 45942-45948.

Swingle,M.R., Honkanen,R.E., and Ciszak,E.M. (2004). Structural basis for the catalytic activity of human serine/threonine protein phosphatase-5. J Biol Chem. *279*, 33992-33999.

Taipale,M., Jarosz,D.F., and Lindquist,S. (2010). HSP90 at the hub of protein homeostasis: emerging mechanistic insights. Nat. Rev. Mol Cell Biol *11*, 515-528.

Toogun,O.A., Dezwaan,D.C., and Freeman,B.C. (2008). The hsp90 molecular chaperone modulates multiple telomerase activities. Mol Cell Biol *28*, 457-467.

Trepel,J., Mollapour,M., Giaccone,G., and Neckers,L. (2010). Targeting the dynamic HSP90 complex in cancer. Nat. Rev. Cancer *10*, 537-549.

Tsutsumi,S., Mollapour,M., Graf,C., Lee,C.T., Scroggins,B.T., Xu,W., Haslerova,L., Hessling,M., Konstantinova,A.A., Trepel,J.B., Panaretou,B., Buchner,J., Mayer,M.P., Prodromou,C., and Neckers,L. (2009). Hsp90 charged-linker truncation reverses the functional consequences of weakened hydrophobic contacts in the N domain. Nat. Struct. Mol Biol *16*, 1141-1147.

Vaughan,C.K., Gohlke,U., Sobott,F., Good,V.M., Ali,M.M., Prodromou,C., Robinson,C.V., Saibil,H.R., and Pearl,L.H. (2006). Structure of an Hsp90-Cdc37-Cdk4 complex. Mol Cell *23*, 697-707.

Vaughan,C.K., Mollapour,M., Smith,J.R., Truman,A., Hu,B., Good,V.M., Panaretou,B., Neckers,L., Clarke,P.A., Workman,P., Piper,P.W., Prodromou,C., and Pearl,L.H. (2008). Hsp90-dependent activation of protein kinases is regulated by chaperone-targeted dephosphorylation of Cdc37. Mol Cell *31*, 886-895.

Wandinger,S.K., Suhre,M.H., Wegele,H., and Buchner,J. (2006). The phosphatase Ppt1 is a dedicated regulator of the molecular chaperone Hsp90. EMBO J *25*, 367-376.

Wang,X., Venable,J., LaPointe,P., Hutt,D.M., Koulov,A.V., Coppinger,J., Gurkan,C., Kellner,W., Matteson,J., Plutner,H., Riordan,J.R., Kelly,J.W., Yates,J.R., III, and Balch,W.E. (2006). Hsp90 cochaperone Aha1 downregulation rescues misfolding of CFTR in cystic fibrosis. Cell *127*, 803-815.

Weaver,A.J., Sullivan,W.P., Felts,S.J., Owen,B.A., and Toft,D.O. (2000). Crystal structure and activity of human p23, a heat shock protein 90 co-chaperone. J Biol Chem. *275*, 23045-23052.

Wegele,H., Wandinger,S.K., Schmid,A.B., Reinstein,J., and Buchner,J. (2006). Substrate transfer from the chaperone Hsp70 to Hsp90. J Mol Biol *356*, 802-811.

Weikl,T., Abelmann,K., and Buchner,J. (1999). An unstructured C-terminal region of the Hsp90 co-chaperone p23 is important for its chaperone function. J Mol Biol *293*, 685-691.

Whitesell,L. and Lindquist,S.L. (2005). HSP90 and the chaperoning of cancer. Nat. Rev. Cancer *5*, 761-772.

Young,J.C., Hoogenraad,N.J., and Hartl,F.U. (2003). Molecular chaperones Hsp90 and Hsp70 deliver preproteins to the mitochondrial import receptor Tom70. Cell *112*, 41-50.

Zhang,M., Kadota,Y., Prodromou,C., Shirasu,K., and Pearl,L.H. (2010). Structural basis for assembly of Hsp90-Sgt1-CHORD protein complexes: implications for chaperoning of NLR innate immunity receptors. Mol Cell *39*, 269-281.

Zhao,R., Davey,M., Hsu,Y.C., Kaplanek,P., Tong,A., Parsons,A.B., Krogan,N., Cagney,G., Mai,D., Greenblatt,J., Boone,C., Emili,A., and Houry,W.A. (2005). Navigating the chaperone network: an integrative map of physical and genetic interactions mediated by the hsp90 chaperone. Cell *120*, 715-727.

Zhao,R., Kakihara,Y., Gribun,A., Huen,J., Yang,G., Khanna,M., Costanzo,M., Brost,R.L., Boone,C., Hughes,T.R., Yip,C.M., and Houry,W.A. (2008). Molecular chaperone Hsp90 stabilizes Pih1/Nop17 to maintain R2TP complex activity that regulates snoRNA accumulation. J Cell Biol *180*, 563-578.

Zhao,Y.G., Gilmore,R., Leone,G., Coffey,M.C., Weber,B., and Lee,P.W. (2001). Hsp90 phosphorylation is linked to its chaperoning function. Assembly of the reovirus cell attachment protein. J Biol Chem. *276*, 32822-32827.

Zhou,Q., Agoston,A.T., Atadja,P., Nelson,W.G., and Davidson,N.E. (2008). Inhibition of histone deacetylases promotes ubiquitin-dependent proteasomal degradation of DNA methyltransferase 1 in human breast cancer cells. Mol Cancer Res. *6*, 873-883.

Zhu,X.J., Liu,X., Jin,Q., Cai,Y., Yang,Y., and Zhou,T. (2010). The L279P mutation of nuclear distribution gene C (NudC) influences its chaperone activity and lissencephaly protein 1 (LIS1) stability. J Biol Chem. *285*, 29903-29910.

11 Declaration

I, Joanna Soroka, hereby declare that this thesis was prepared by me independently and using only the references and resources stated here. The work has so far not been submitted to any audit commission. Parts of this work have been published in scientific journals.

Hiermit erkläre ich, Joanna Soroka, dass ich die vorliegende Arbeit selbständig verfasst und keine anderen als die angegebenen Quellen und Hilfsmittel verwendet habe. Die Arbeit wurde bisher keiner Prüfungskommission vorgelegt. Teile dieser Arbeit wurde in wissenschaftlichen Journalen veröffentlicht.

_____

Joanna Soroka

12 Publications

Richter K., **Soroka J.**, Skalniak L., Leskovar A., Hessling M., Reinstein J., Buchner J. (2008)
Conserved conformational changes in the ATPase cycle of human Hsp90
J Biol Chem. 283, 17757-17765

Li J., **Soroka J.**, Buchner J. (2011)
The Hsp90 chaperone machinery: conformational dynamics and regulation by co-chaperones
BBA review

Soroka J.; Wandinger S.; Mäusbacher N.; Schreiber T.; Richter K.; Daub H.; Buchner J. (2012)
Conformational switching of the molecular chaperone Hsp90 via regulated phosphorylation
Mol Cell, accepted

13 Acknowledgments

This PhD thesis was prepared at the Technische Universität München, Department Chemie, Lehrstuhl Biotechnologie under supervision of Prof. Dr. Johannes Buchner from September 2007 to November 2011.

I would like to express my gratitude to my research advisor Prof. Dr. Johannes Buchner for giving me a good opportunity to work in his group, his guidance, support and encouragement during every stage of my research work. I thank Dr. Henrik Daub for our fruitful collaboration which has led to publications and for his constructive suggestions and comments. My appreciation goes to Dr. Sebastian Wandinger and Dr. Klaus Richter for their involvement in this project and useful discussions. I thank my lab mates and technicians who helped me throughout this academic exploration and our secretary Mrs. Susanne Hilber for being always helpful and understanding. I am appreciative to all practical students for their assistance and contribution to this work. I am also thankful to all people that I have met at the University for their great friendship.

Finally, I am deeply grateful to Muzio (without you, I could not have completed this project), and to my family for supporting me throughout the years.